Cassini Ultraviolet Imaging Spectrograph

Ring Solar Occultation Atlas
Volume 2: Revs 172 - 279

Version: 1.0
June 18, 2018

Table of Contents

The table lists all solar occultations observed by UVIS over the course of the Cassini mission. The table includes the rev number, whether the occultation was ingress or egress, the radial range sampled in the ring plane, the instrument integration period, solar elevation angle of the occultation, and duration of the occultation.

For each occultation there are four graphical products: (1) a plot of the total signal collected as a function of ring plane radius (the data have been binned spectrally); (2) the nominal radial resolution as a function of ring plane radius; (3) the azimuthal look angle as a function of ring plane radius; (4) a geometric rendering of Saturn from the point of view of Cassini at the temporal midpoint of the occultation. The nominal radial resolution does not include effects due to the nonzero angular dimensions of the Sun, diffraction, or smearing. The geometric rendering includes the UVIS EUV Solar occultation window field of view.

Occultations are presented chronologically in the order they were observed. In order to keep the file sizes small, the atlas is divided into volumes.

Introduction

The Cassini UVIS Extreme Ultraviolet Channel (EUV) had a solar port offset 20 degrees from the main UVIS optical axis to allow safe solar viewing. This was co-aligned with the Visual and Infrared Mapping Spectrometer (VIMS) solar port so that both instruments could observe the Sun simultaneously. Solar occultations by Saturn's atmosphere, Titan's atmosphere, the plumes of Enceladus, and Saturn's rings were observed. Because of the finite angular size of the solar disk projected onto the rings as seen from Cassini and longer integration times, the nominal spatial resolution of the ring solar occultations is much worse than that of the stellar occultations.

On the first ring solar occultation on "rev 9" it was discovered that an offset between the VIMS and UVIS solar fields of view resulted in the Sun falling just at the edge of the UVIS field of view when the VIMS solar boresight was pointed at the Sun. This resulted in an unusual occultation profile for rev 9 that also, coincidentally, passed near a particularly dust region of the F ring, resulting in a prominent diffraction signal (Becker et al. 2018). Most future occultations used UVIS pointing because that enabled both VIMS and UVIS to see the full solar disk due to the differences in instrument field of view shapes and sizes. The misalignment of rev 9 was approximately re-produced on the solar occultations on revs 90, 172 and 181.

Description of Data Products in the Atlas

The data are shown summed in the spectral dimension and plotted as a function of nominal ring plane intercept of the line of sight to the Sun. The data plots are at the full temporal resolution recorded. The summary table identifies the integration period for each occultation.

Two additional geometry plots are included for each occultation: (1) the radial ring plane resolution of the occultation (in the frame of Saturn, not accounting for ring particle motion, size of the solar disk, or diffraction); and (2) the value of ϕ, an angle measured in the ring plane in the counterclockwise sense from the outward radial vector at the measurement point to the direction to the Sun projected into the ring plane. Thus, an observation where the look vector to the Sun is tangent to the rings has ϕ=90 degrees.

On the page following the data plots, a geometry visualization is shown at a time near the middle of the occultation. The position of the UVIS EUV solar port field of view is labeled on each of these plots. Occultations that cut a chord across the rings, are presented here as separate "Ingress" and "Egress" occultations, referring to the portion of the occultation where the observation point is approaching or receding from Saturn, respectively.

Document assembled by Joshua Colwell, UVIS Co-Investigator, University of Central Florida, with the assistance of Tina Notrika, UCF.

References

1. Becker, T. M., J. E. Colwell, L. W. Esposito, N. O. Attree, C. D. Murray 2018. Cassini UVIS Solar Occultations by Saturn's F Ring and the Detection of Collision-Produced Micron-Sized Dust. *Icarus* **306**, 171-199, doi:10.1016/j.icarus.2018.02.006.
2. Esposito, L. W., J. E. Colwell, and W. E. McClintock 1998. Cassini UVIS Observations of Saturn's Rings. *Planet. Space Sci.* **46**, 1221-1235.
3. Esposito, L. W., C. A. Barth, J. E. Colwell, G. M. Lawrence, W. E. McClintock, A. I. F. Stewart, H. U. Keller, , A. Korth, H. Lauche, M. Festou, A. L. Lane, C. J. Hansen, J. N. Maki, R. A. West, H. Jahn, R. Reulke, K. Warlich, D. E. Shemansky, and Y. L. Yung 2004. The Cassini Ultraviolet Imaging Spectrograph Investigation. *Space Sci. Rev.* **115**, 299-361.

Rev	Ing/Eg	Year/Day	B0	ϕ (degrees)	Radius (km)	Int. Period (s)	Duration (minutes)	I0 (counts/int.)	Background (counts/int.)
9	I	2005-159	-21.45	281.96-281.67	168,669-66,033	4	144.5	8.0E+03	6.0E+02
11	I	2005-196	-21.07	284.83-286.18	116,000-53,978	4	81.7	4.0E+05	1.0E+03
28	I	2006-257	-15.86	281.20-230.96	128,084-87,624	37	633.9	2.5E+06	4.0E+03
28	E	2006-258	-15.86	234.16-230.96	87,490-87,624	37	31.4	2.5E+06	4.0E+03
43	I	2007-114	-12.76	41.24-78.81	126,232-100,226	5.5	38.8	4.7E+05	4.0E+02
43	E	2007-114	-12.76	78.81-139.77	100,226-205,453	5.5	129.4	4.7E+05	6.0E+02
55	I	2008-003	-9	314.11-258.18	172,488-96,962	4	40.1	3.2E+05	8.0E+02
55	E	2008-003	-9	258.18-207.70	96.962-151,727	4	73	3.2E+05	1.0E+03
59	I	2008-051	-8.27	331.78-262.26	194,733-68,372	4	34.3	3.2E+05	1.2E+04
59	E	2008-051	-8.27	262.26-257.22	68,372-68,628	4	1.1	3.2E+05	1.2E+04
62	I	2008-083	-7.79	337.93-264.72	257,380-74,524	4	41.7	3.2E+05	2.1E+03
62	E	2008-083	-7.79	264.72-192.75	74,524-238,015	4	38.3	3.2E+05	2.1E+03
65	I	2008-111	-7.36	332.21-266.13	206,054-83,837	1	30.2	8.1E+04	1.0E+02
65	E	2008-111	-7.36	266.13-194.65	83,837-262,873	1	40	8.1E+04	1.5E+02
66	I	2008-121	-7.21	337.36-266.20	261,953-85,115	1	38.9	7.8E+04	5.5E+02
66	E	2008-121	-7.21	266.20-194.49	85,115-270,107	1	40.2	7.8E+04	7.0E+02
90	I	2008-298	-4.49	346.51-268.82	445,890-95,719	2	36.3	4.0E+03	Unknown
90	E	2008-298	-4.49	268.82-206.69	95,719-204,613	2	15	4.3E+03	Unknown
172	I	2012-267	15.9	320.48-308.40	150,286-78,637	1	70.1	4.0E+03	6.0E+01
181	E	2013-044	17.5	147.36-153.60	100,304-148,010	1	35.3	1.8E+03	6.0E+01
239	I	2016-221	26.4	348.95-254.61	157,454-119,150	2	59.1	1.5E+05	1.0E+02
239	E	2016-221	26.4	103.36-134.95	59,983-150,709	2	151.6	1.5E+05	4.0E+02
241	I	2016-245	26.5	4.58-64.53	161,762-81,459	2	212.4	1.5E+05	1.0E+02
241	E	2016-245	26.5	64.53-116.75	81,459-132,557	2	158.7	Unknown	4.0E+02
243	I	2016-269	26.5	53.17-65.08	71,084-69,558	2	22.1	1.4E+05	Unknown
243	E	2016-269	26.5	65.08-119.41	69,558-118,986	2	146	1.4E+05	4.0E+02
245	I	2016-288	26.5	16.56-66.62	147,966-95,457	2	181.5	1.4E+05	4.0E+02
245	E	2016-288	26.5	66.62-82.74	95,457-99,340	2	44.1	Unknown	Unknown
249	I	2016-325	26.6	17.64-67.75	148,772-96,097	1	194.8	5.1E+04	1.0E+02
249	E	2016-325	26.6	67.75-117.77	96,097-148,630	1	194.3	5.1E+04	1.0E+02
254	I	2016-361	26.6	11.24-69.07	146,194-78,903	1	221.3	6.5E+04	1.5E+02

254	E	2016-361	26.6	69.07-126.58	78,903-145,372	1	218.9	6.5E+04	2.0E+02
257	I	2017-017	26.7	6.64-16.07	145,205-111,292	1	71.6	6.5E+04	Unknown
261	E	2017-046	26.7	118.88-143.42	68,714-147,371	1	159.6	6.5E+04	2.0E+02
263	E	2017-060	26.7	133.09-143.50	75,268-113,102	1	73.6	Unknown	2.0E+02
265	E	2017-074	26.7	146.20-152.35	95,650-147,462	1	95.1	6.4E+04	2.0E+02
267	E	2017-089	26.7	152.28-156.80	95,293-153,775	1	105.6	6.6E+04	2.0E+02
269	I	2017-103	26.7	348.26-349.55	157,777-117,823	1	72.1	6.4E+04	Unknown
271	E	2017-116	26.7	171.30-169.90	126,863-174,743	1	87.1	6.7E+04	Unknown
279	I	2017-168	26.7	321.49-267.36	127,778-77,483	1	180.1	Unknown	1.0E+02
279	E	2017-168	26.7	267.36-214.41	77,483-126,099	1	173.8	Unknown	1.0E+02

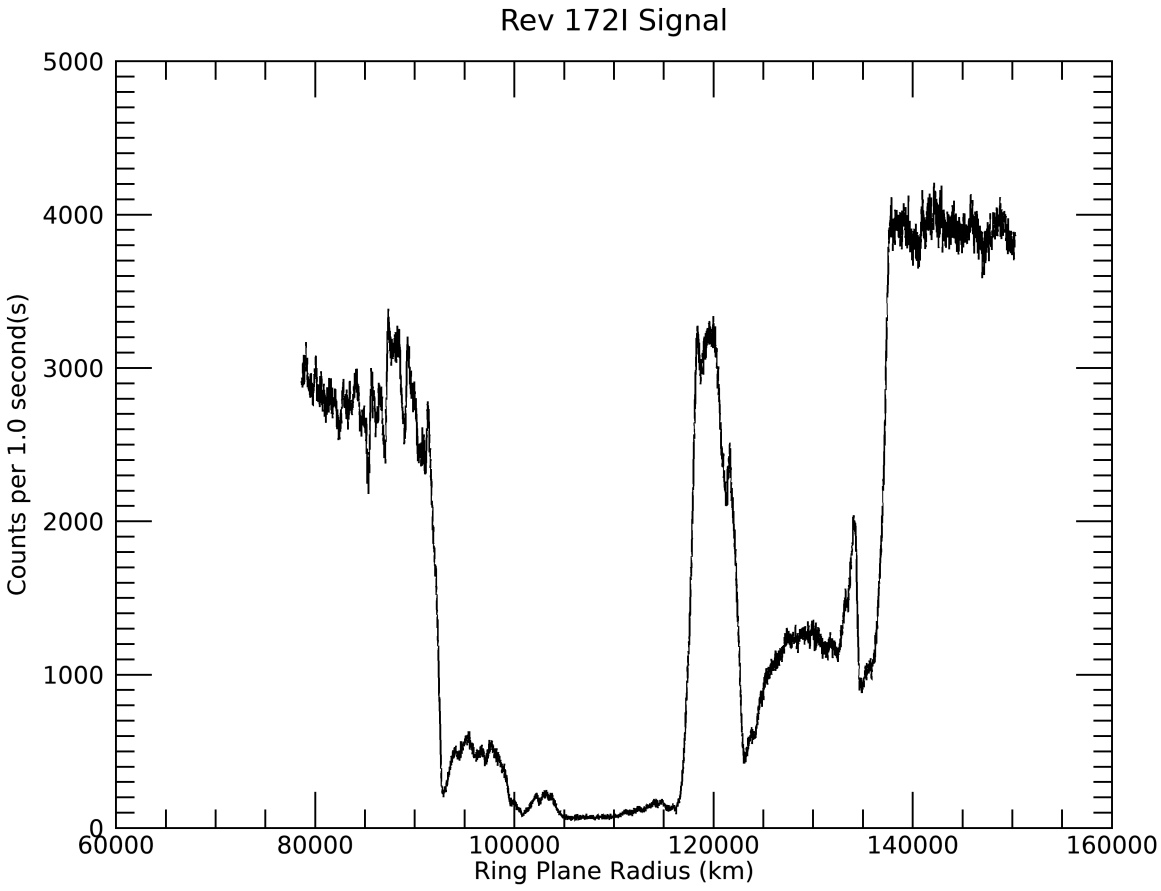
Rev 172I Signal
5000
4000
3000
2000
1000
0
Counts per 1.0 second(s)
60000
80000
100000
120000
140000
160000
Ring Plane Radius (km)

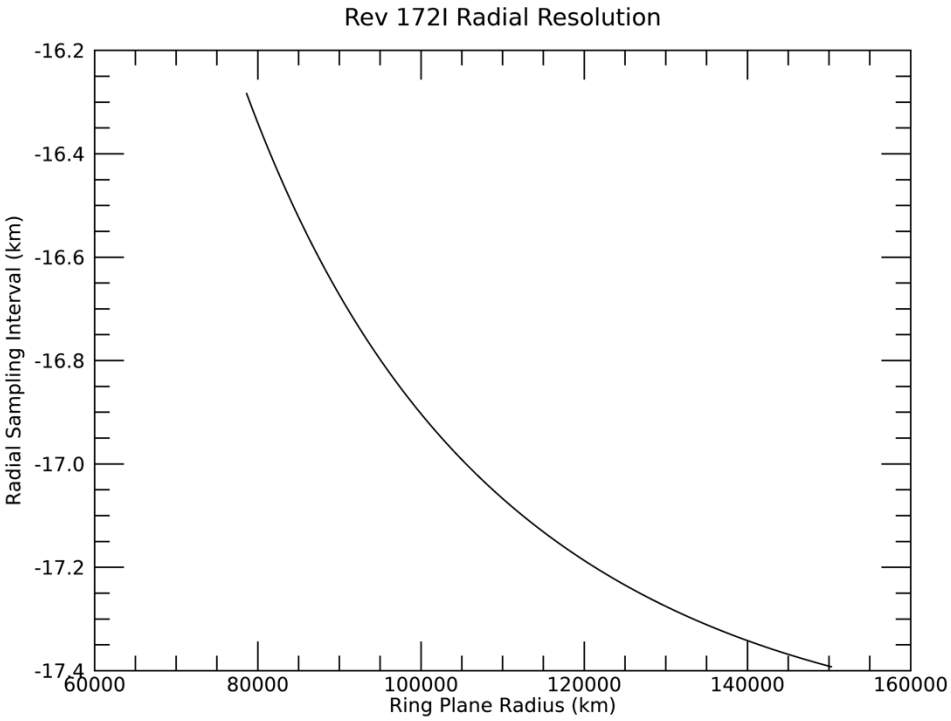
Rev 172I Radial Resolution
Radial Sampling Interval (km)
-16.2
-16.4
-16.6
-16.8
-17.0
-17.2
-17.4
60000
80000
100000
120000
140000
160000
Ring Plane Radius (km)

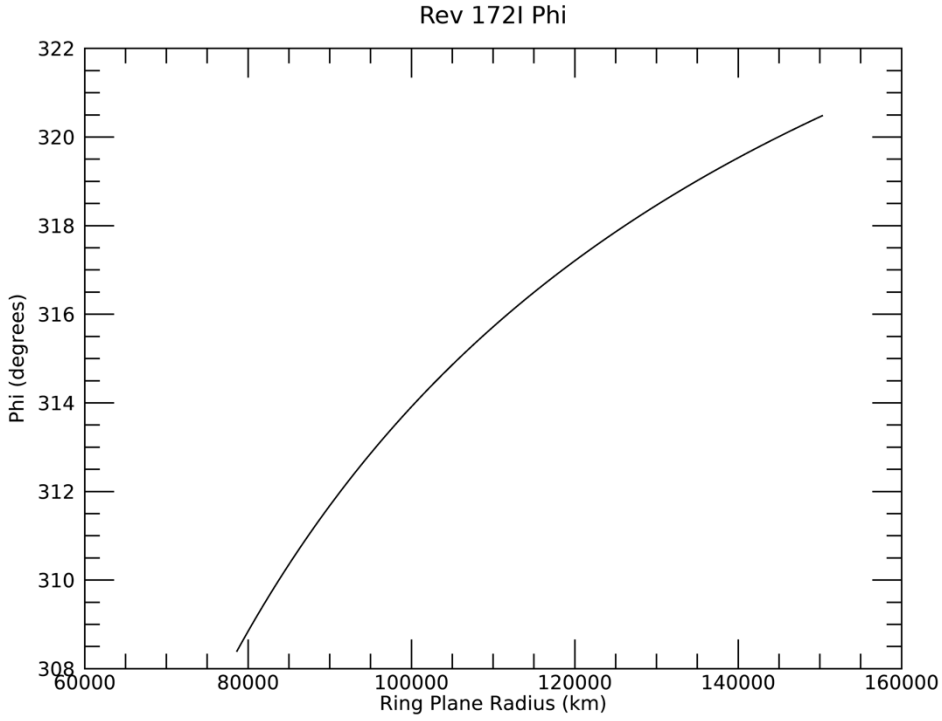
Rev 172I Phi
Phi (degrees)
322
320
318
316
314
312
310
308
60000
80000
100000
120000
140000
160000
Ring Plane Radius (km)

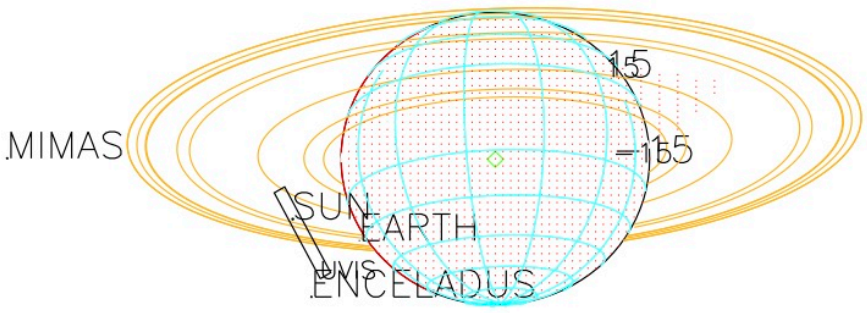

2012-268T00:07:00.000 571621.96 km

Target RA/dec: 21.86, 11.91

Subsolar lat/lon: 13.06, -10.66

Sub-s/c lat/lon: -15.11, 161.01

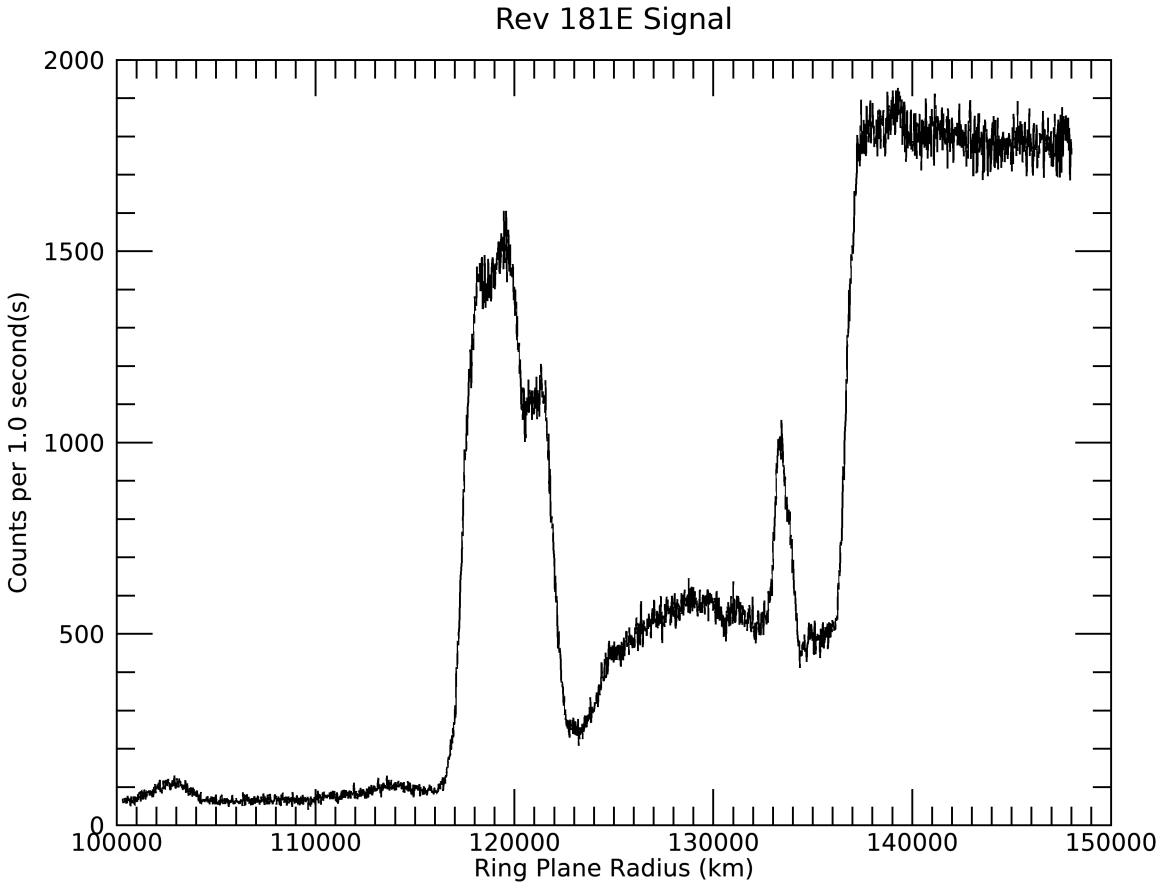
Rev 181E Signal
2000
1500
1000
500
0
Counts per 1.0 second(s)
100000
110000
120000
130000
140000
150000
Ring Plane Radius (km)

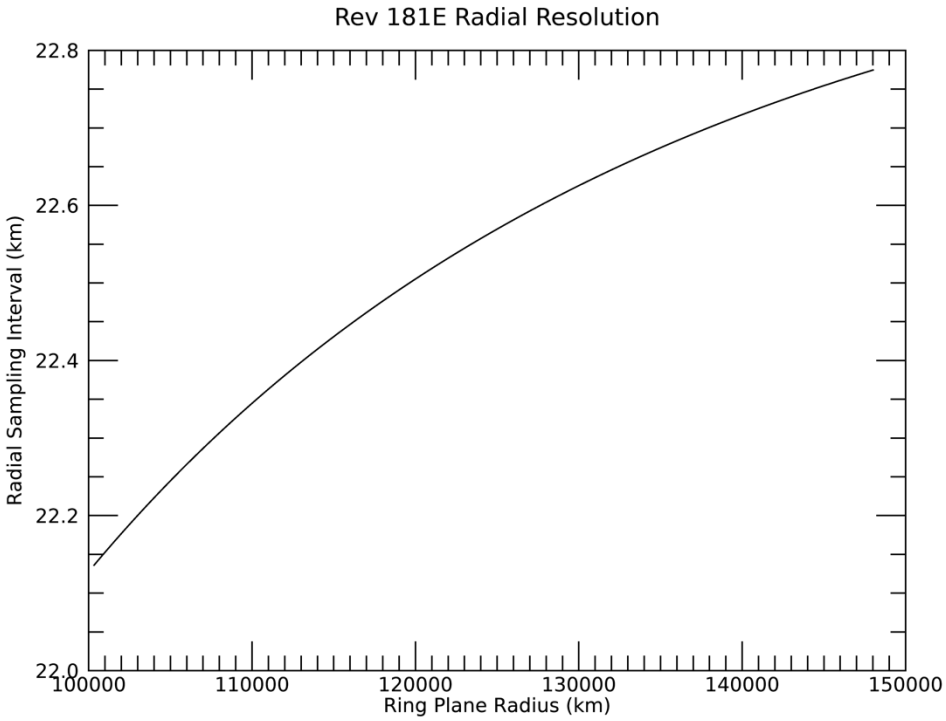
Rev 181E Radial Resolution
Radial Sampling Interval (km)
22.8
22.6
22.4
22.2
22.0
100000
110000
120000
130000
140000
150000
Ring Plane Radius (km)

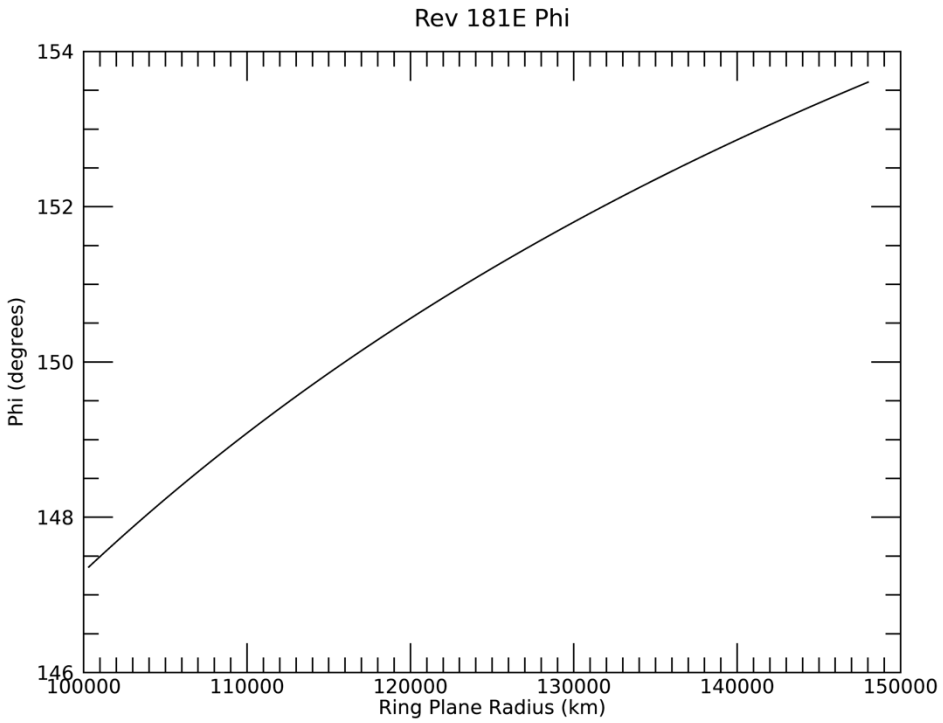
Rev 181E Phi
Phi (degrees)
154
152
150
148
146
100000
110000
120000
130000
140000
150000
Ring Plane Radius (km)

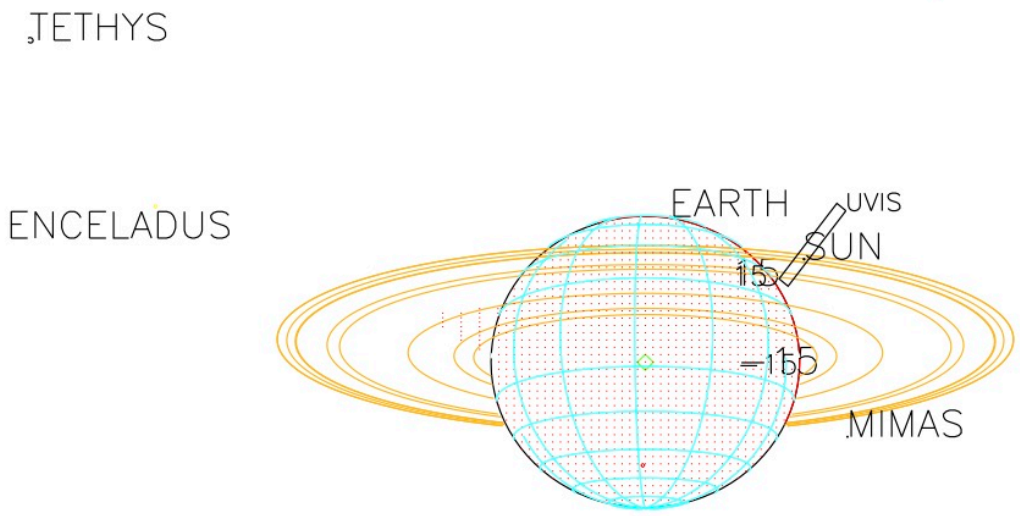

2013-044T23:19:00.000 556807.88 km

Target RA/dec: 40.72, 7.22

Subsolar lat/lon: 14.43, -2.75

Sub-s/c lat/lon: -11.43, -176.06

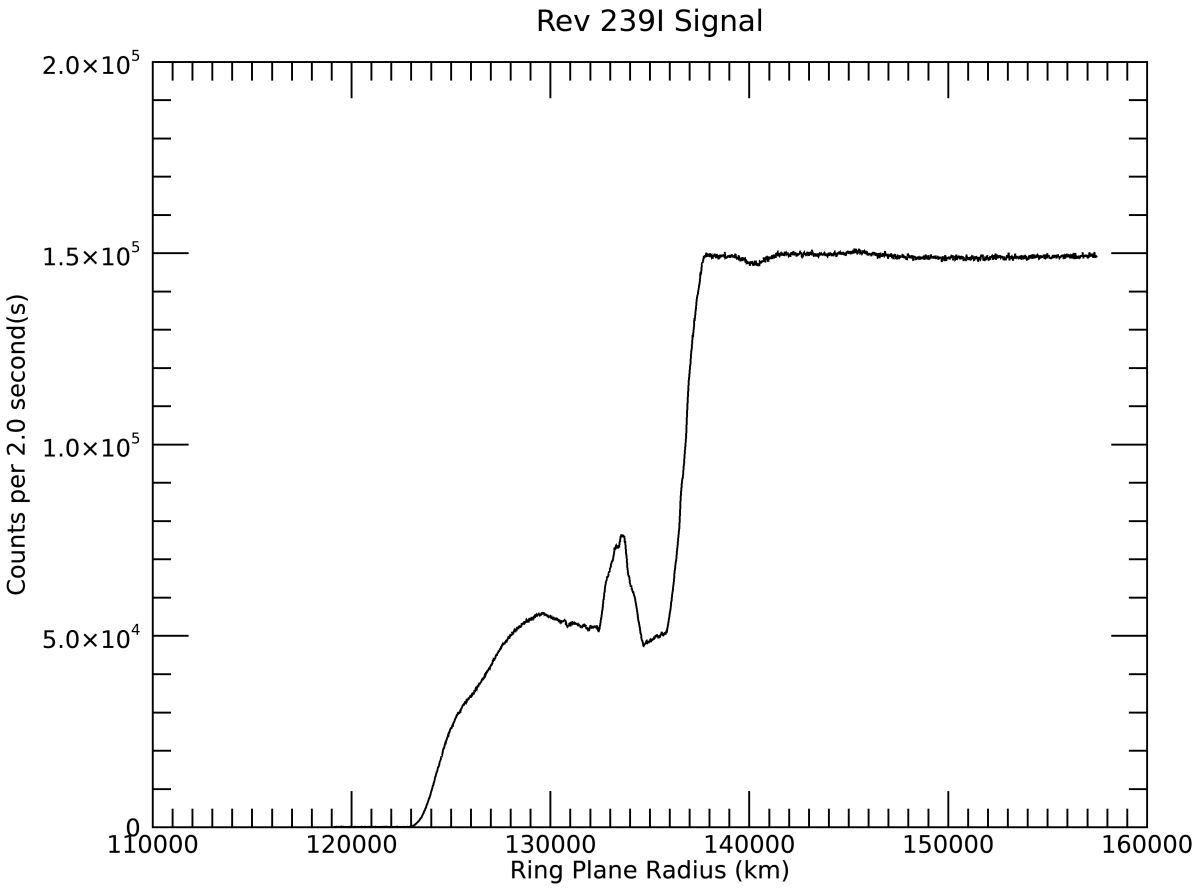
Rev 239I Signal
2.0×10^5
1.5×10^5
1.0×10^5
5.0×10^4
0
Counts per 2.0 second(s)
110000
120000
130000
140000
150000
160000
Ring Plane Radius (km)

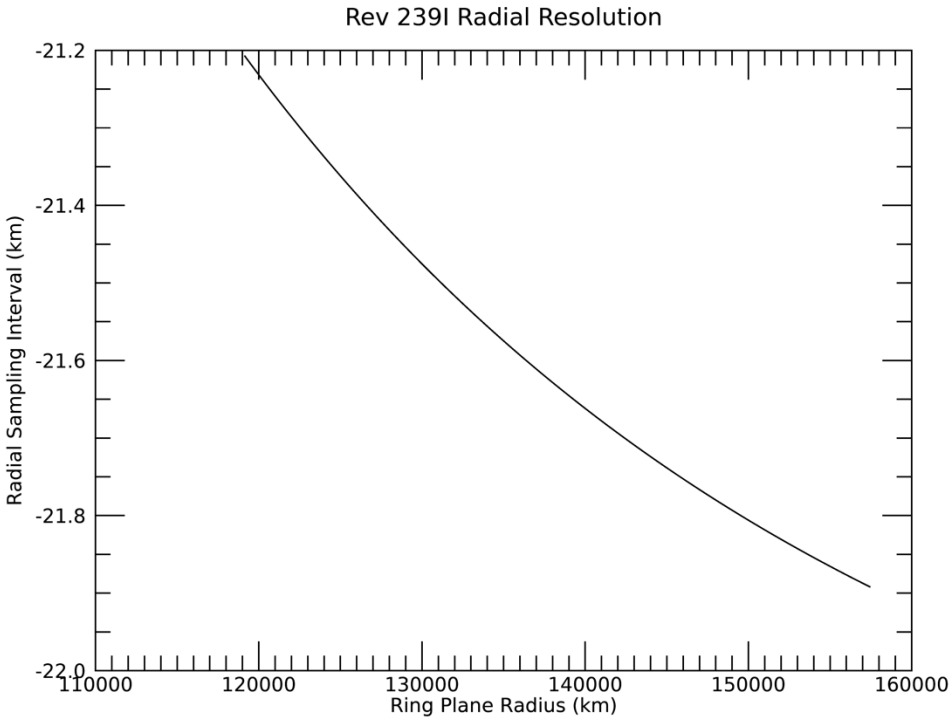
Rev 239I Radial Resolution
-21.2
-21.4
-21.6
-21.8
-22.0
Radial Sampling Interval (km)
110000
120000
130000
140000
150000
160000
Ring Plane Radius (km)

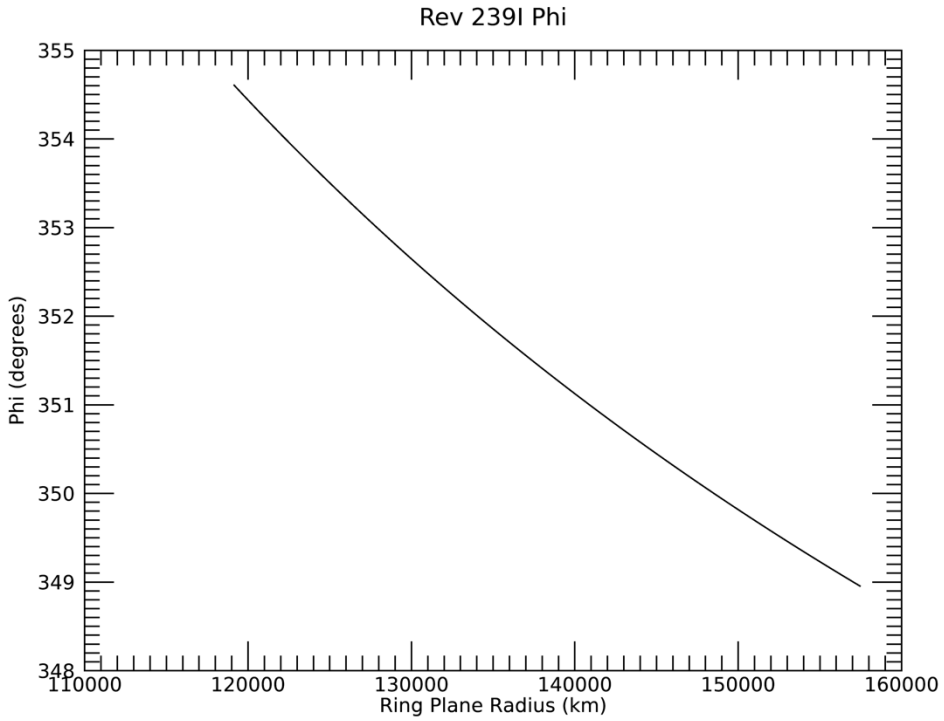
Rev 239I Phi
355
354
353
352
351
350
349
348
Phi (degrees)
110000
120000
130000
140000
150000
160000
Ring Plane Radius (km)

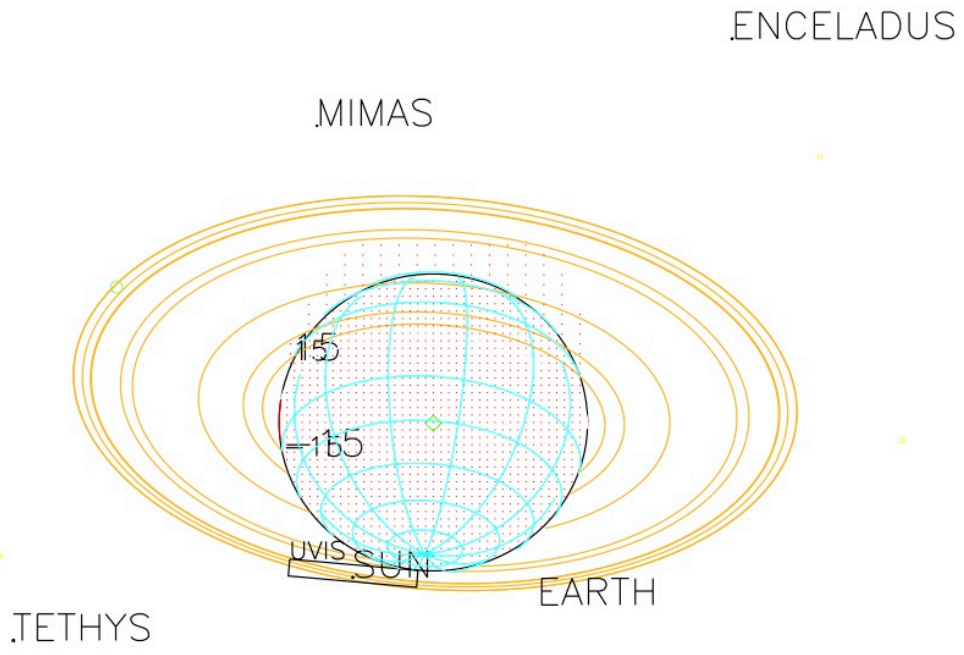

2016-221T22:21:00.000 784079.95 km
Target RA/dec: 71.34, 25.27
Subsolar lat/lon: 21.99, 141.42
Sub-s/c lat/lon: -26.18, -40.83

HYPERION

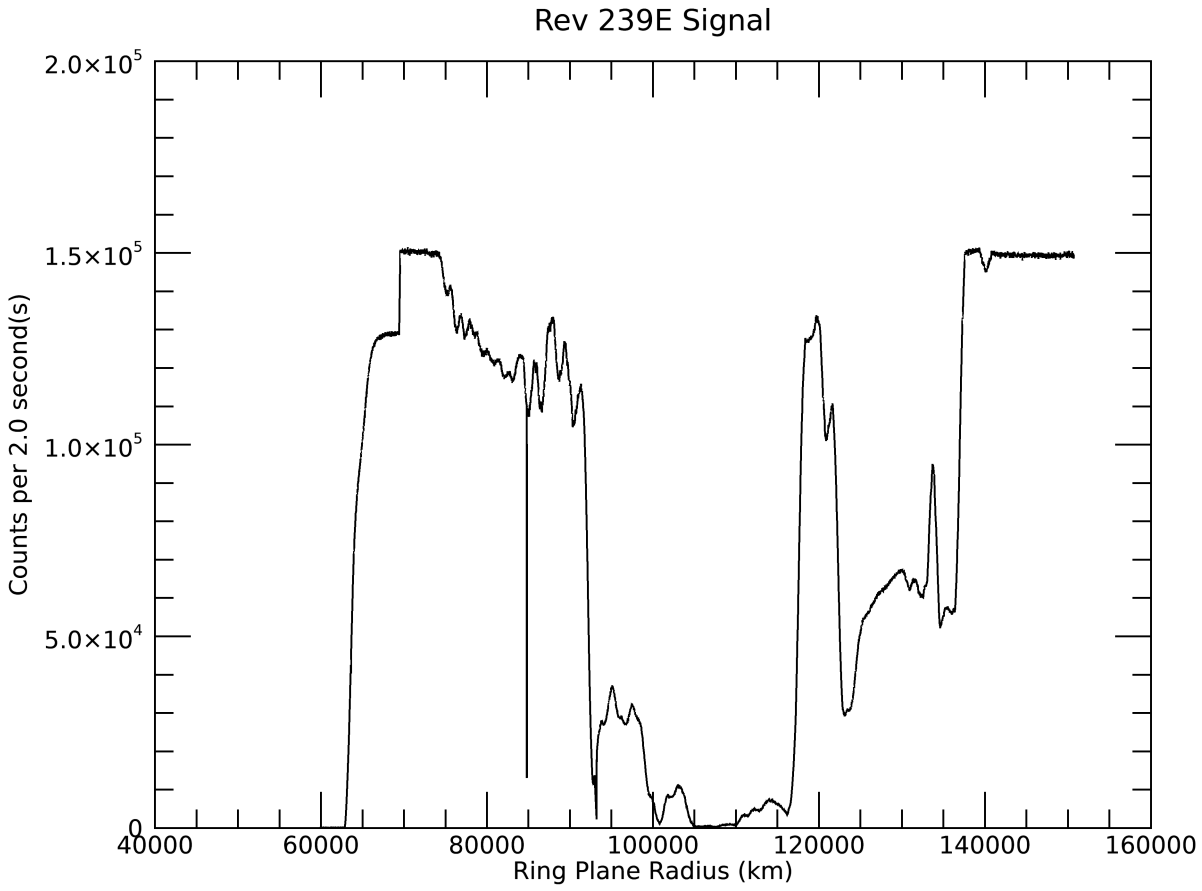
Rev 239E Signal
2.0×10^5
1.5×10^5
1.0×10^5
5.0×10^4
0
Counts per 2.0 second(s)
40000
60000
80000
100000
120000
140000
160000
Ring Plane Radius (km)

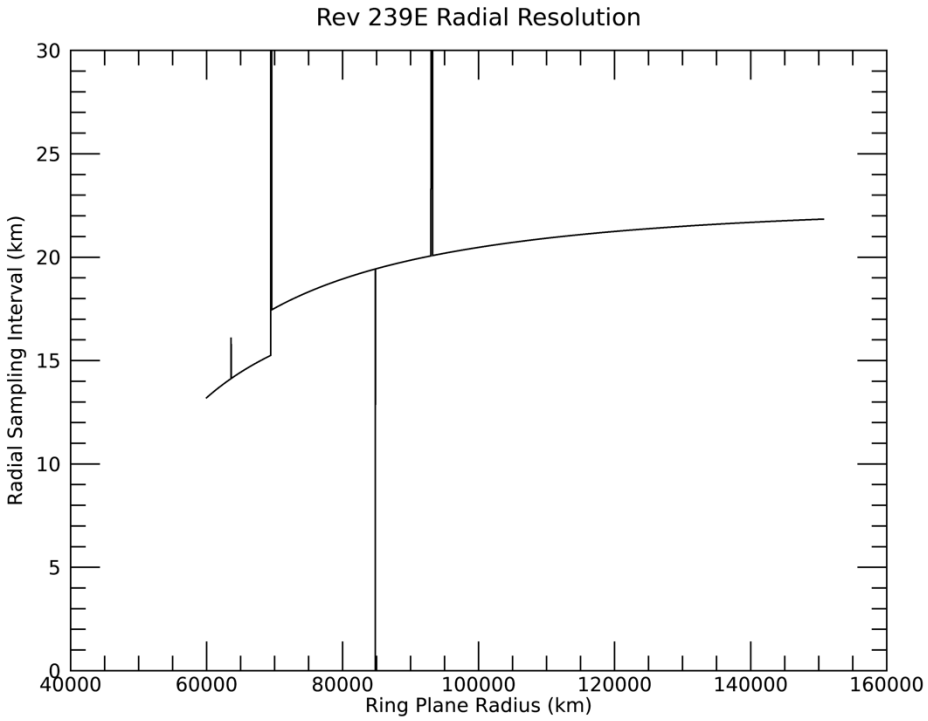
Rev 239E Radial Resolution
Radial Sampling Interval (km)
Ring Plane Radius (km)
0
5
10
15
20
25
30
40000
60000
80000
100000
120000
140000
160000

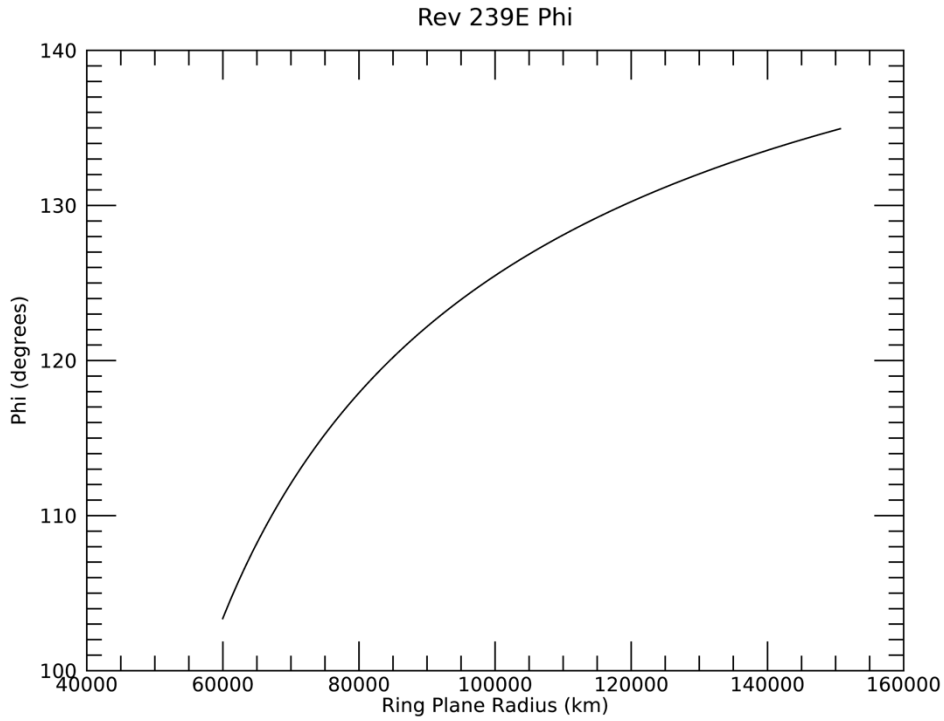
Rev 239E Phi
Phi (degrees)
Ring Plane Radius (km)
100
110
120
130
140
40000
60000
80000
100000
120000
140000
160000

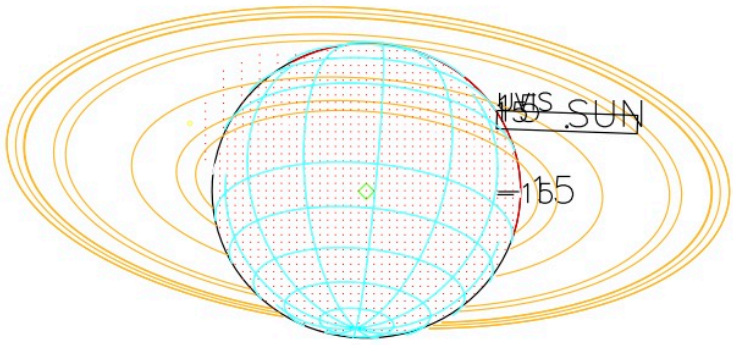

2016-222T03:42:00.000 852673.91 km

Target RA/dec: 79.45, 19.51

Subsolar lat/lon: 21.99, -39.31

Sub-s/c lat/lon: -20.58, 146.41

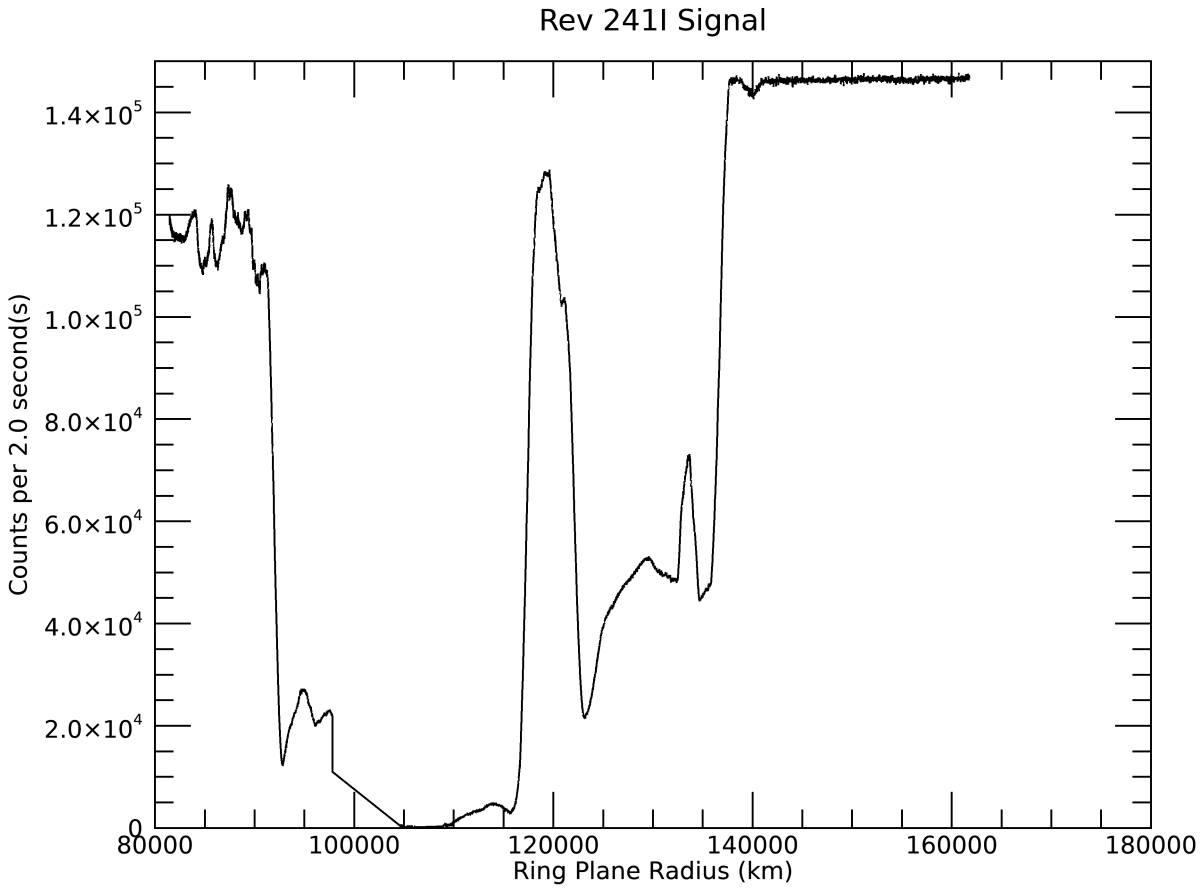
Rev 241I Signal
Counts per 2.0 second(s)
1.4×10^5
1.2×10^5
1.0×10^5
8.0×10^4
6.0×10^4
4.0×10^4
2.0×10^4
0
80000
100000
120000
140000
160000
180000
Ring Plane Radius (km)

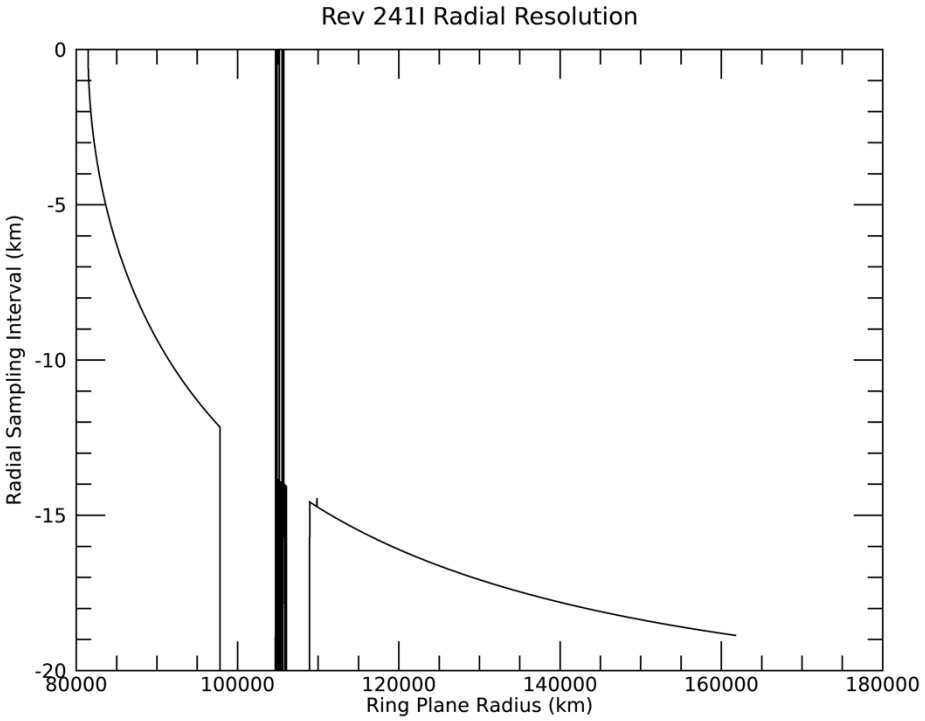
Rev 241I Radial Resolution
Radial Sampling Interval (km)
0
-5
-10
-15
-20
80000
100000
120000
140000
160000
180000
Ring Plane Radius (km)

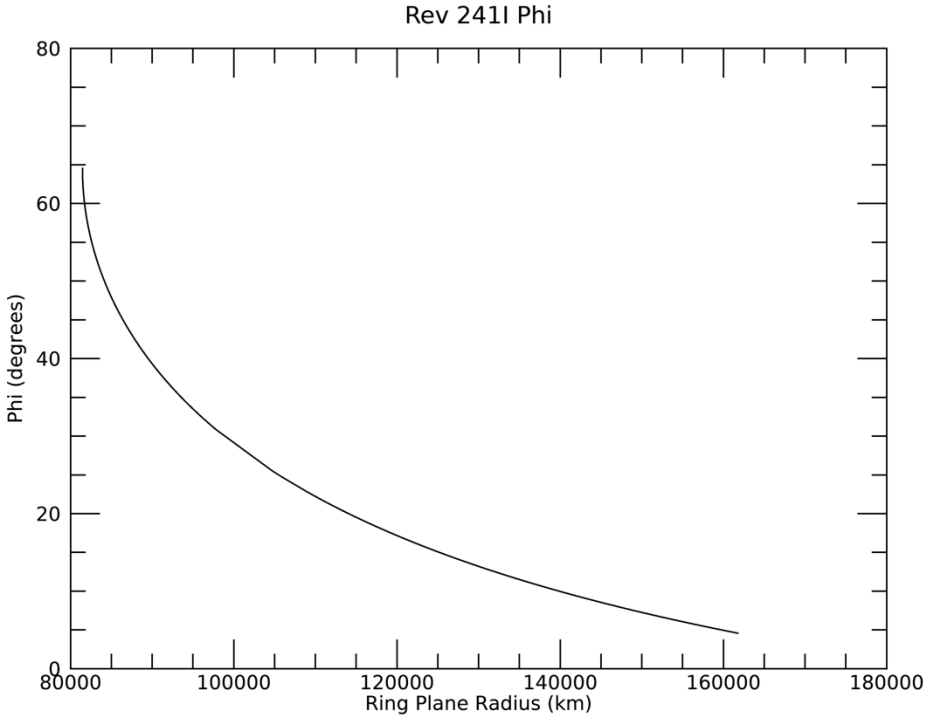
Rev 241I Phi
Phi (degrees)
80
60
40
20
0
80000
100000
120000
140000
160000
180000
Ring Plane Radius (km)

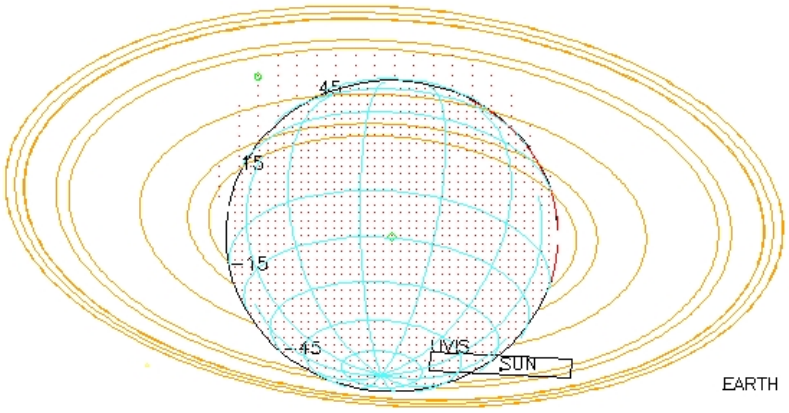

MIMAS

EARTH

DIONE

ENCELADUS

RHEA

2016-245T19:30:00.000 798996.92 km
Target RA/dec: 77.59, 24.57
Subsolar lat/lon: 22.04, −140.55
Sub-s/c lat/lon: −25.18, 42.89

TITAN

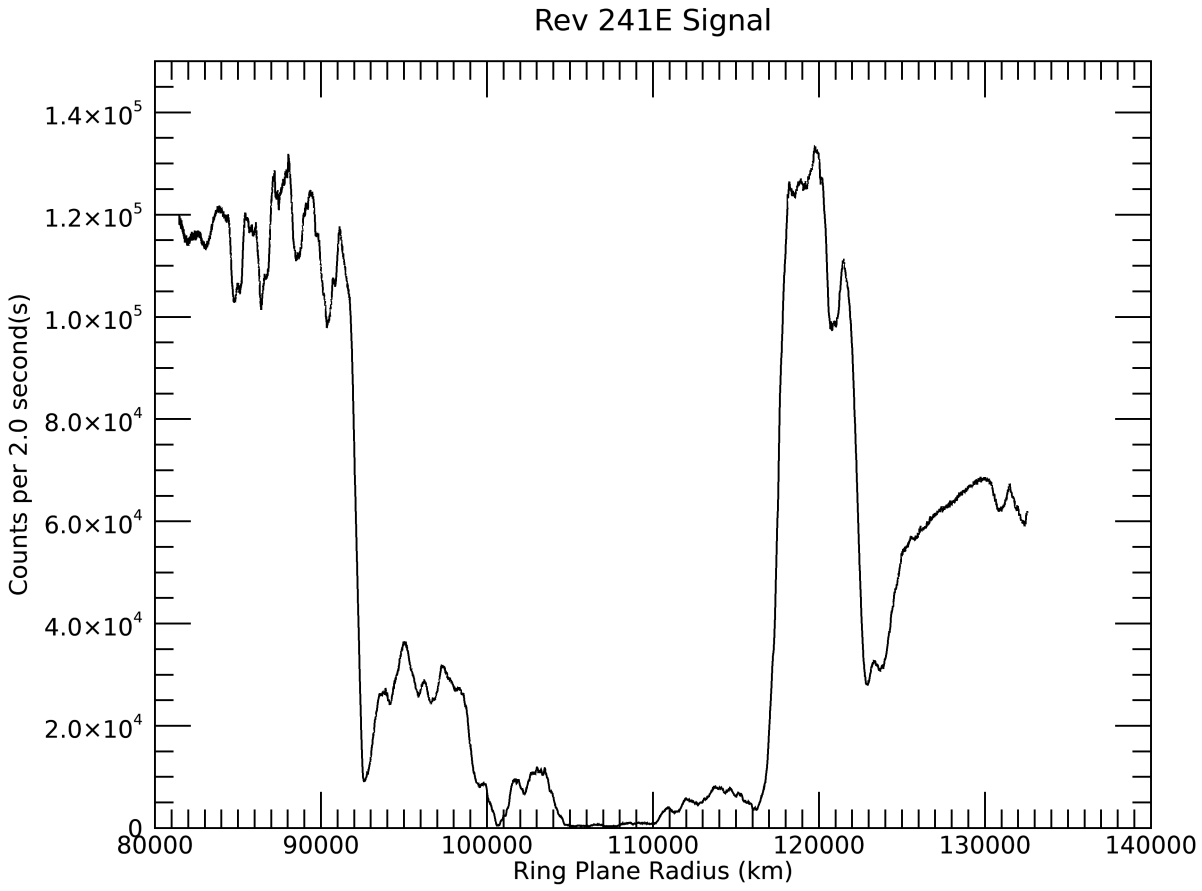
Rev 241E Signal
Counts per 2.0 second(s)
1.4×10^5
1.2×10^5
1.0×10^5
8.0×10^4
6.0×10^4
4.0×10^4
2.0×10^4
0
80000
90000
100000
110000
120000
130000
140000
Ring Plane Radius (km)

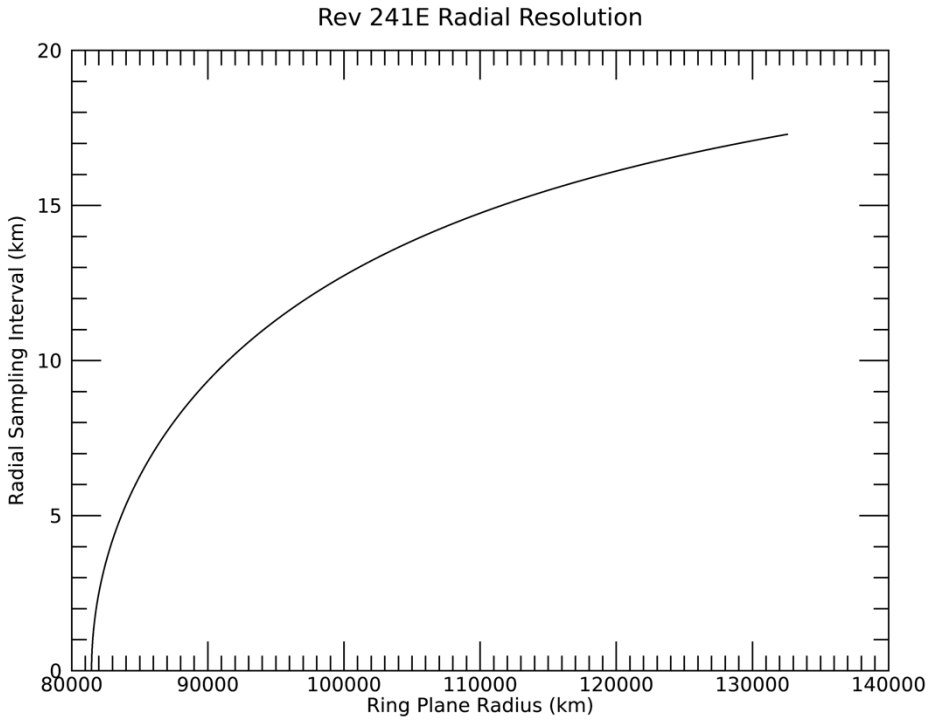
Rev 241E Radial Resolution
Radial Sampling Interval (km)
0
5
10
15
20
80000
90000
100000
110000
120000
130000
140000
Ring Plane Radius (km)

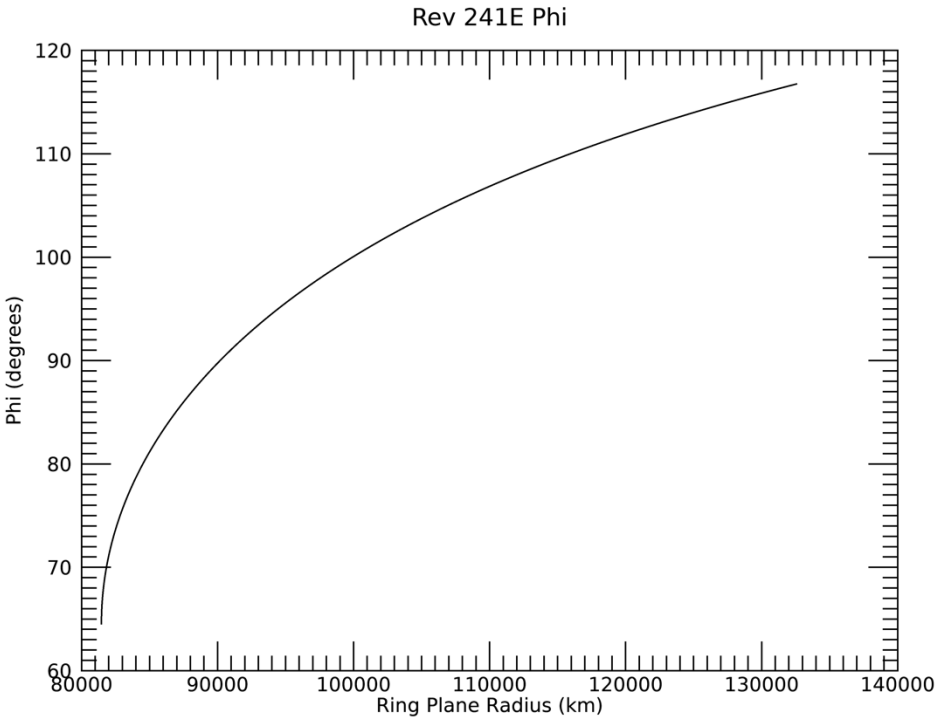
Rev 241E Phi
Phi (degrees)
60
70
80
90
100
110
120
80000
90000
100000
110000
120000
130000
140000
Ring Plane Radius (km)

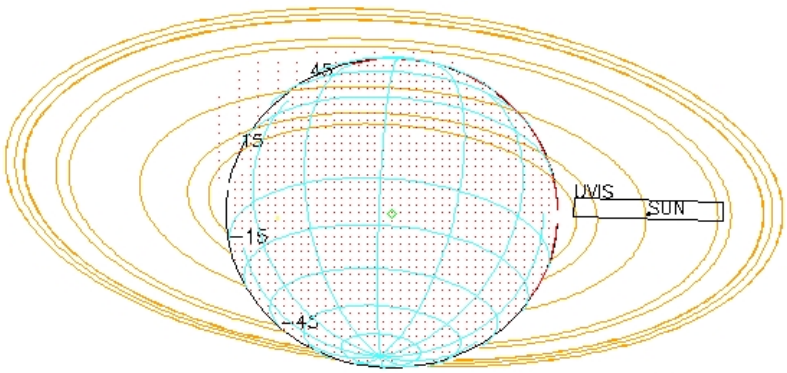

EARTH

TI

MIMAS

ENCELADUS

RHEA

TITAN

2016-245T22:30:00.000 840530.04 km
Target RA/dec: 81.37, 21.28
Subsolar lat/lon: 22.04, 118.11
Sub-s/c lat/lon: −22.01, −54.83

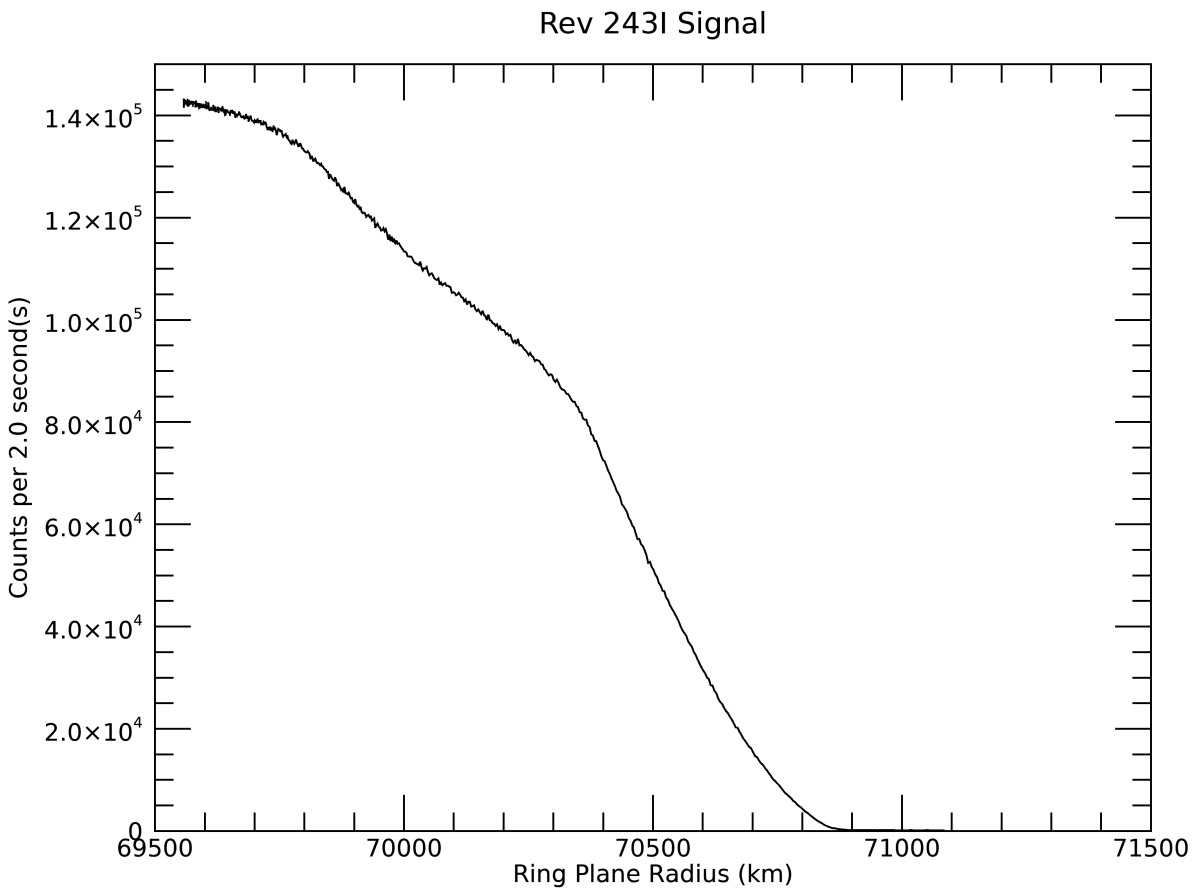
Rev 243I Signal
Counts per 2.0 second(s)
1.4×10^5
1.2×10^5
1.0×10^5
8.0×10^4
6.0×10^4
4.0×10^4
2.0×10^4
0
69500
70000
70500
71000
71500
Ring Plane Radius (km)

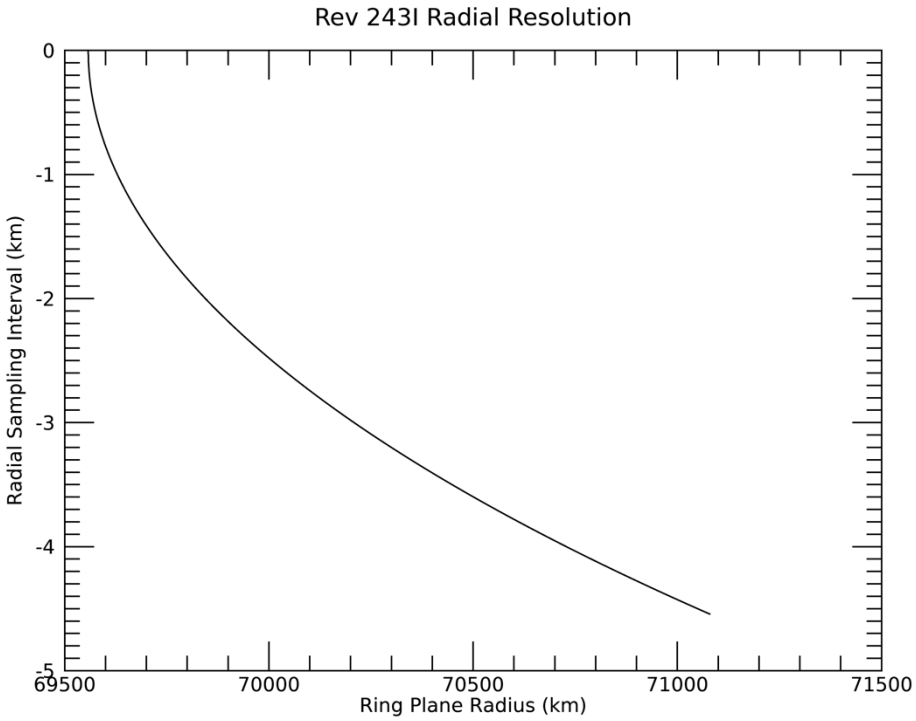
Rev 243I Radial Resolution
Radial Sampling Interval (km)
0
-1
-2
-3
-4
-5
69500
70000
70500
71000
71500
Ring Plane Radius (km)

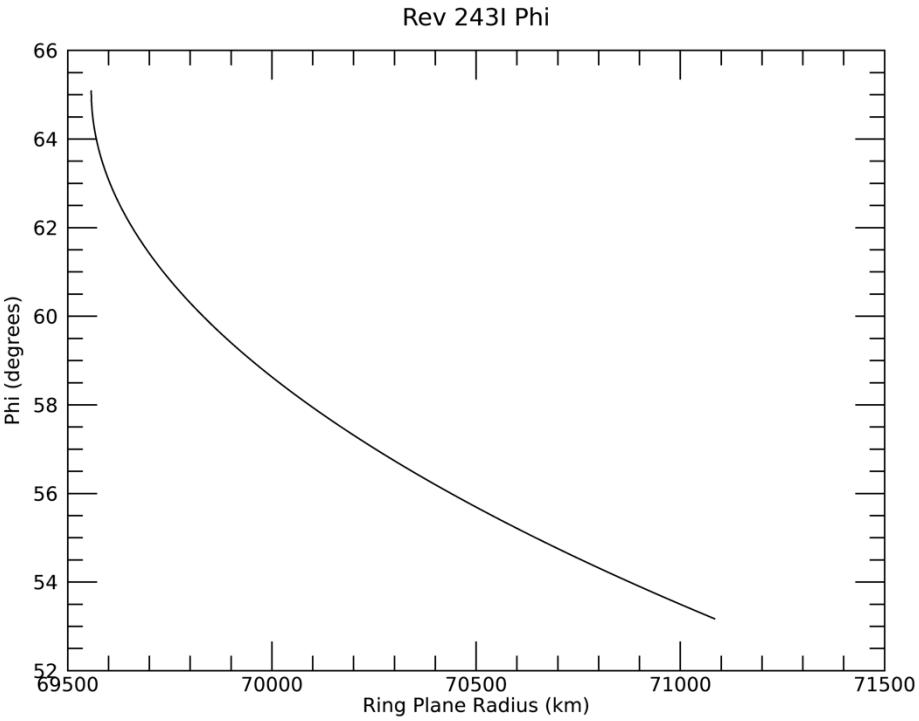
Rev 243I Phi
Phi (degrees)
66
64
62
60
58
56
54
52
69500
70000
70500
71000
71500
Ring Plane Radius (km)

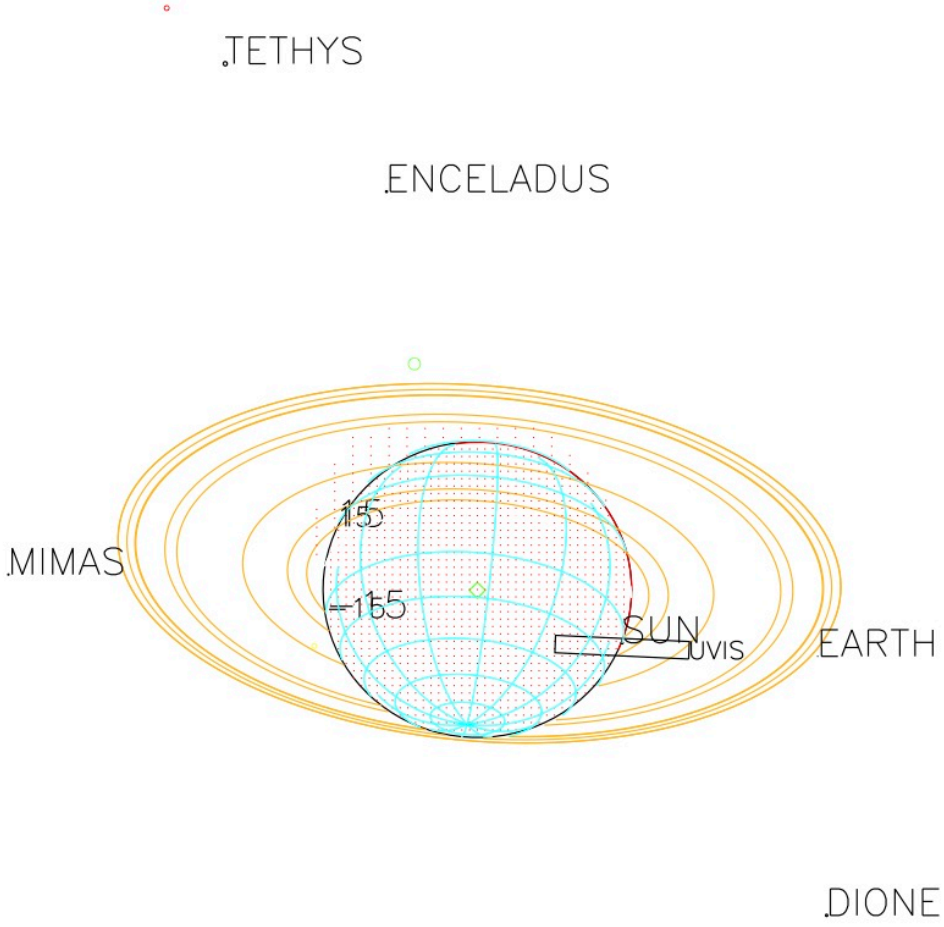

2016−269T19:31:00.000 815037.88 km

Target RA/dec: 79.61, 22.68

Subsolar lat/lon: 22.08, −159.36

Sub−s/c lat/lon: −23.37, 25.20

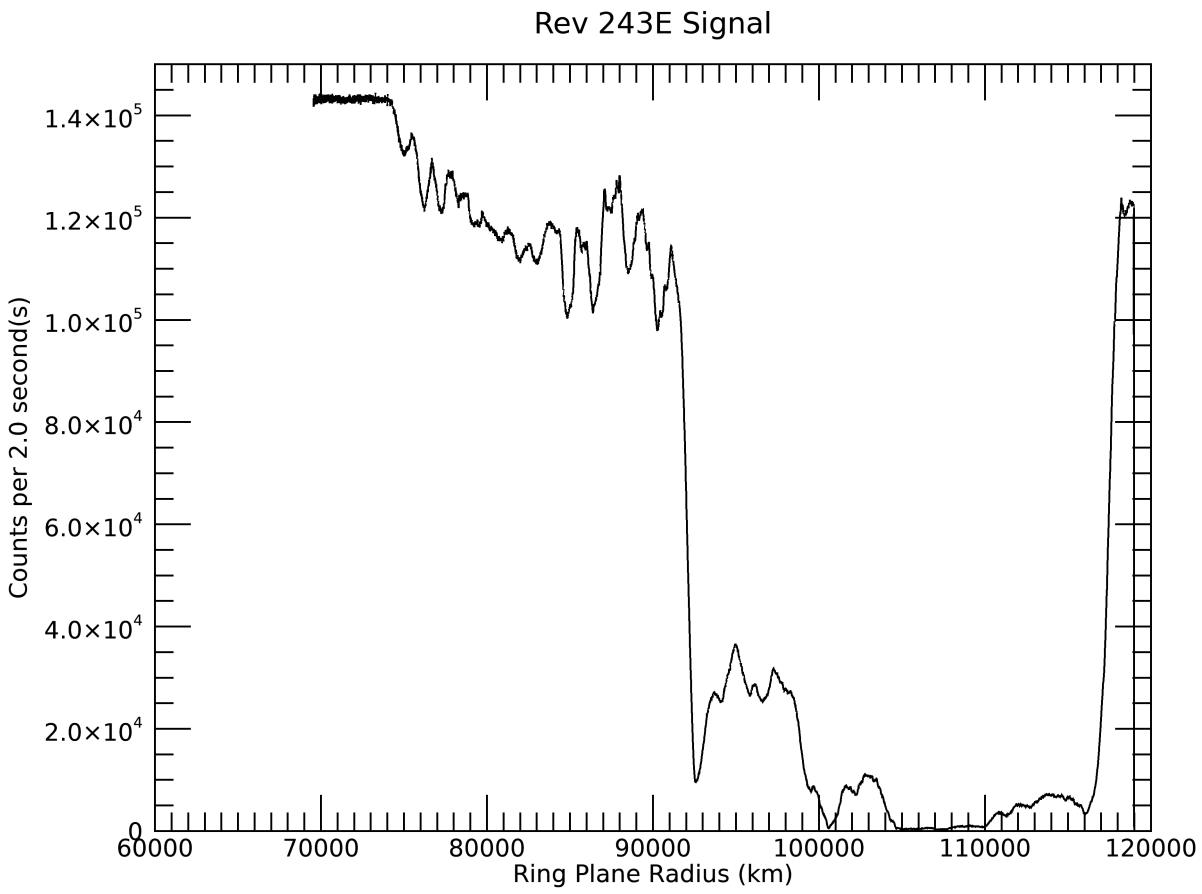
Rev 243E Signal
Counts per 2.0 second(s)
1.4×10^5
1.2×10^5
1.0×10^5
8.0×10^4
6.0×10^4
4.0×10^4
2.0×10^4
0
60000
70000
80000
90000
100000
110000
120000
Ring Plane Radius (km)

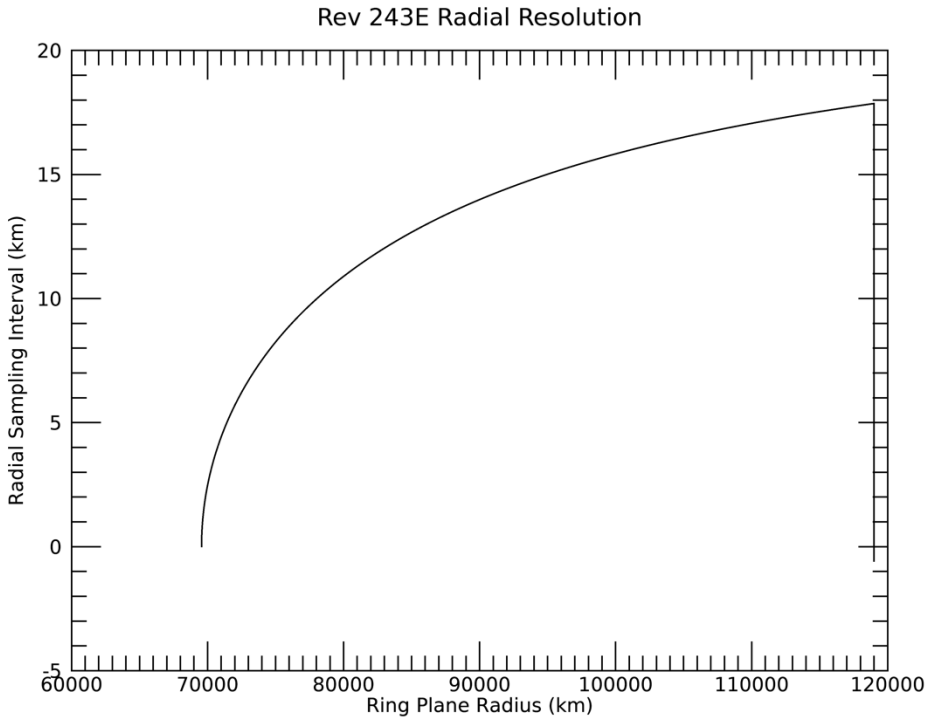
Rev 243E Radial Resolution
Radial Sampling Interval (km)
20
15
10
5
0
-5
60000
70000
80000
90000
100000
110000
120000
Ring Plane Radius (km)

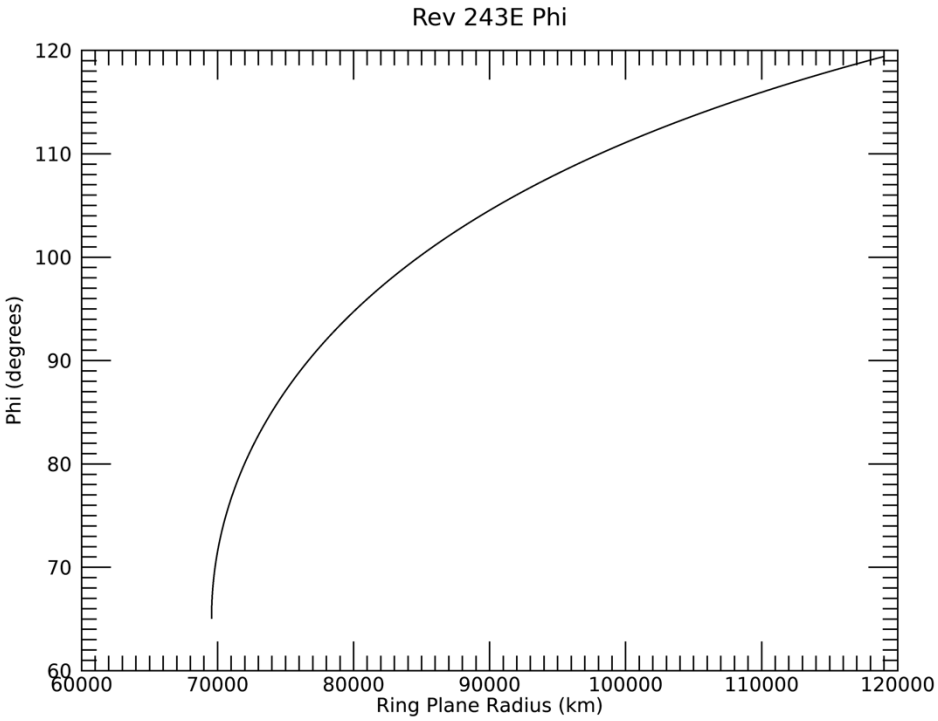
Rev 243E Phi
Phi (degrees)
120
110
100
90
80
70
60
60000
70000
80000
90000
100000
110000
120000
Ring Plane Radius (km)

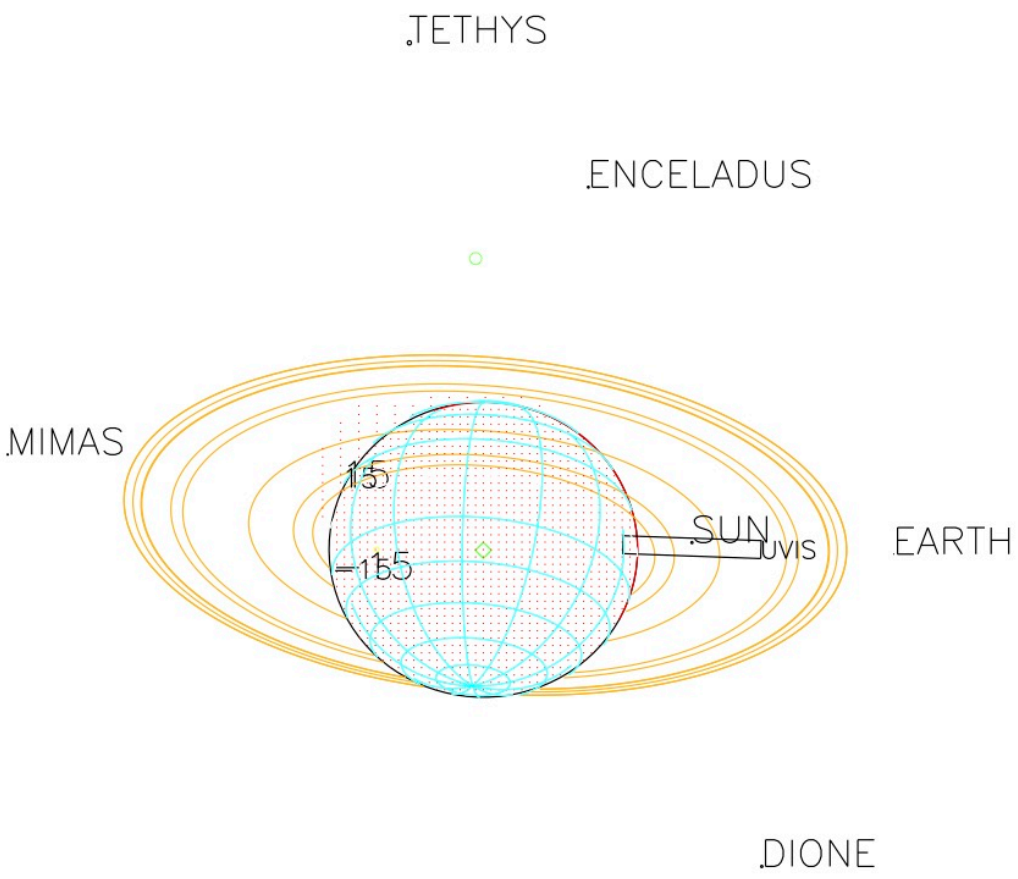

2016-269T20:56:00.000 834890.62 km

Target RA/dec: 81.34, 21.15

Subsolar lat/lon: 22.08, 152.79

Sub-s/c lat/lon: -21.90, -21.00

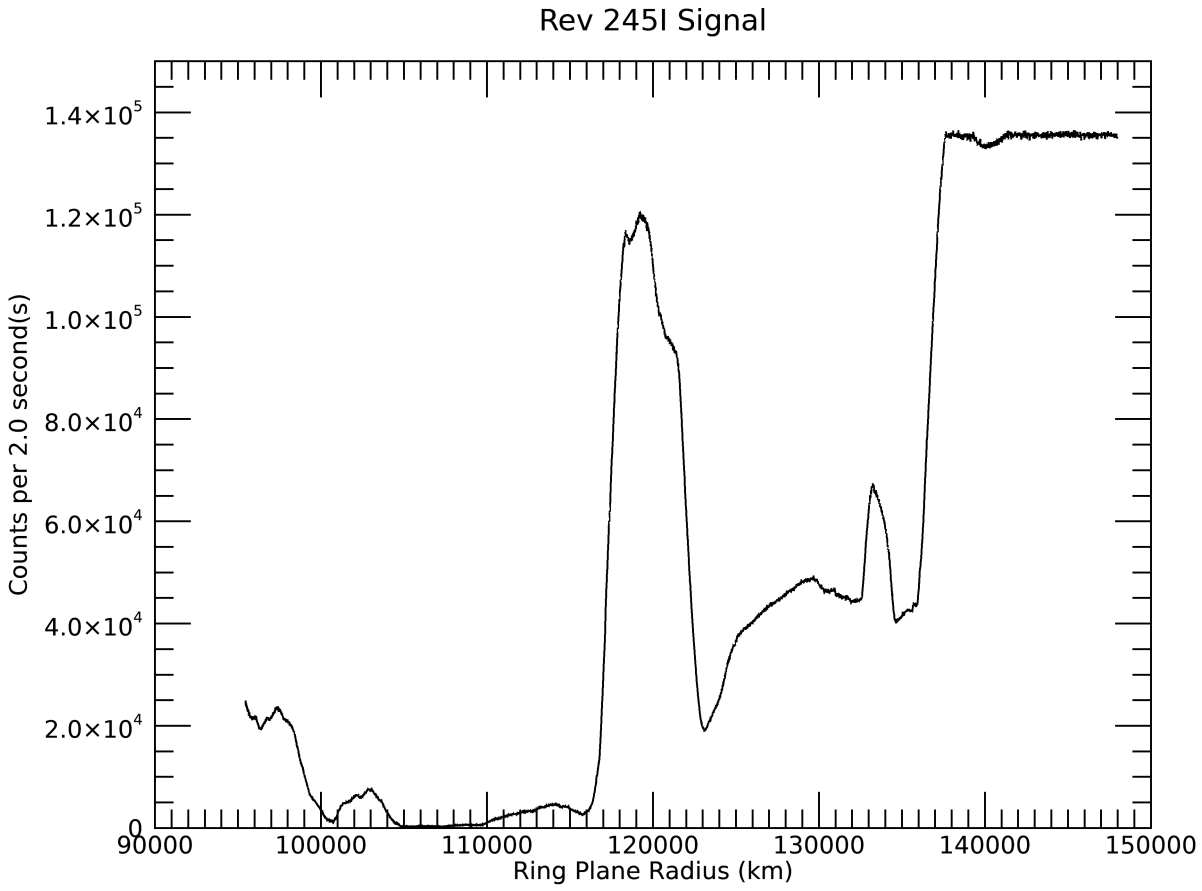
Rev 245I Signal
Counts per 2.0 second(s)
1.4×10^5
1.2×10^5
1.0×10^5
8.0×10^4
6.0×10^4
4.0×10^4
2.0×10^4
0
90000
100000
110000
120000
130000
140000
150000
Ring Plane Radius (km)

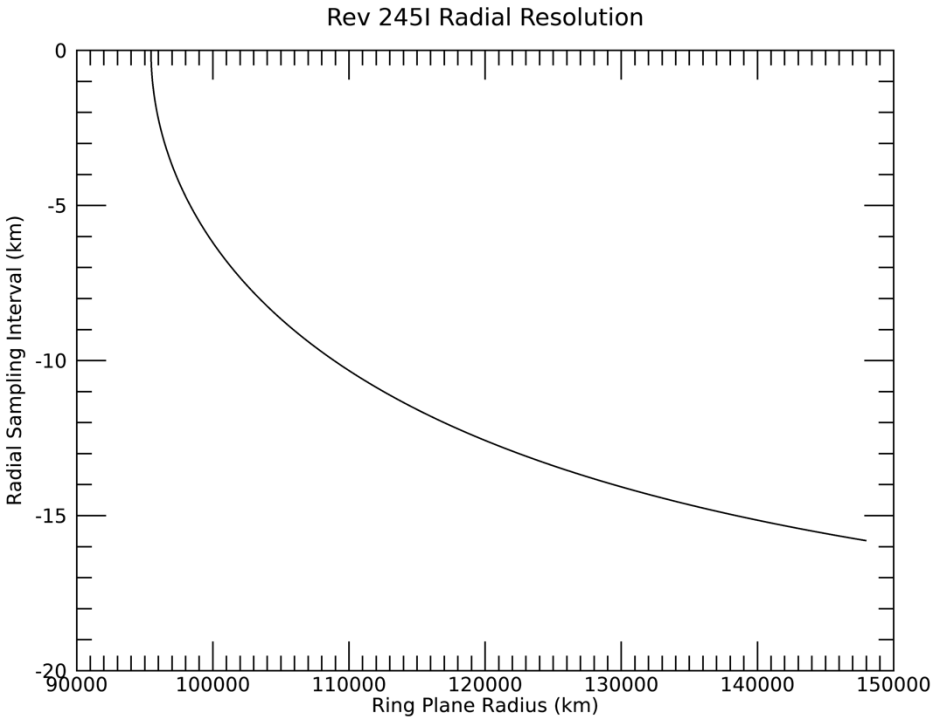
Rev 245I Radial Resolution
Radial Sampling Interval (km)
0
-5
-10
-15
-20
90000
100000
110000
120000
130000
140000
150000
Ring Plane Radius (km)

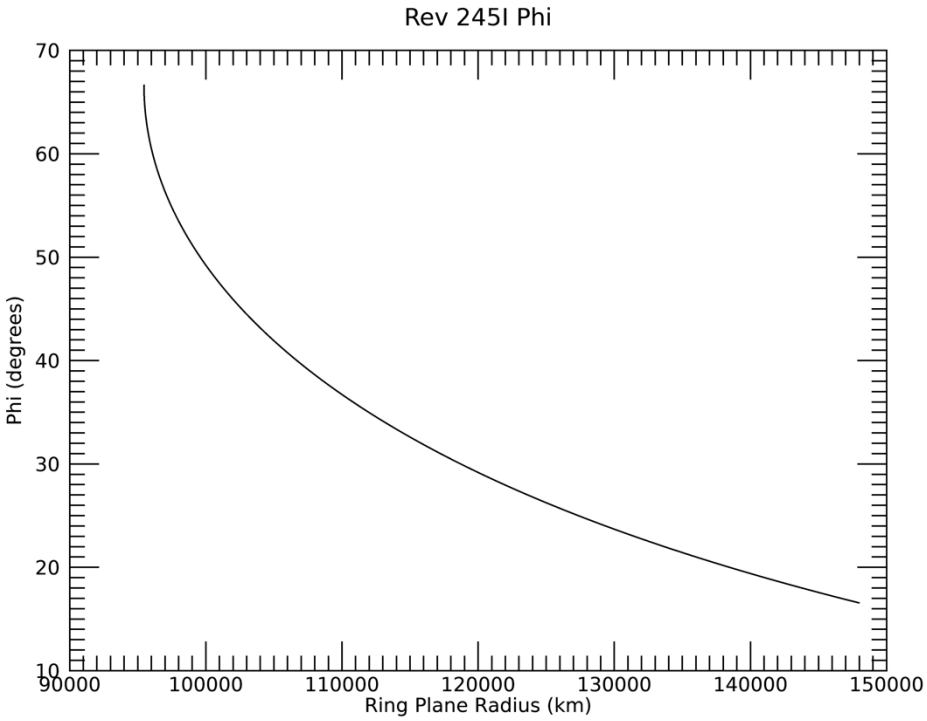
Rev 245I Phi
Phi (degrees)
70
60
50
40
30
20
10
90000
100000
110000
120000
130000
140000
150000
Ring Plane Radius (km)

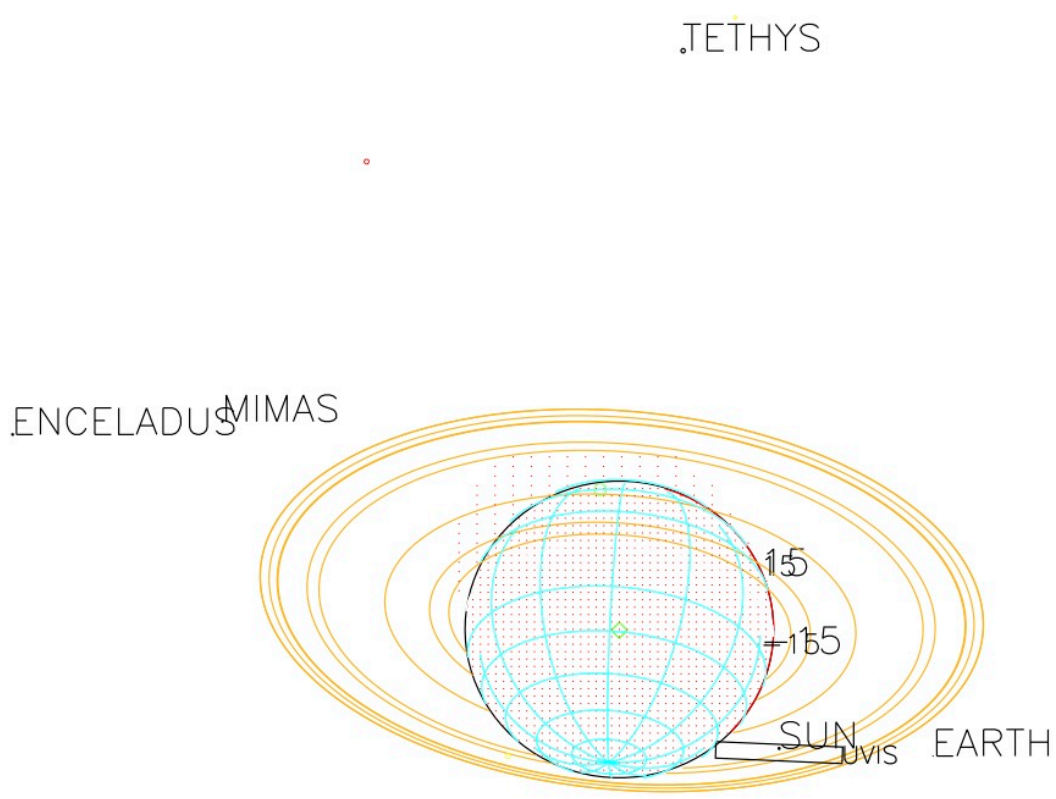

2016-288T18:51:00.000 769058.87 km

Target RA/dec: 80.94, 24.69

Subsolar lat/lon: 22.11, -61.28

Sub-s/c lat/lon: -25.08, 124.21

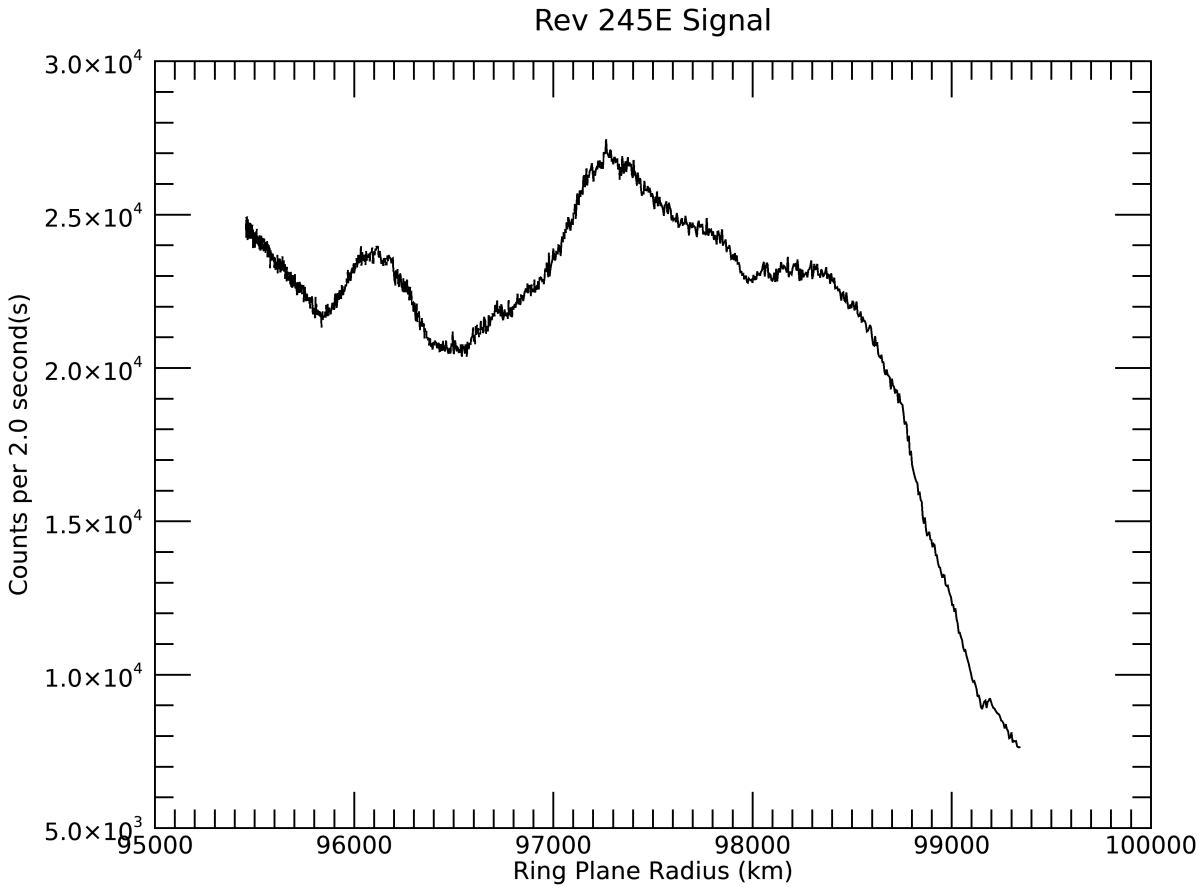
Rev 245E Signal
3.0×10^4
2.5×10^4
2.0×10^4
1.5×10^4
1.0×10^4
5.0×10^3
Counts per 2.0 second(s)
95000
96000
97000
98000
99000
100000
Ring Plane Radius (km)

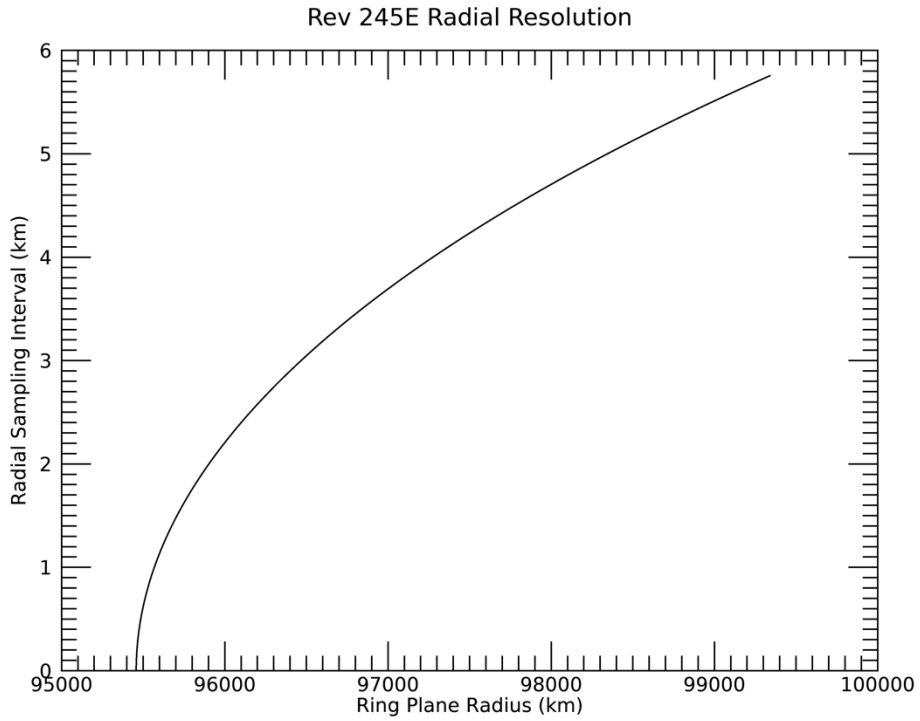
Rev 245E Radial Resolution
Radial Sampling Interval (km)
0
1
2
3
4
5
6
95000
96000
97000
98000
99000
100000
Ring Plane Radius (km)

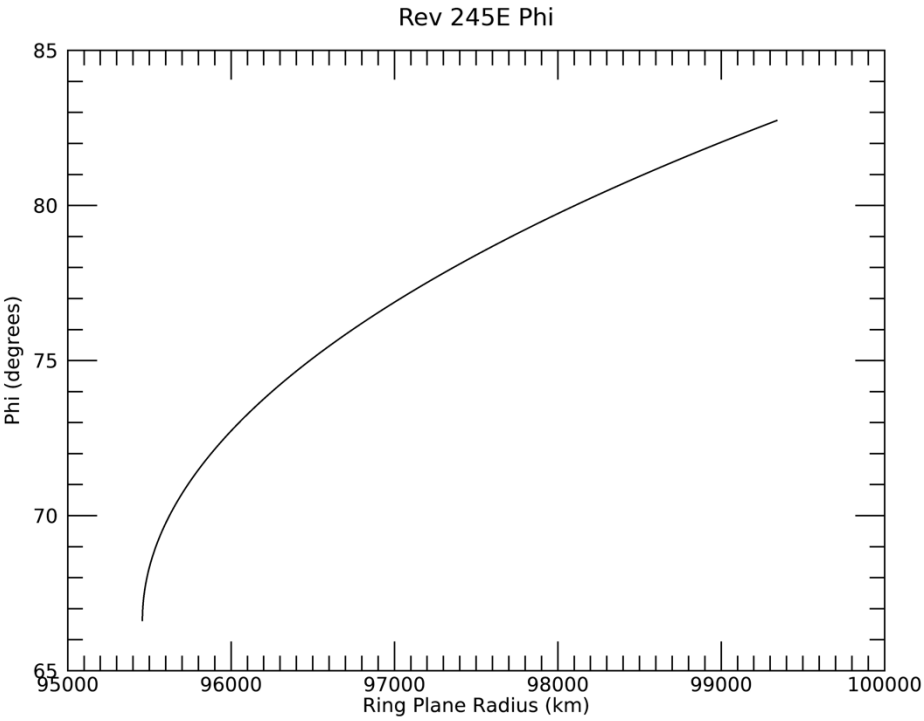
Rev 245E Phi
Phi (degrees)
65
70
75
80
85
95000
96000
97000
98000
99000
100000
Ring Plane Radius (km)

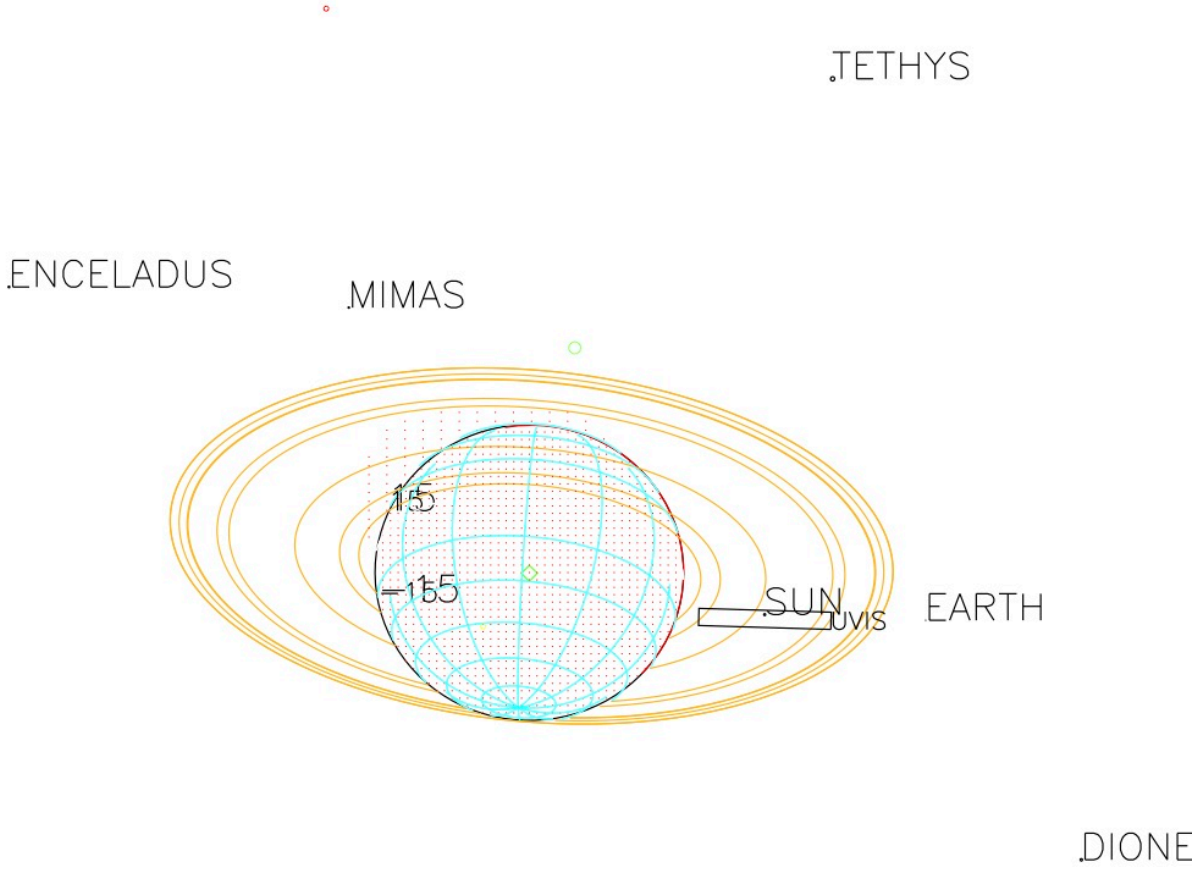

2016−288T20:43:00.000 798793.97 km

Target RA/dec: 83.02, 22.58

Subsolar lat/lon: 22.11, −124.34

Sub−s/c lat/lon: −23.05, 63.10

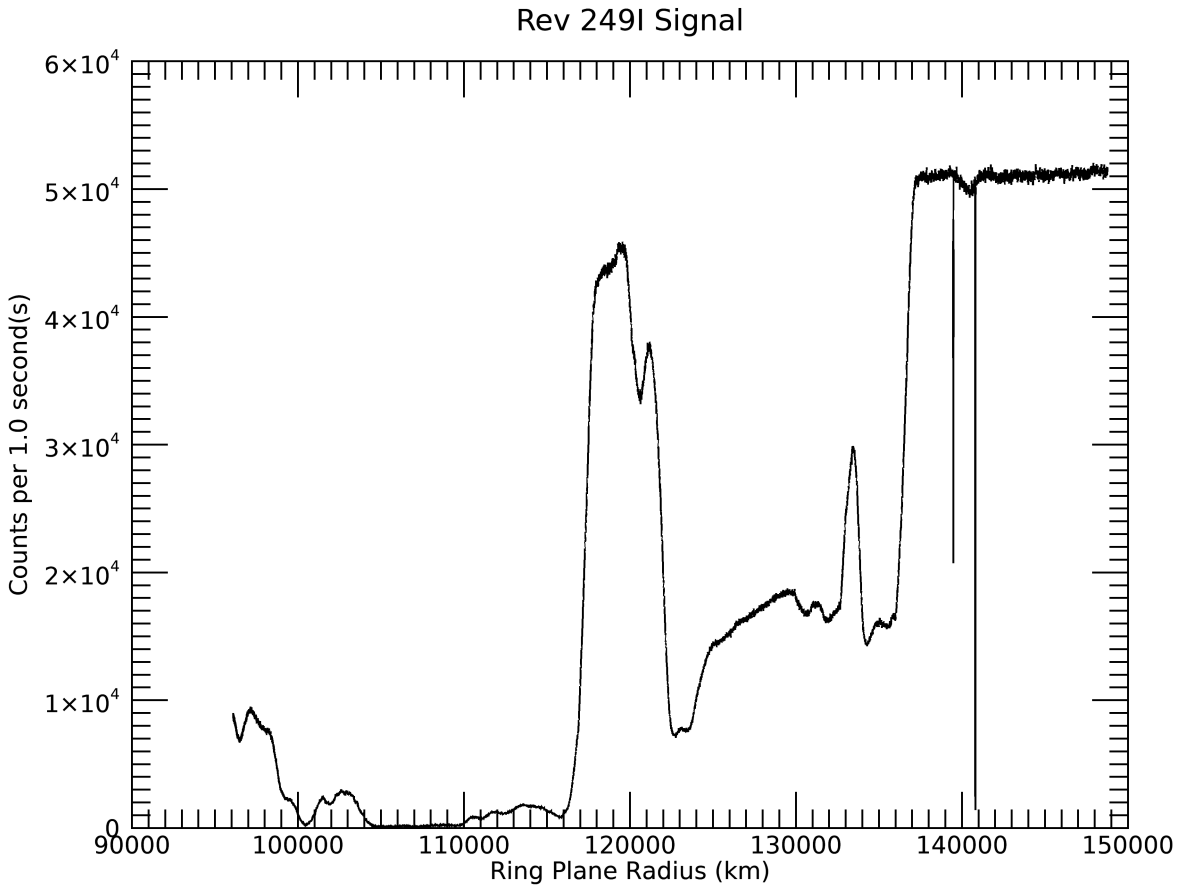
Rev 249I Signal
6×10^4
5×10^4
4×10^4
3×10^4
2×10^4
1×10^4
0
Counts per 1.0 second(s)
90000
100000
110000
120000
130000
140000
150000
Ring Plane Radius (km)

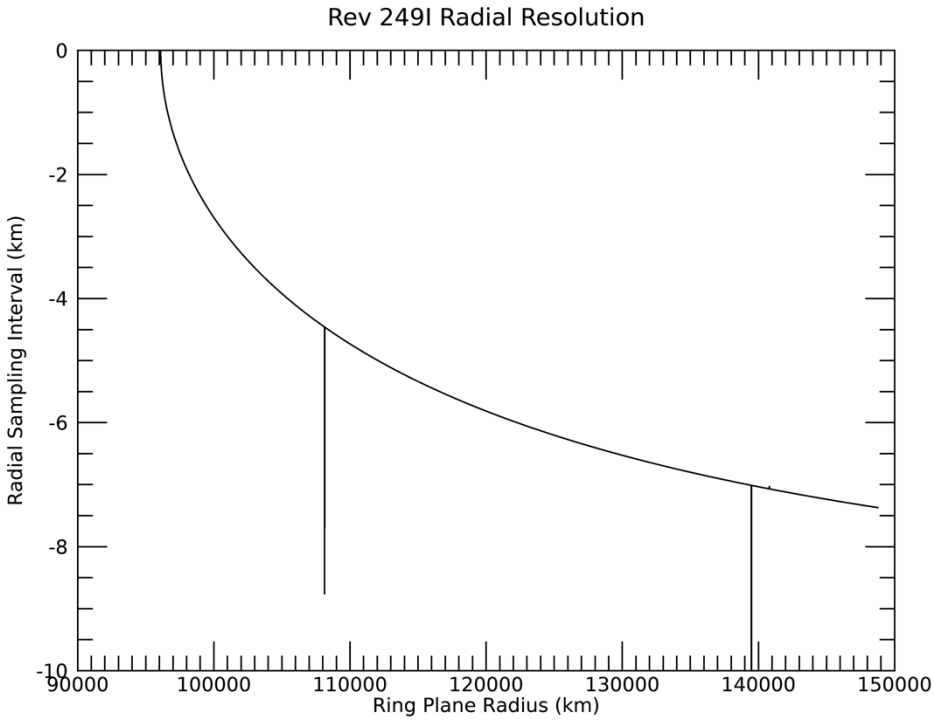
Rev 249I Radial Resolution
Radial Sampling Interval (km)
0
-2
-4
-6
-8
-10
90000
100000
110000
120000
130000
140000
150000
Ring Plane Radius (km)

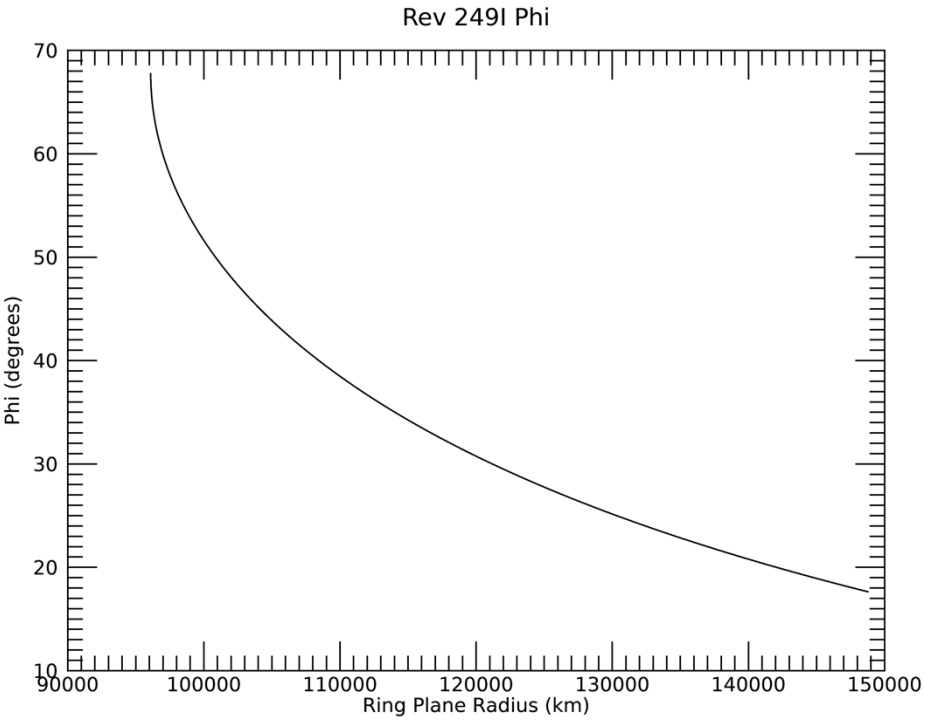
Rev 249I Phi
Phi (degrees)
70
60
50
40
30
20
10
90000
100000
110000
120000
130000
140000
150000
Ring Plane Radius (km)

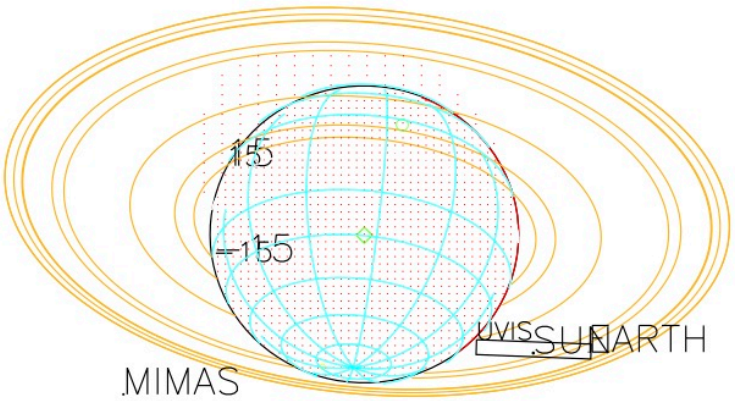

DIONE

MIMAS

TETHY

ENCELADUS

TITAN

2016-325T06:47:00.000 694253.79 km

Target RA/dec: 82.97, 25.20

Subsolar lat/lon: 22.16, -131.78

Sub-s/c lat/lon: -25.43, 54.64

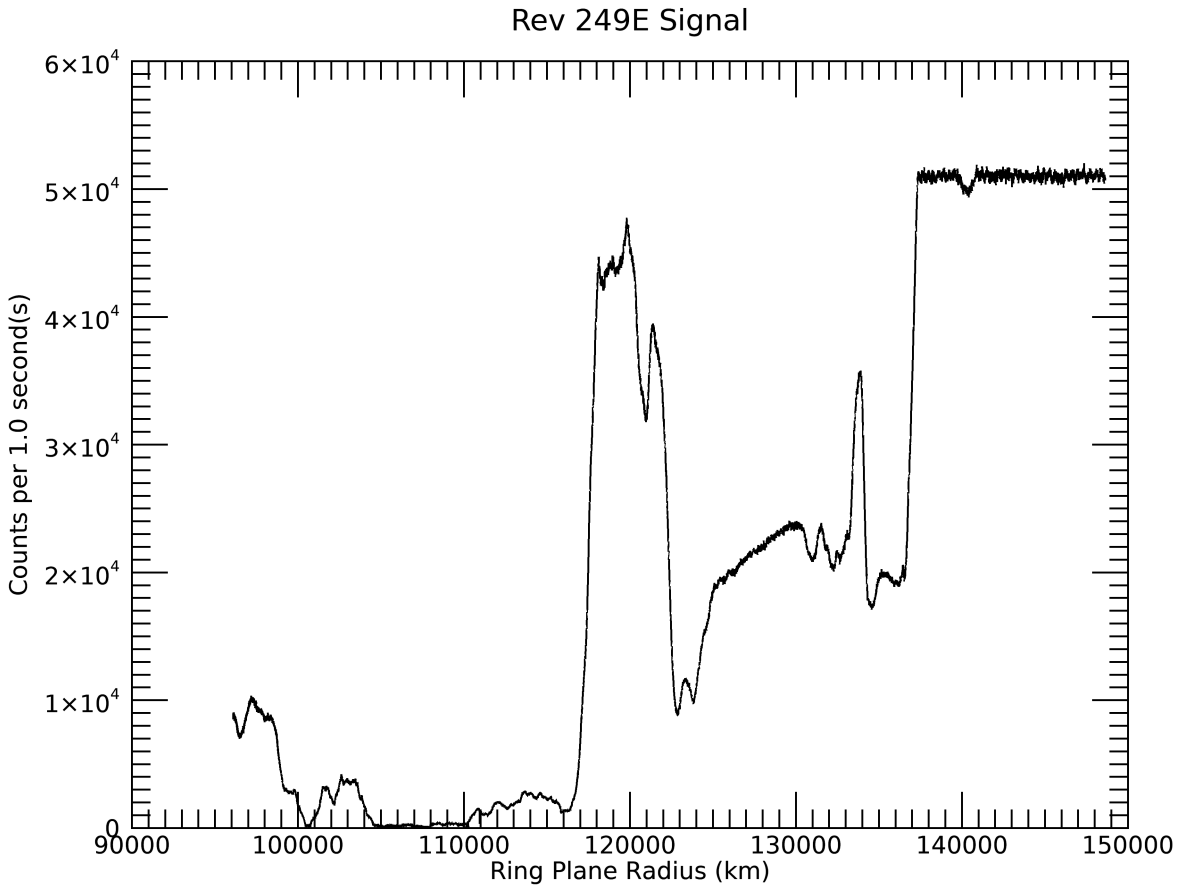
Rev 249E Signal
6×10^4
5×10^4
4×10^4
3×10^4
2×10^4
1×10^4
0
Counts per 1.0 second(s)
90000
100000
110000
120000
130000
140000
150000
Ring Plane Radius (km)

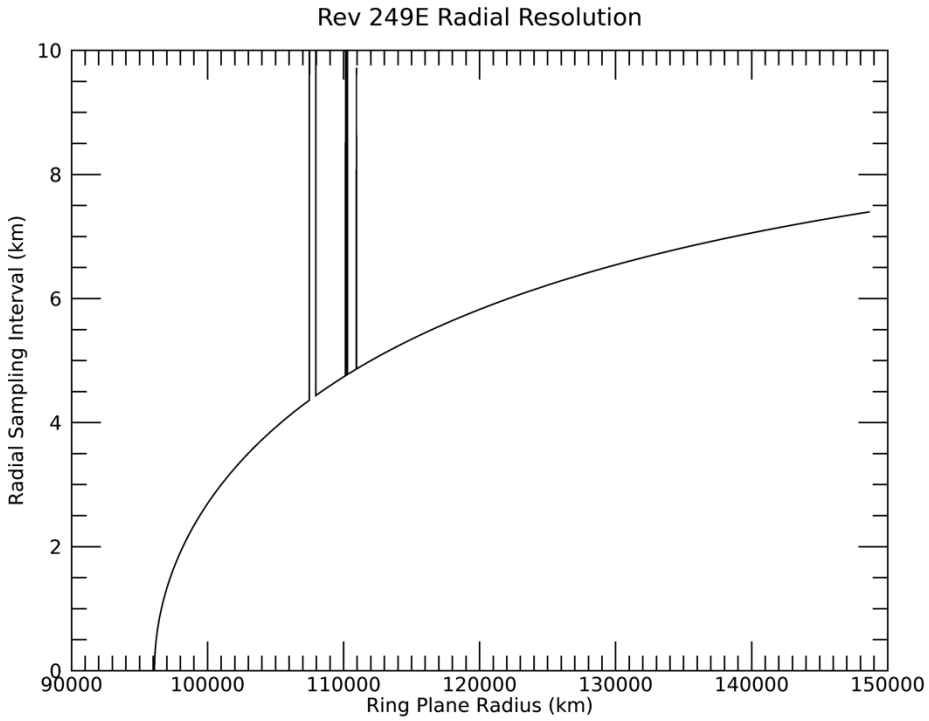
Rev 249E Radial Resolution
Radial Sampling Interval (km)
0
2
4
6
8
10
90000
100000
110000
120000
130000
140000
150000
Ring Plane Radius (km)

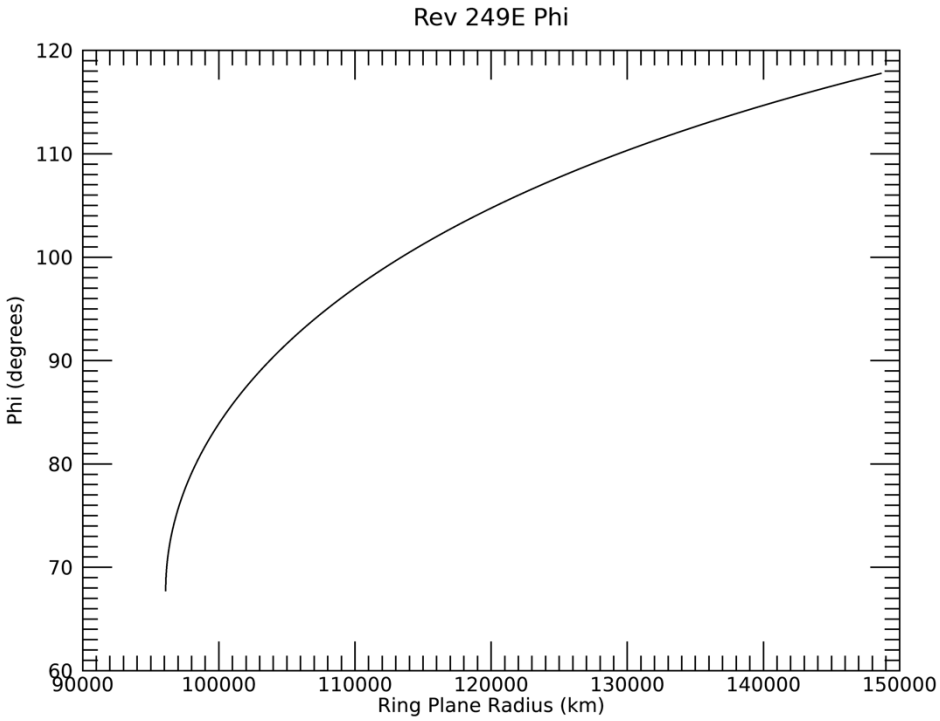
Rev 249E Phi
Phi (degrees)
60
70
80
90
100
110
120
90000
100000
110000
120000
130000
140000
150000
Ring Plane Radius (km)

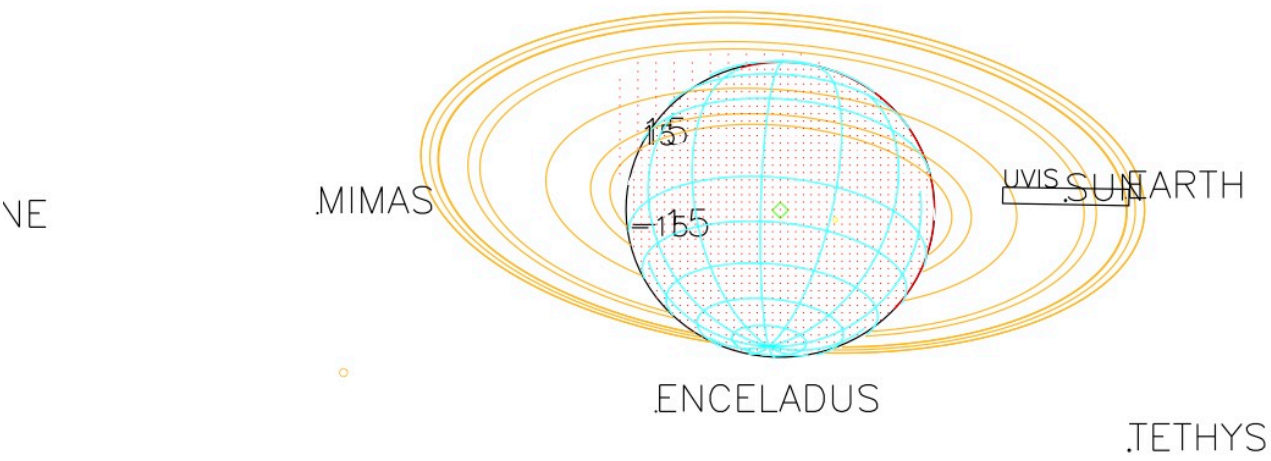

2016−325T10:01:00.000 756115.77 km

Target RA/dec: 86.17, 21.42

Subsolar lat/lon: 22.16, 119.00

Sub−s/c lat/lon: −21.83, −51.66

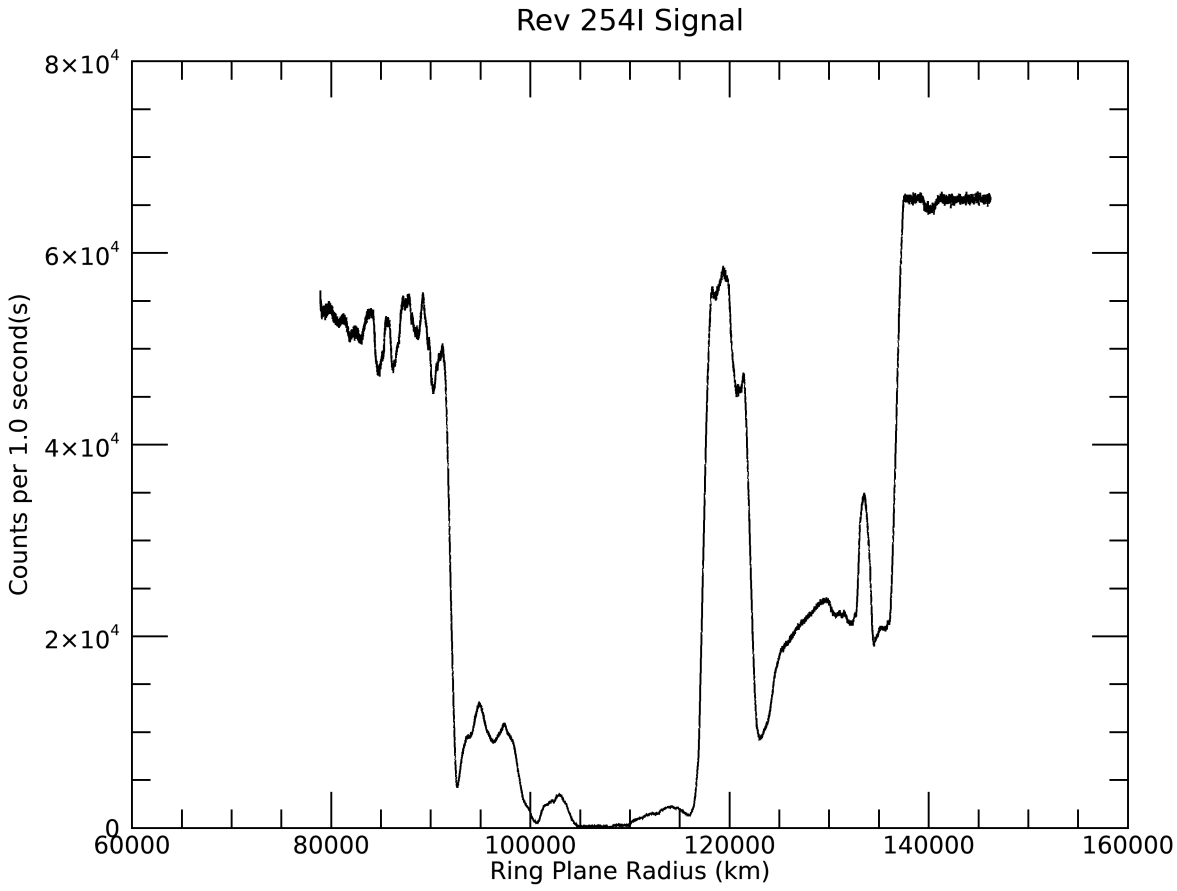
Rev 254I Signal
8×10^4
6×10^4
4×10^4
2×10^4
0
Counts per 1.0 second(s)
60000
80000
100000
120000
140000
160000
Ring Plane Radius (km)

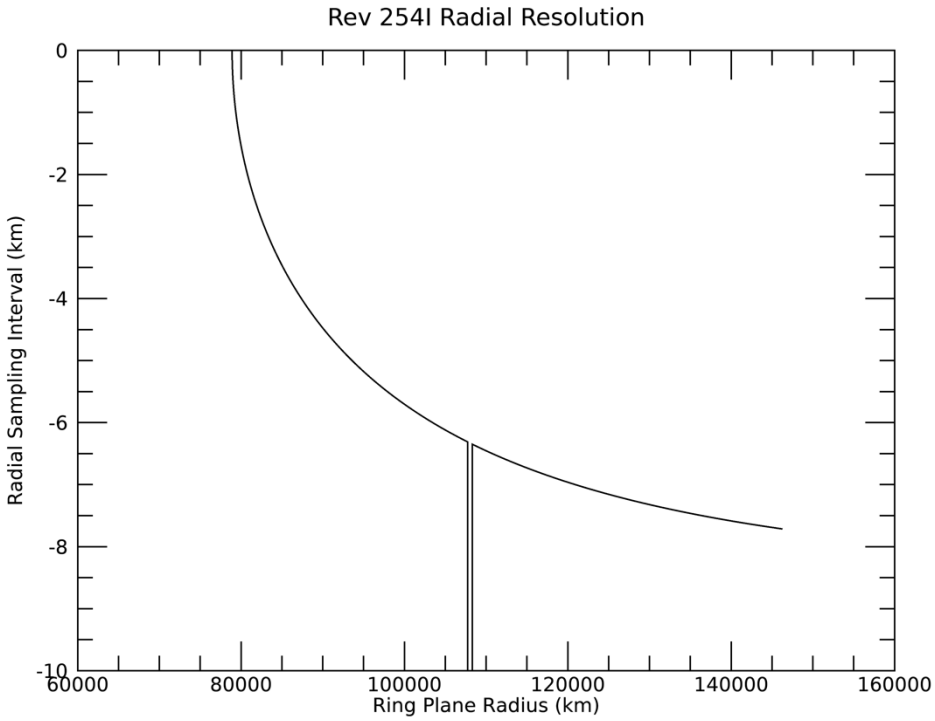
Rev 254I Radial Resolution
Radial Sampling Interval (km)
0
-2
-4
-6
-8
-10
60000
80000
100000
120000
140000
160000
Ring Plane Radius (km)

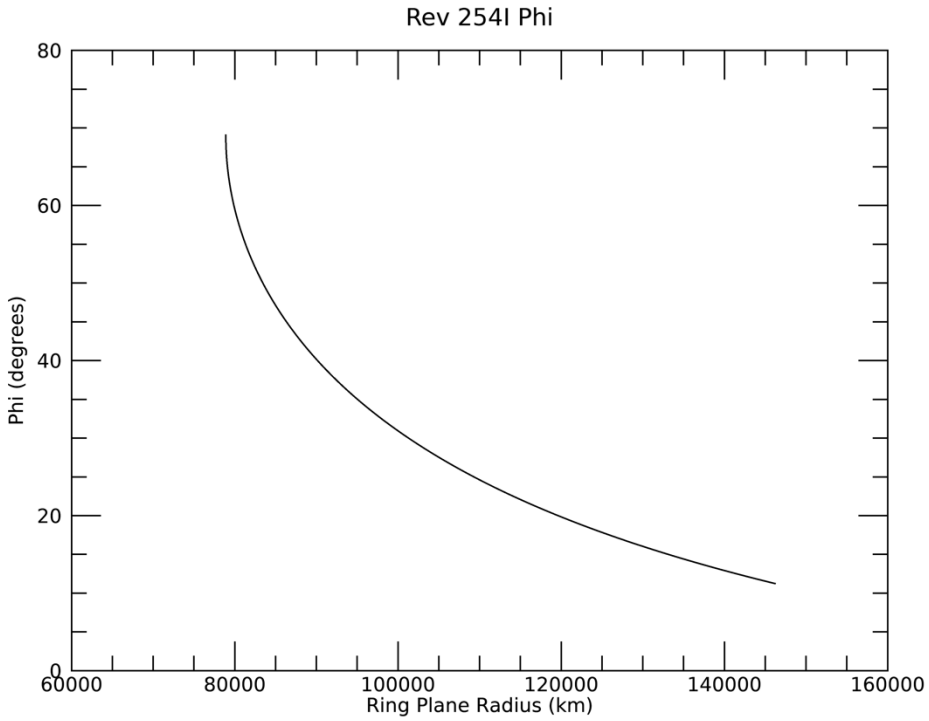
Rev 254I Phi
Phi (degrees)
80
60
40
20
0
60000
80000
100000
120000
140000
160000
Ring Plane Radius (km)

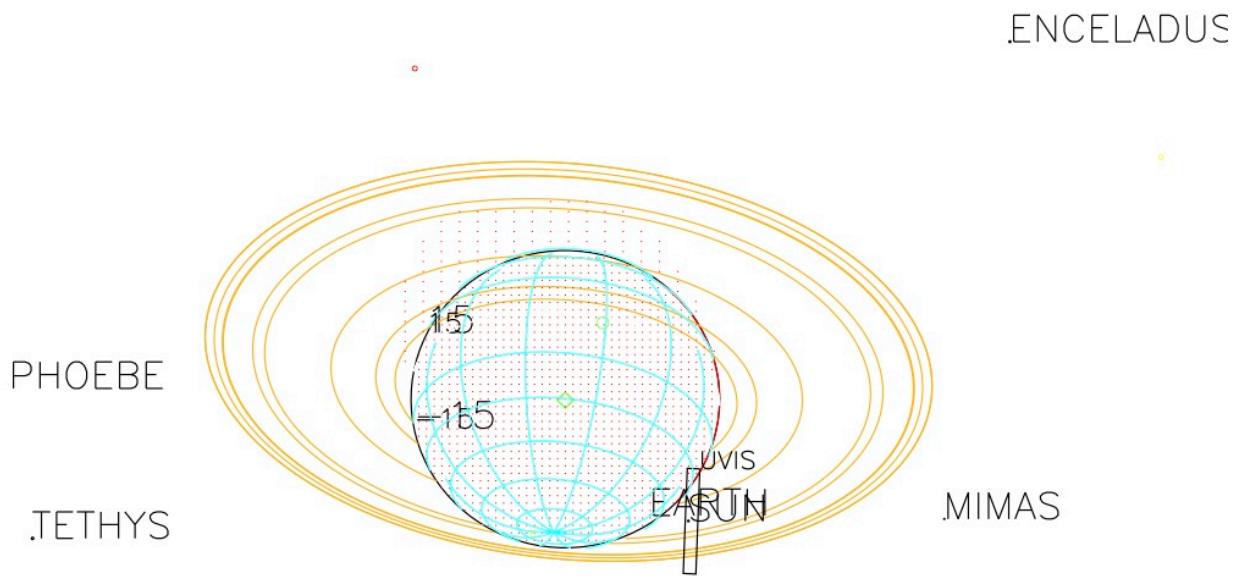

2016-361T18:36:00.000 611805.65 km

Target RA/dec: 83.14, 25.90

Subsolar lat/lon: 22.21, 161.66

Sub-s/c lat/lon: -26.09, -12.90

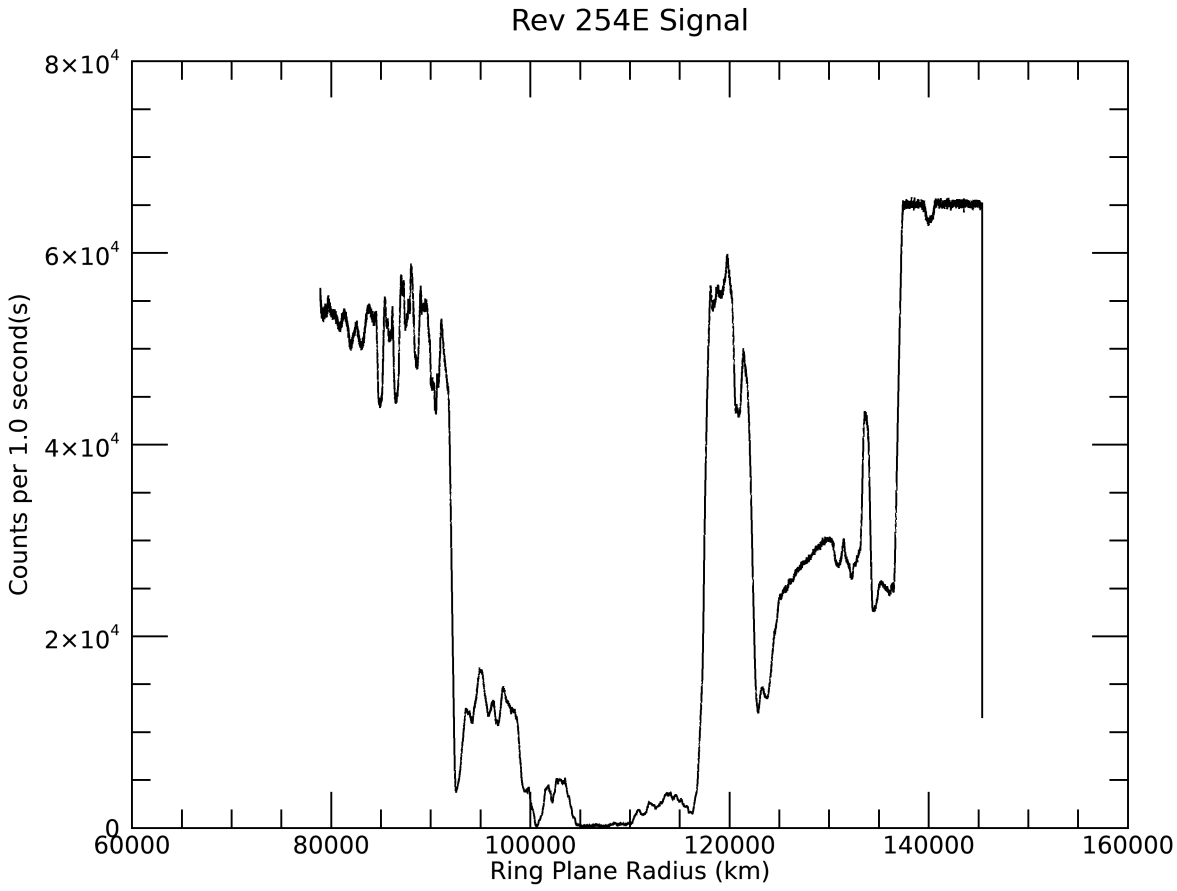
Rev 254E Signal
8×10^4
6×10^4
4×10^4
2×10^4
0
Counts per 1.0 second(s)
60000
80000
100000
120000
140000
160000
Ring Plane Radius (km)

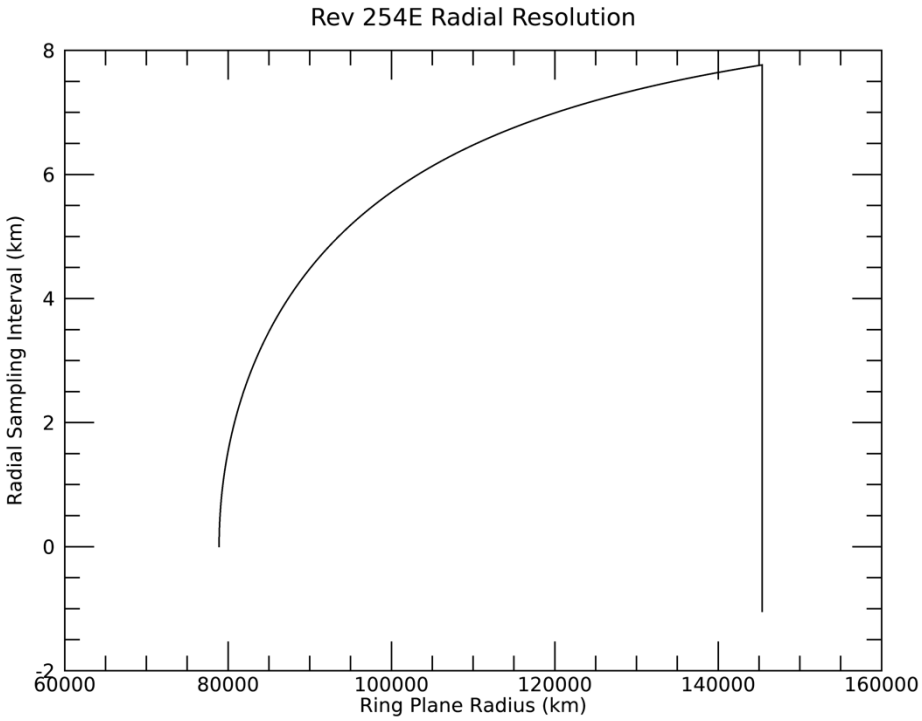
Rev 254E Radial Resolution
Radial Sampling Interval (km)
8
6
4
2
0
-2
60000
80000
100000
120000
140000
160000
Ring Plane Radius (km)

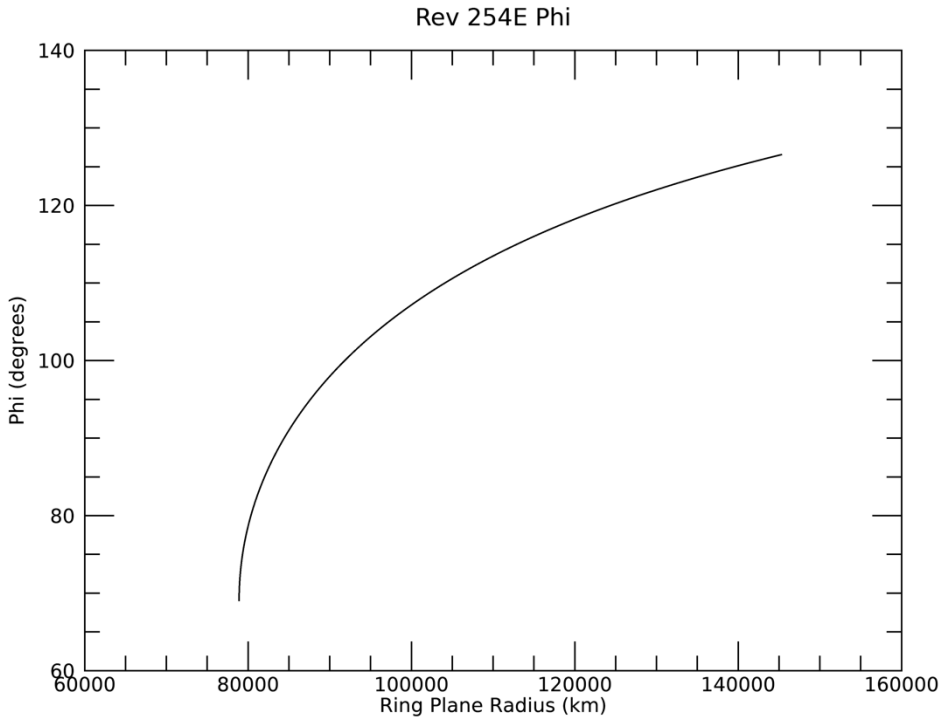
Rev 254E Phi
Phi (degrees)
140
120
100
80
60
60000
80000
100000
120000
140000
160000
Ring Plane Radius (km)

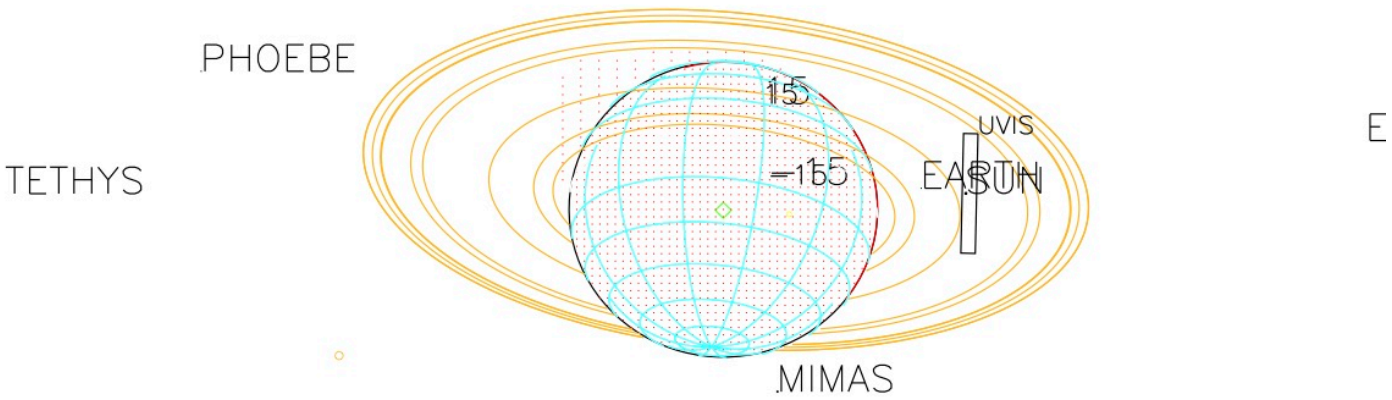

2016−361T22:15:00.000 694142.89 km

Target RA/dec: 86.69, 21.28

Subsolar lat/lon: 22.21, 38.36

Sub−s/c lat/lon: −21.69, −132.99

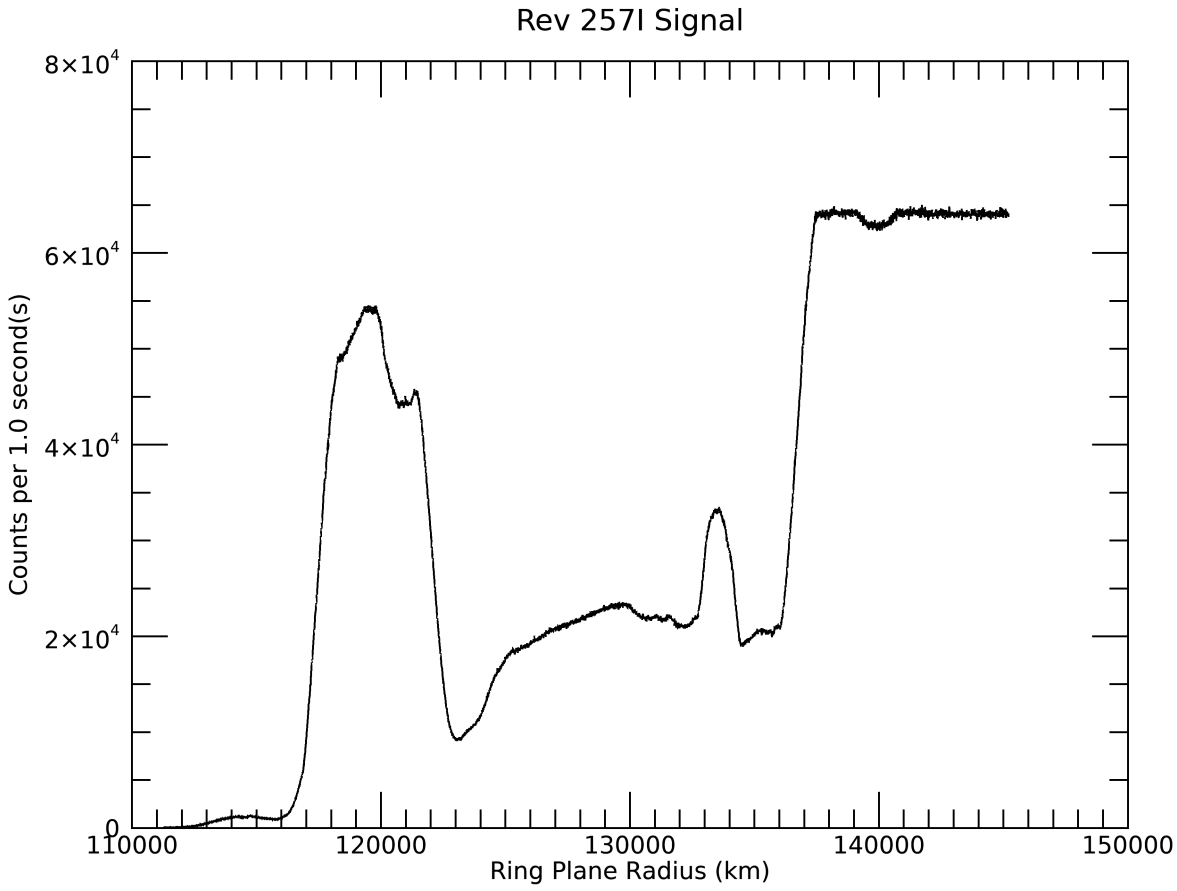
Rev 257I Signal
8×10^4
6×10^4
4×10^4
2×10^4
0
Counts per 1.0 second(s)
110000
120000
130000
140000
150000
Ring Plane Radius (km)

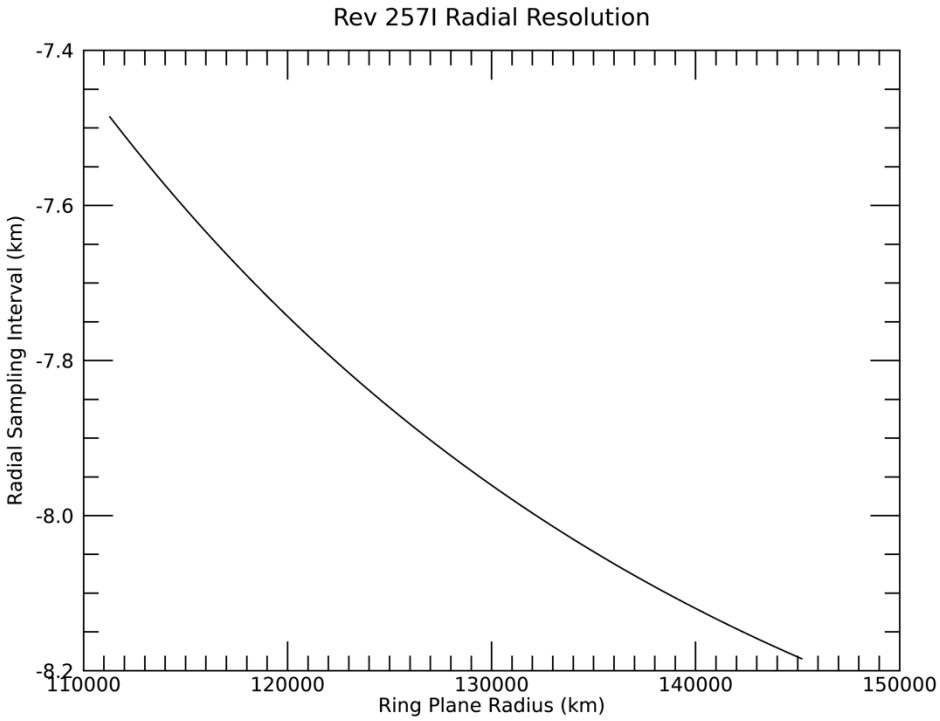
Rev 257I Radial Resolution
-7.4
-7.6
-7.8
-8.0
-8.2
Radial Sampling Interval (km)
110000
120000
130000
140000
150000
Ring Plane Radius (km)

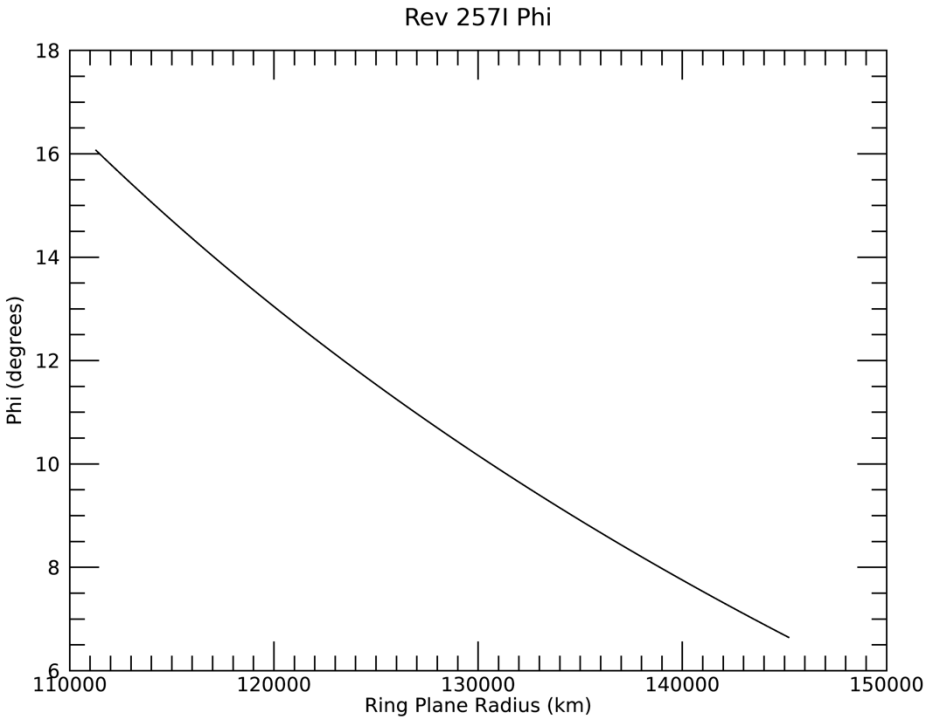
Rev 257I Phi
18
16
14
12
10
8
6
Phi (degrees)
110000
120000
130000
140000
150000
Ring Plane Radius (km)

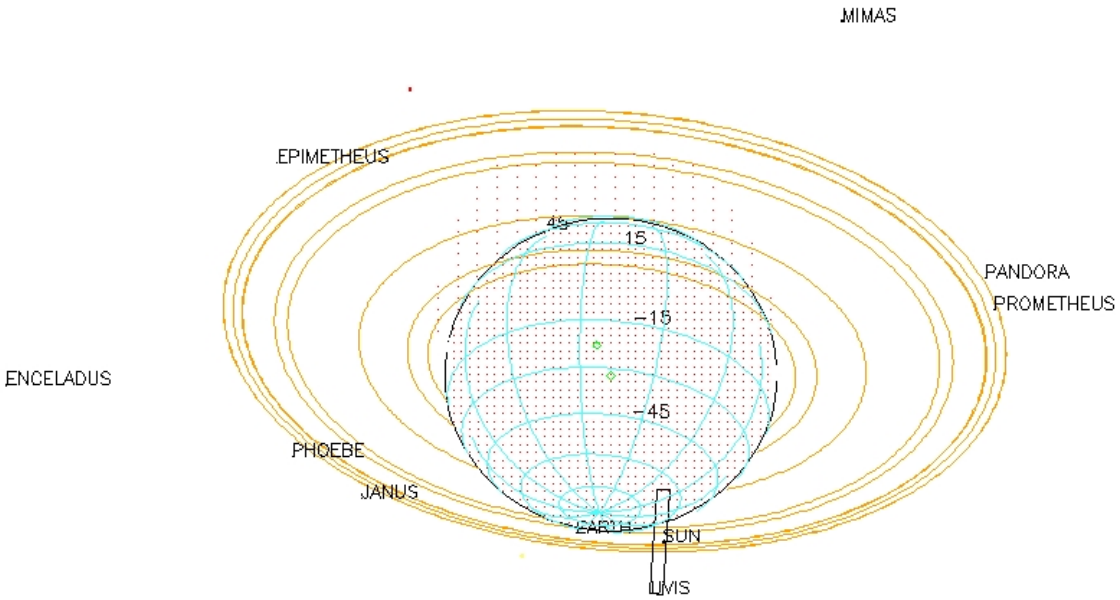

2017-017T04:50:00.000 579989.30 km
Target RA/dec: 81.00, 27.52
Subsolar lat/lon: 22.23, 69.99
Sub-s/c lat/lon: -27.74, -107.35

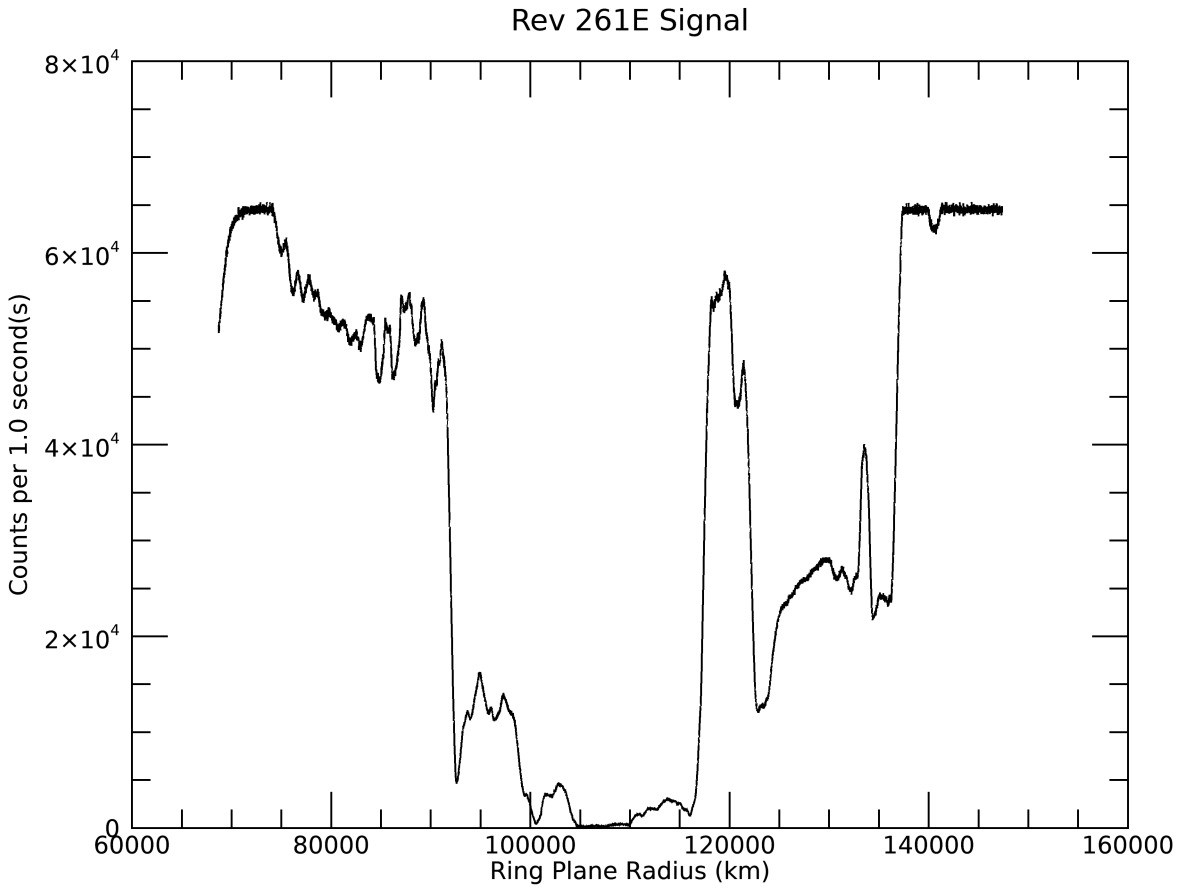
Rev 261E Signal
8×10^4
6×10^4
4×10^4
2×10^4
0
Counts per 1.0 second(s)
60000
80000
100000
120000
140000
160000
Ring Plane Radius (km)

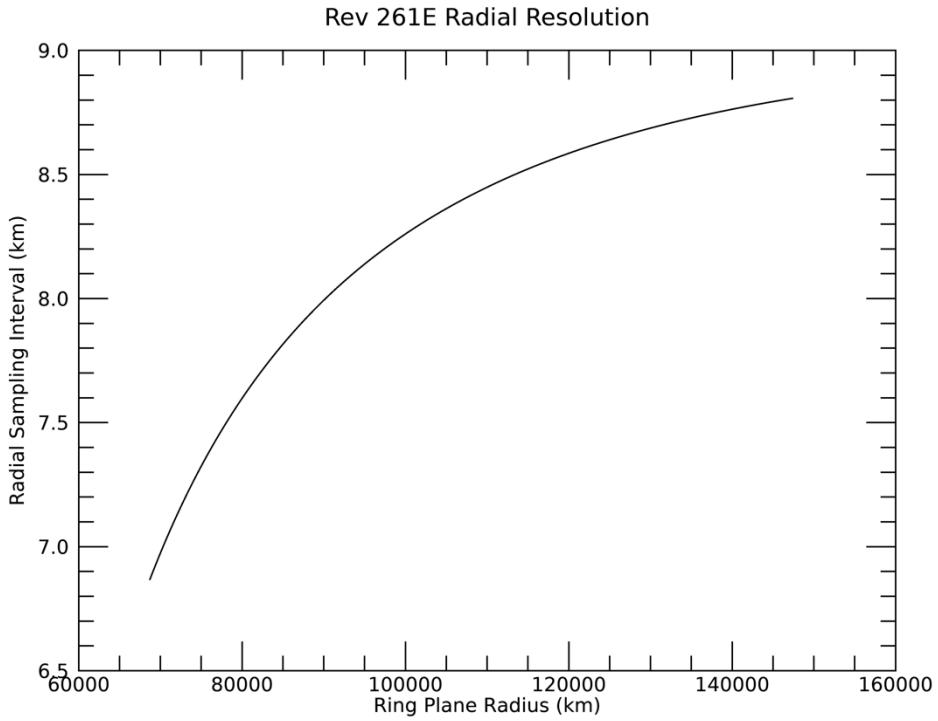
Rev 261E Radial Resolution
Radial Sampling Interval (km)
9.0
8.5
8.0
7.5
7.0
6.5
60000
80000
100000
120000
140000
160000
Ring Plane Radius (km)

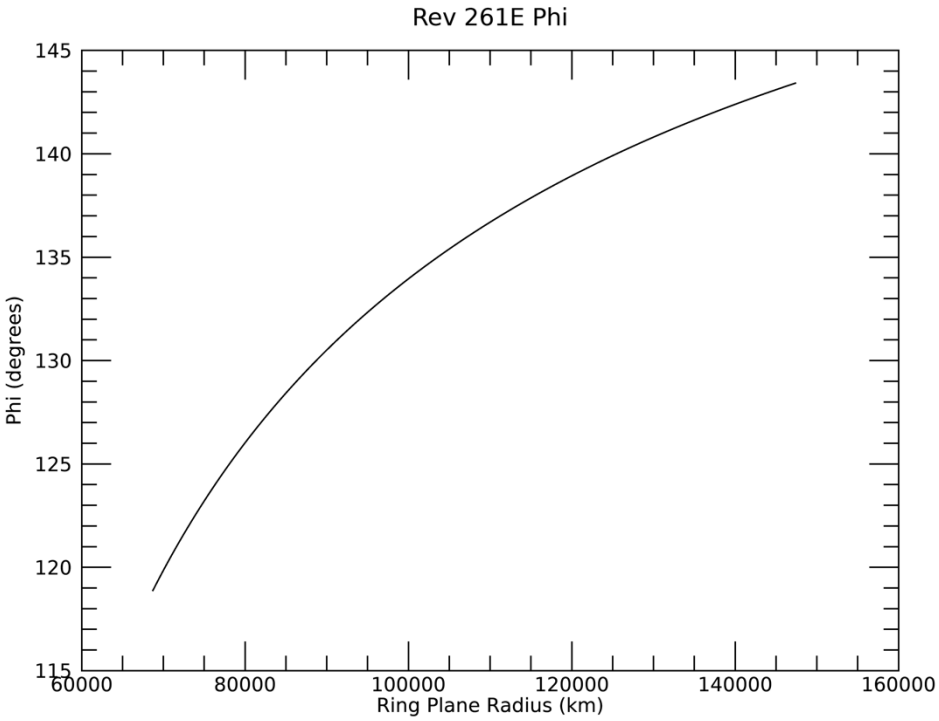
Rev 261E Phi
Phi (degrees)
145
140
135
130
125
120
115
60000
80000
100000
120000
140000
160000
Ring Plane Radius (km)

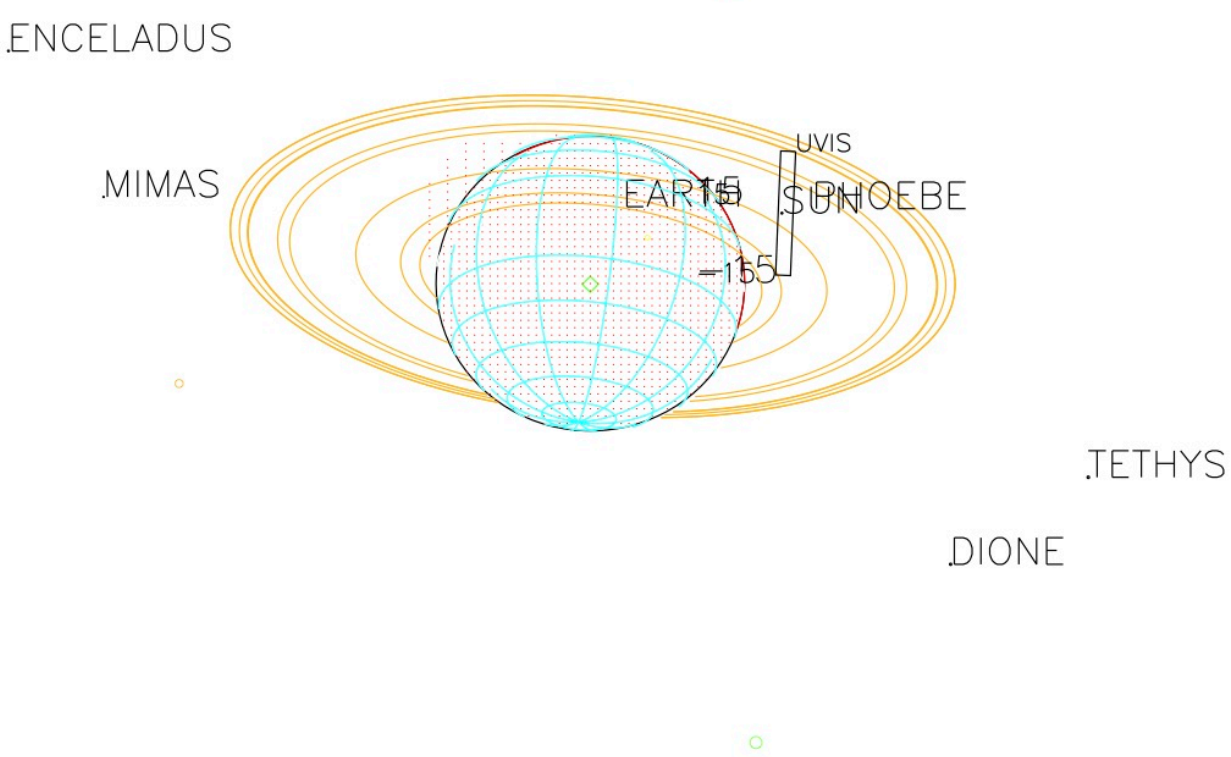

2017-046T04:00:00.000 721766.45 km

Target RA/dec: 86.32, 19.76

Subsolar lat/lon: 22.25, -13.90

Sub-s/c lat/lon: -20.38, 172.52

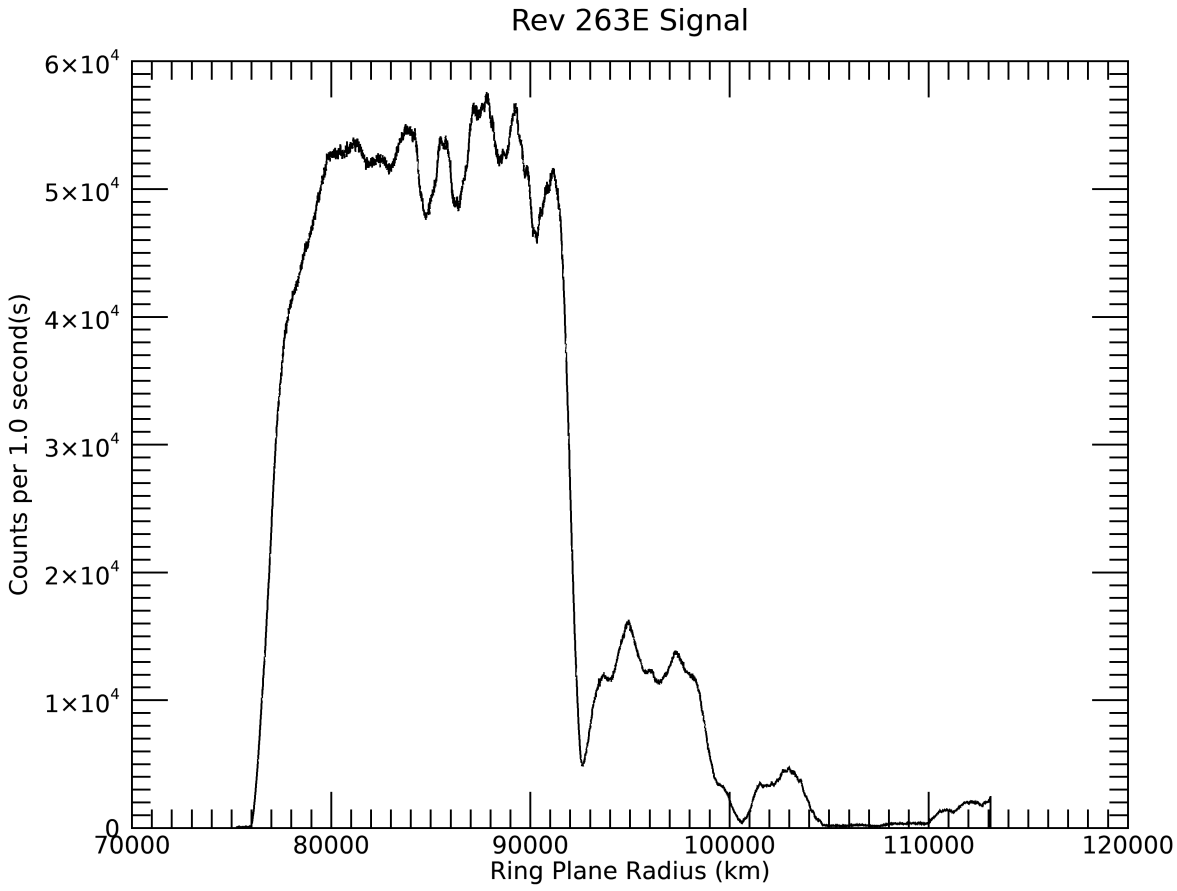
Rev 263E Signal
6×10^4
5×10^4
4×10^4
3×10^4
2×10^4
1×10^4
0
Counts per 1.0 second(s)
70000
80000
90000
100000
110000
120000
Ring Plane Radius (km)

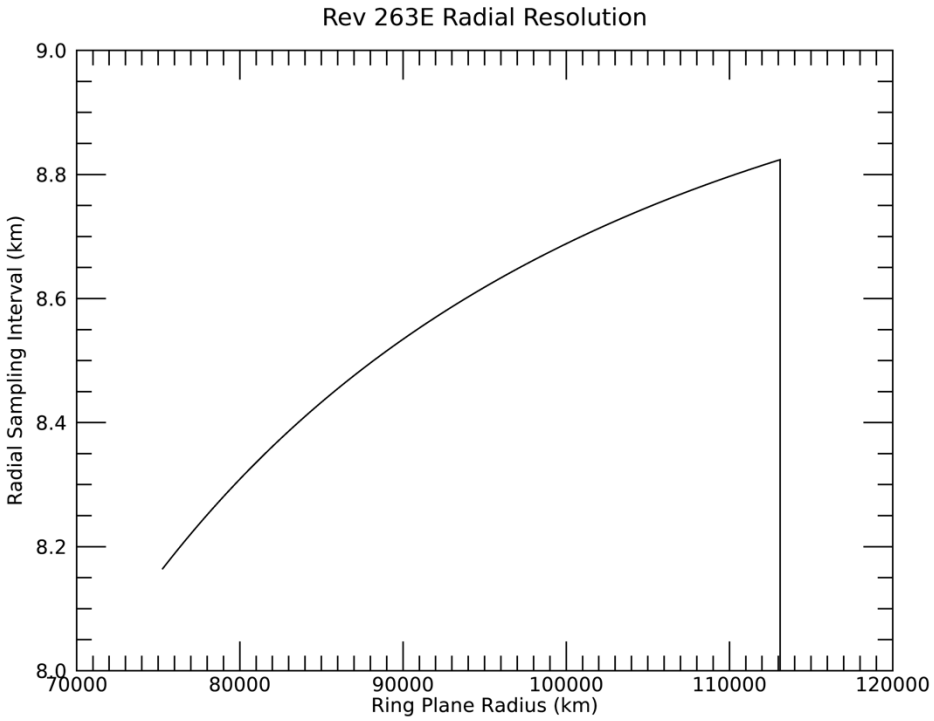
Rev 263E Radial Resolution
Radial Sampling Interval (km)
9.0
8.8
8.6
8.4
8.2
8.0
70000
80000
90000
100000
110000
120000
Ring Plane Radius (km)

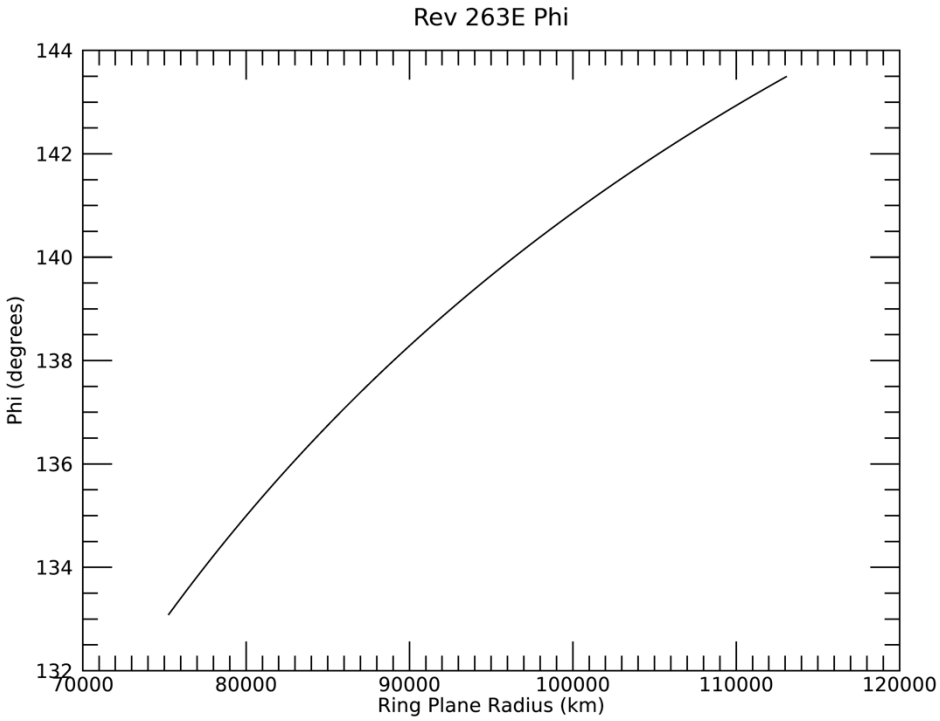
Rev 263E Phi
Phi (degrees)
144
142
140
138
136
134
132
70000
80000
90000
100000
110000
120000
Ring Plane Radius (km)

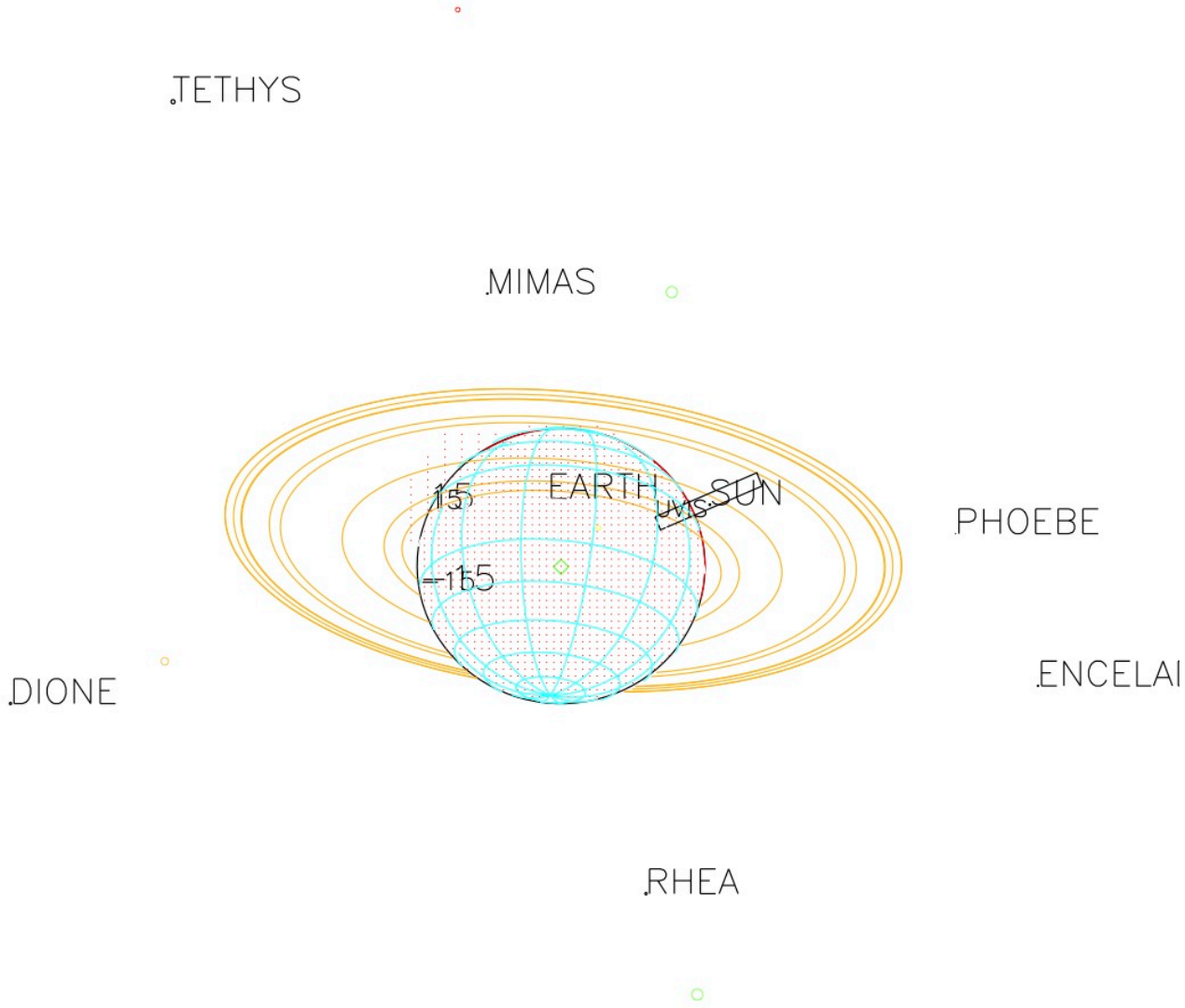

2017-060T11:47:00.000 714527.61 km

Target RA/dec: 85.76, 19.89

Subsolar lat/lon: 22.26, -107.47

Sub-s/c lat/lon: -20.54, 77.90

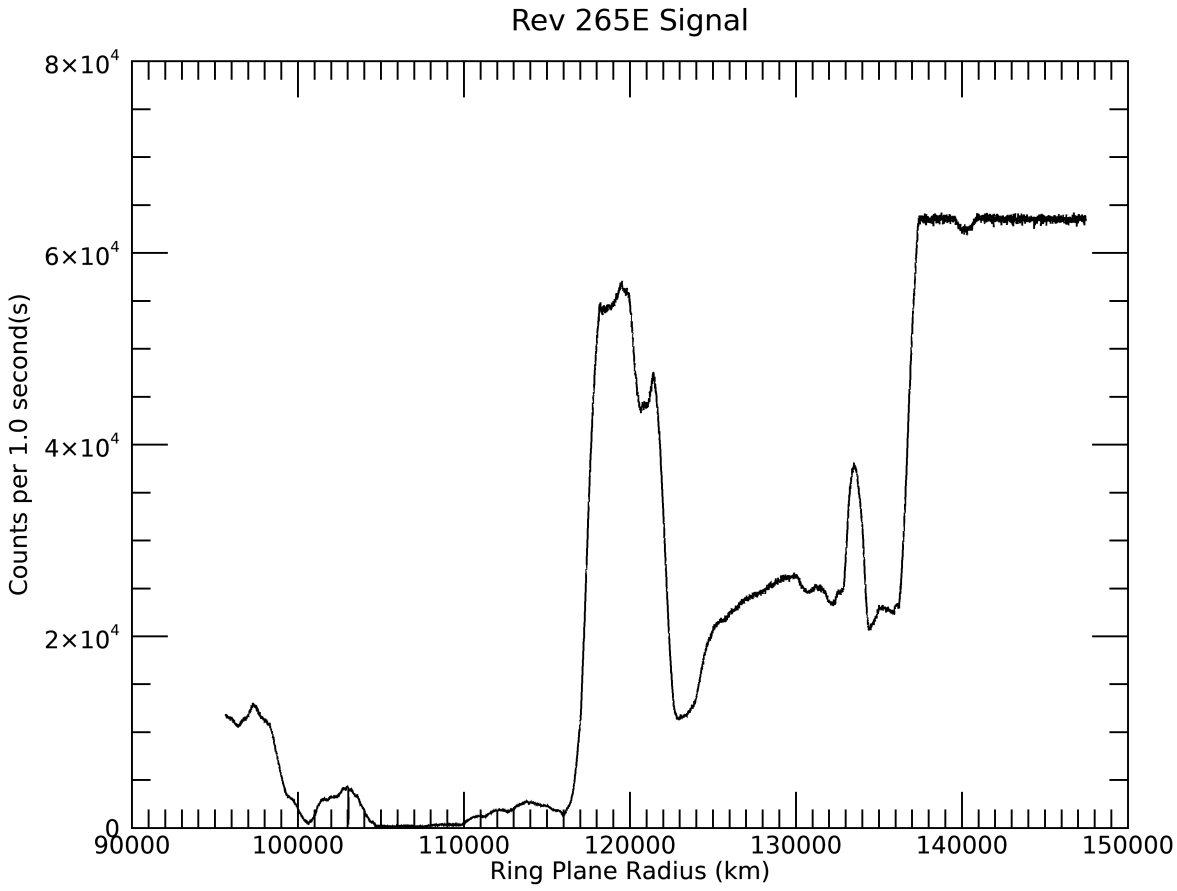
Rev 265E Signal
8×10^4
6×10^4
4×10^4
2×10^4
0
Counts per 1.0 second(s)
90000
100000
110000
120000
130000
140000
150000
Ring Plane Radius (km)

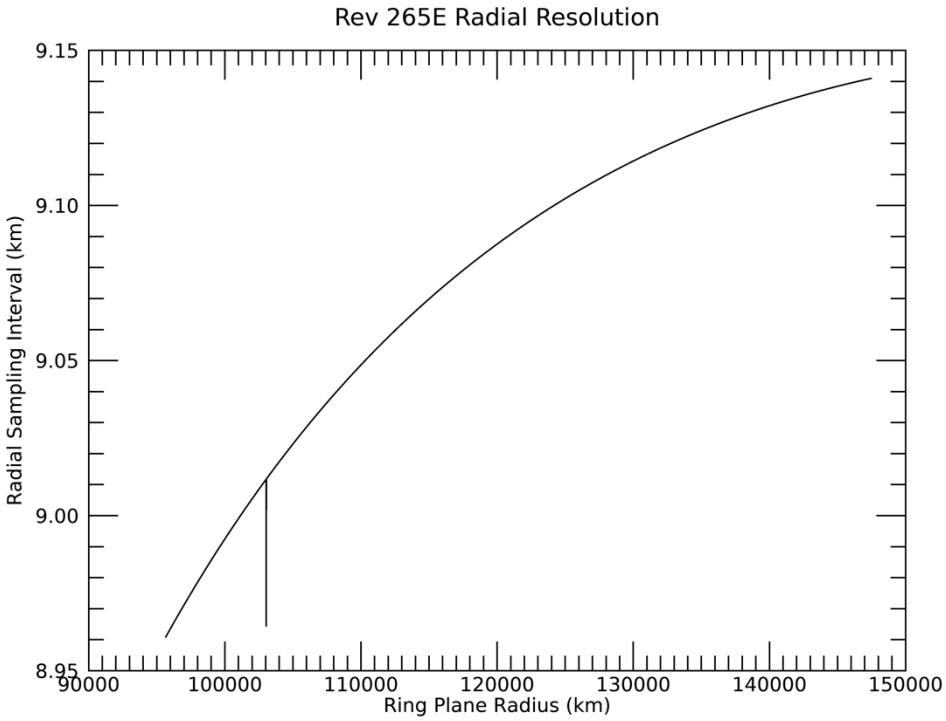
Rev 265E Radial Resolution
Radial Sampling Interval (km)
9.15
9.10
9.05
9.00
8.95
90000
100000
110000
120000
130000
140000
150000
Ring Plane Radius (km)

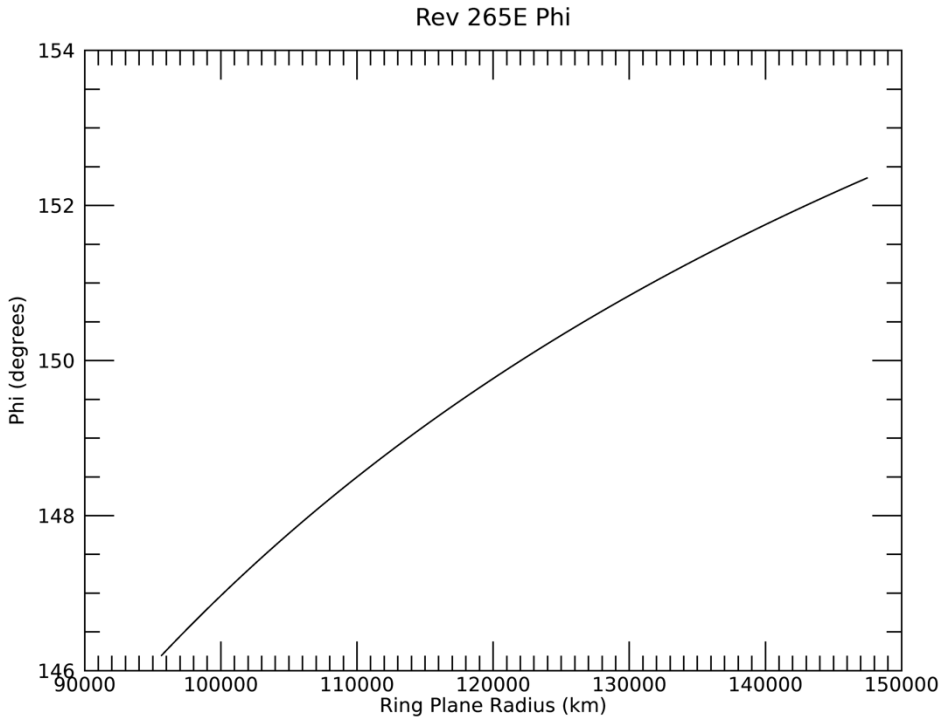
Rev 265E Phi
Phi (degrees)
154
152
150
148
146
90000
100000
110000
120000
130000
140000
150000
Ring Plane Radius (km)

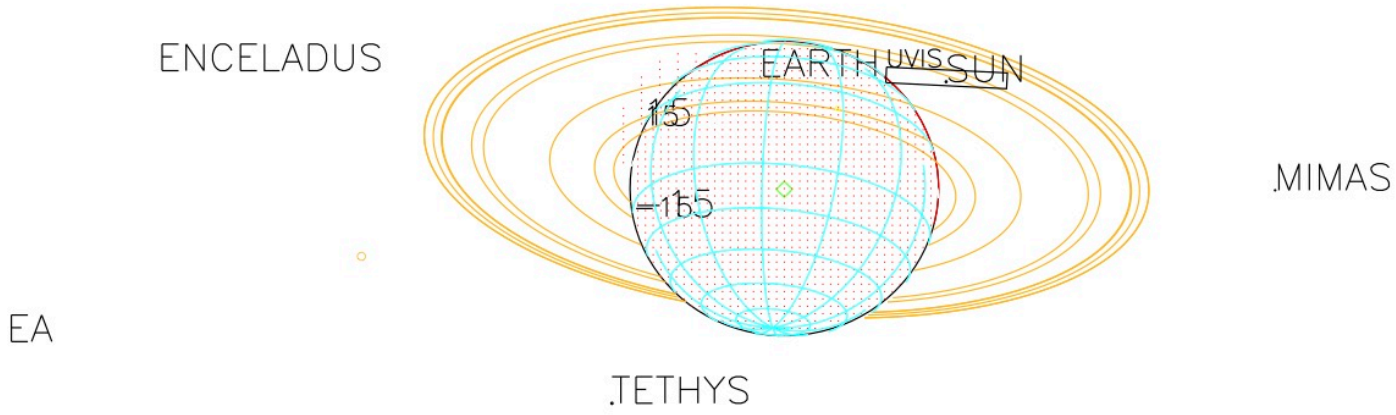

2017−074T20:36:00.000 733863.74 km

Target RA/dec: 86.16, 18.79

Subsolar lat/lon: 22.27, 124.04

Sub−s/c lat/lon: −19.54, −50.76

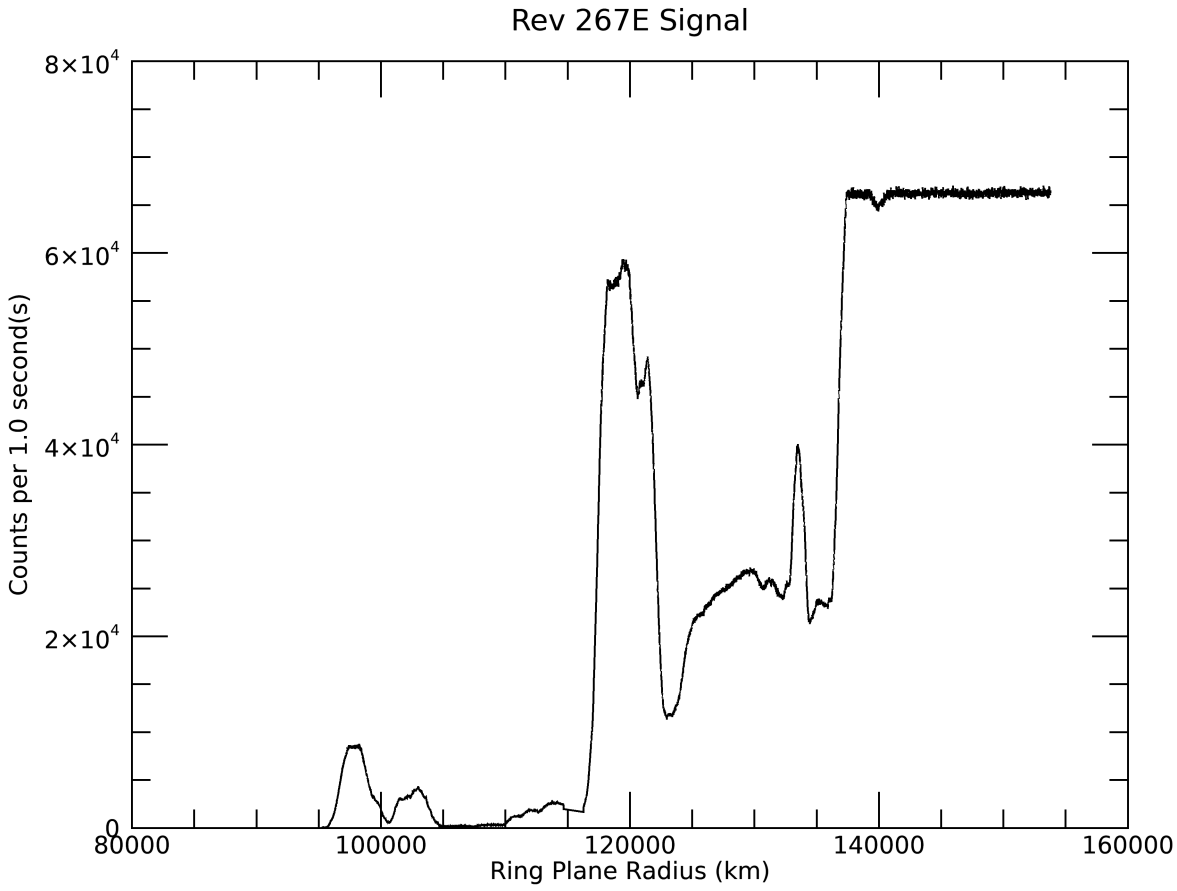
Rev 267E Signal
8×10^4
6×10^4
4×10^4
2×10^4
0
Counts per 1.0 second(s)
80000
100000
120000
140000
160000
Ring Plane Radius (km)

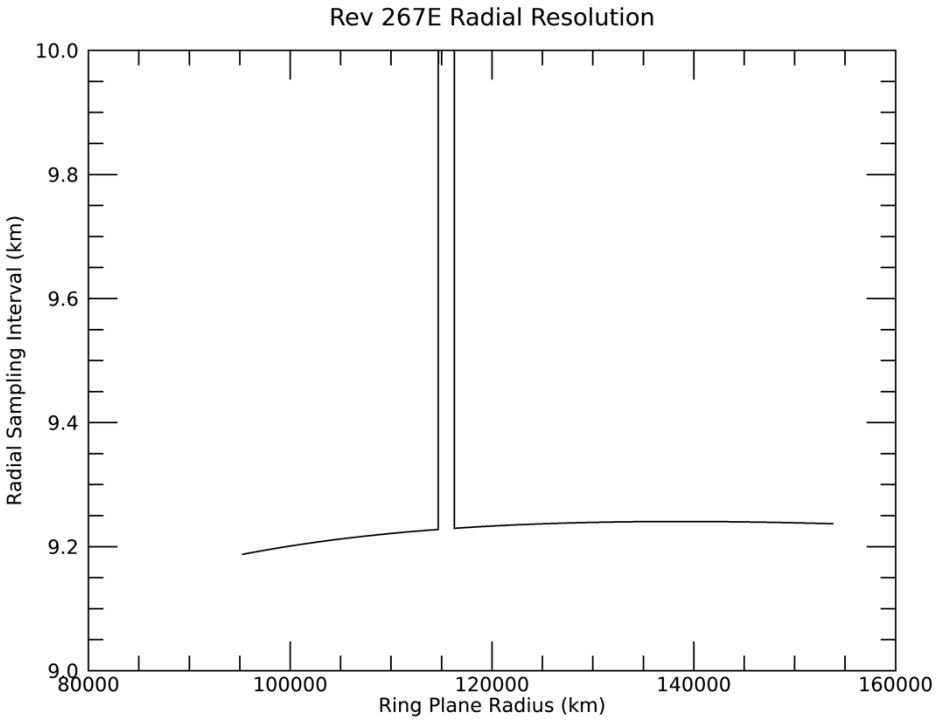
Rev 267E Radial Resolution
Radial Sampling Interval (km)
10.0
9.8
9.6
9.4
9.2
9.0
80000
100000
120000
140000
160000
Ring Plane Radius (km)

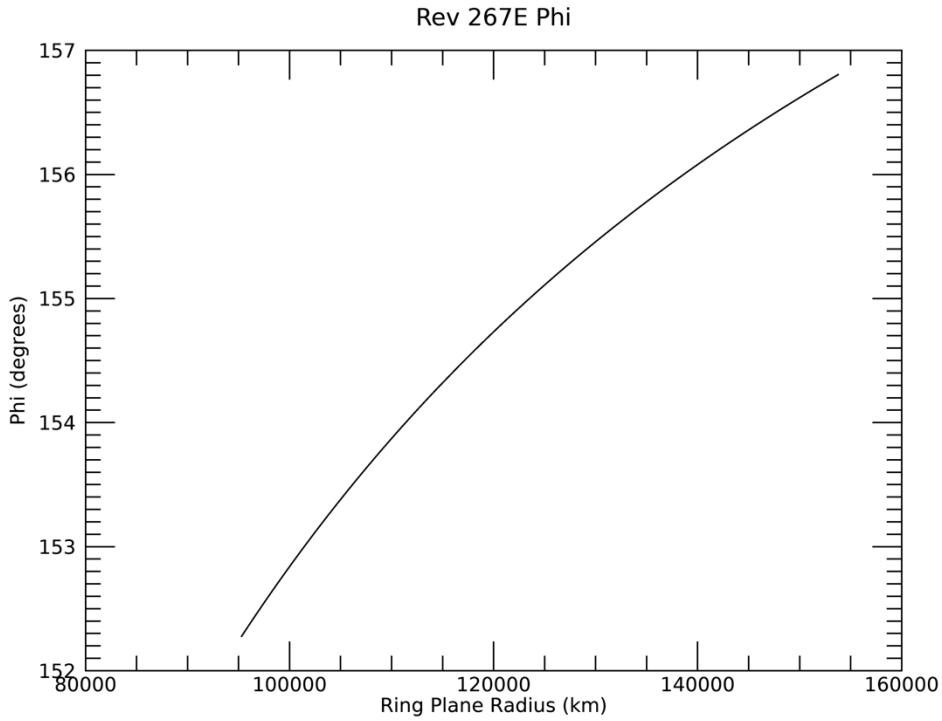
Rev 267E Phi
Phi (degrees)
157
156
155
154
153
152
80000
100000
120000
140000
160000
Ring Plane Radius (km)

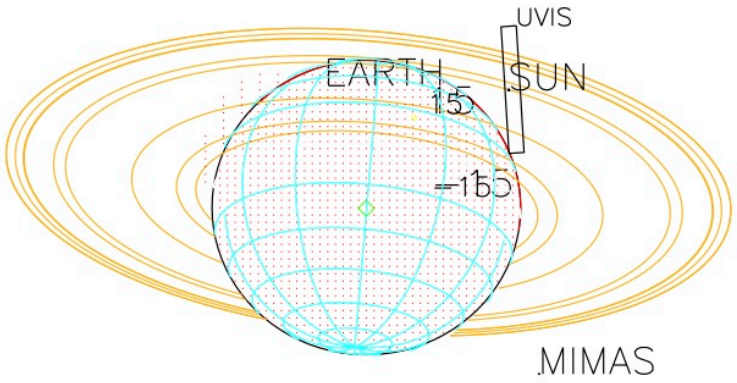

EN

N

HYPERION

2017-089T04:32:00.000 738563.89 km

Target RA/dec: 85.96, 18.52

Subsolar lat/lon: 22.27, 25.40

Sub-s/c lat/lon: -19.32, -150.12

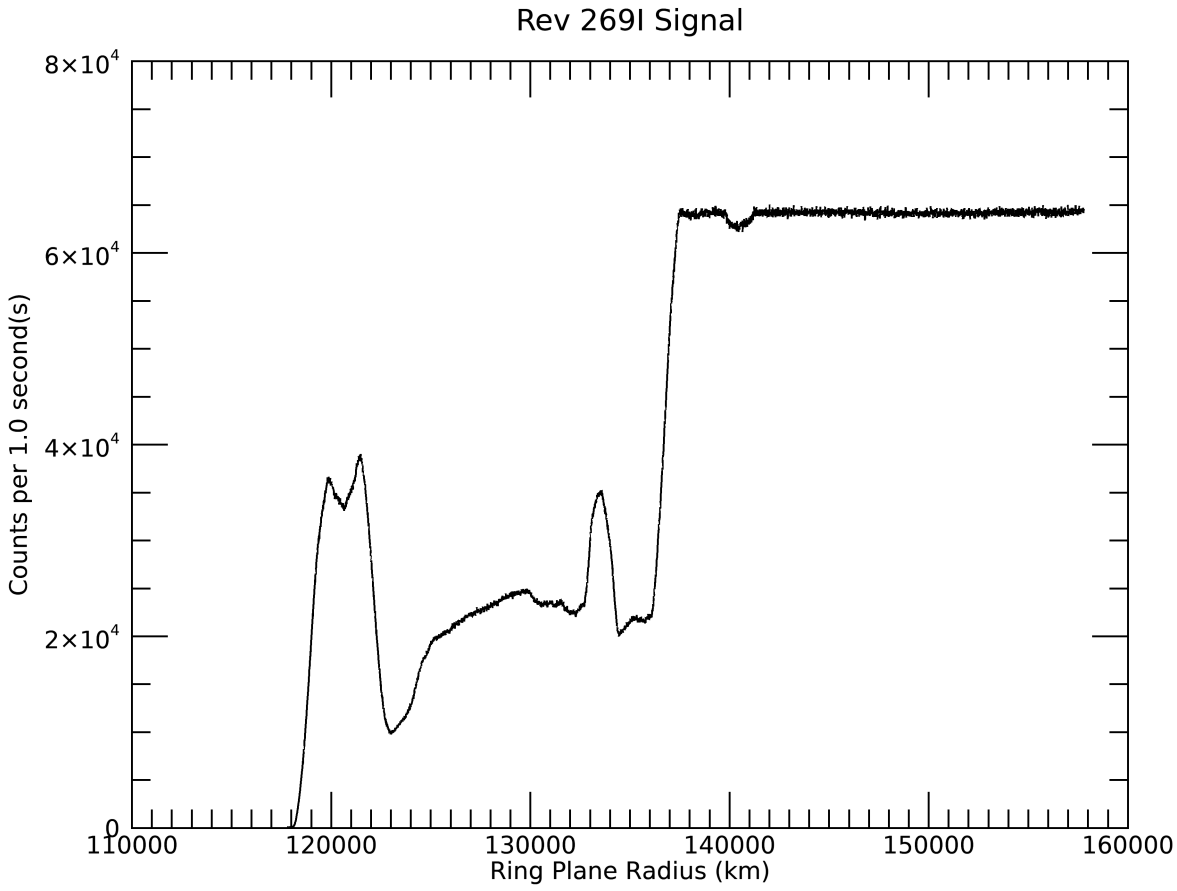
Rev 269I Signal
8×10^4
6×10^4
4×10^4
2×10^4
0
Counts per 1.0 second(s)
110000
120000
130000
140000
150000
160000
Ring Plane Radius (km)

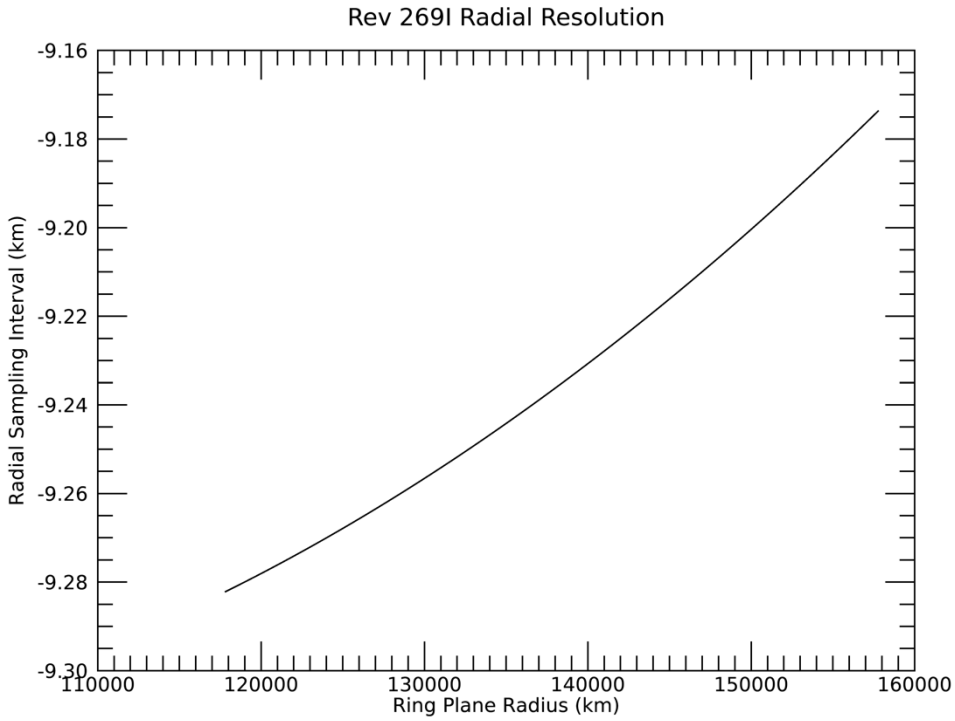
Rev 269I Radial Resolution
-9.16
-9.18
-9.20
-9.22
-9.24
-9.26
-9.28
-9.30
Radial Sampling Interval (km)
110000
120000
130000
140000
150000
160000
Ring Plane Radius (km)

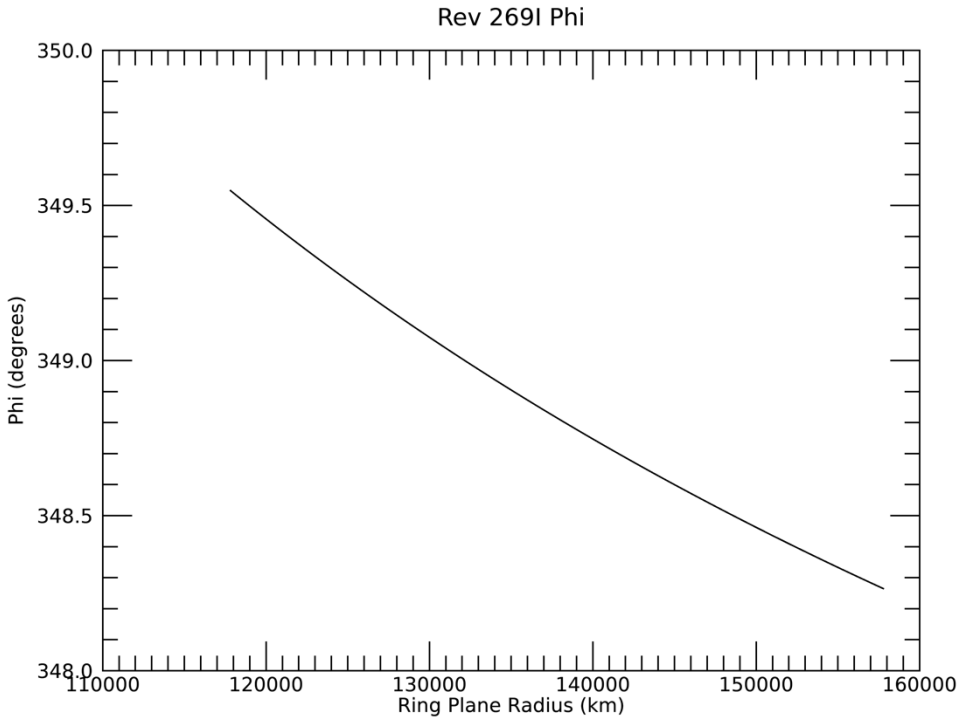
Rev 269I Phi
350.0
349.5
349.0
348.5
348.0
Phi (degrees)
110000
120000
130000
140000
150000
160000
Ring Plane Radius (km)

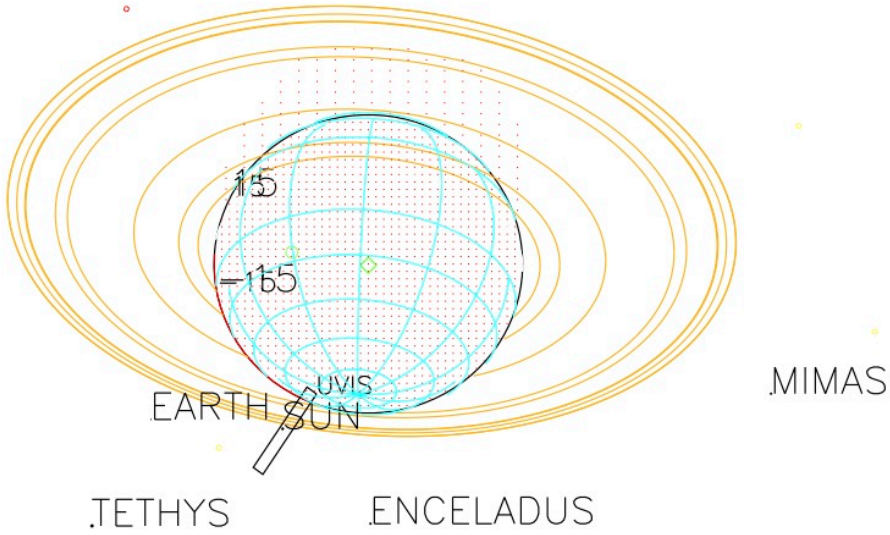

IAPETUS

2017−103T04:46:00.000 566712.74 km

Target RA/dec: 78.12, 28.16

Subsolar lat/lon: 22.28, −173.13

Sub−s/c lat/lon: −28.53, 3.66

TITAN

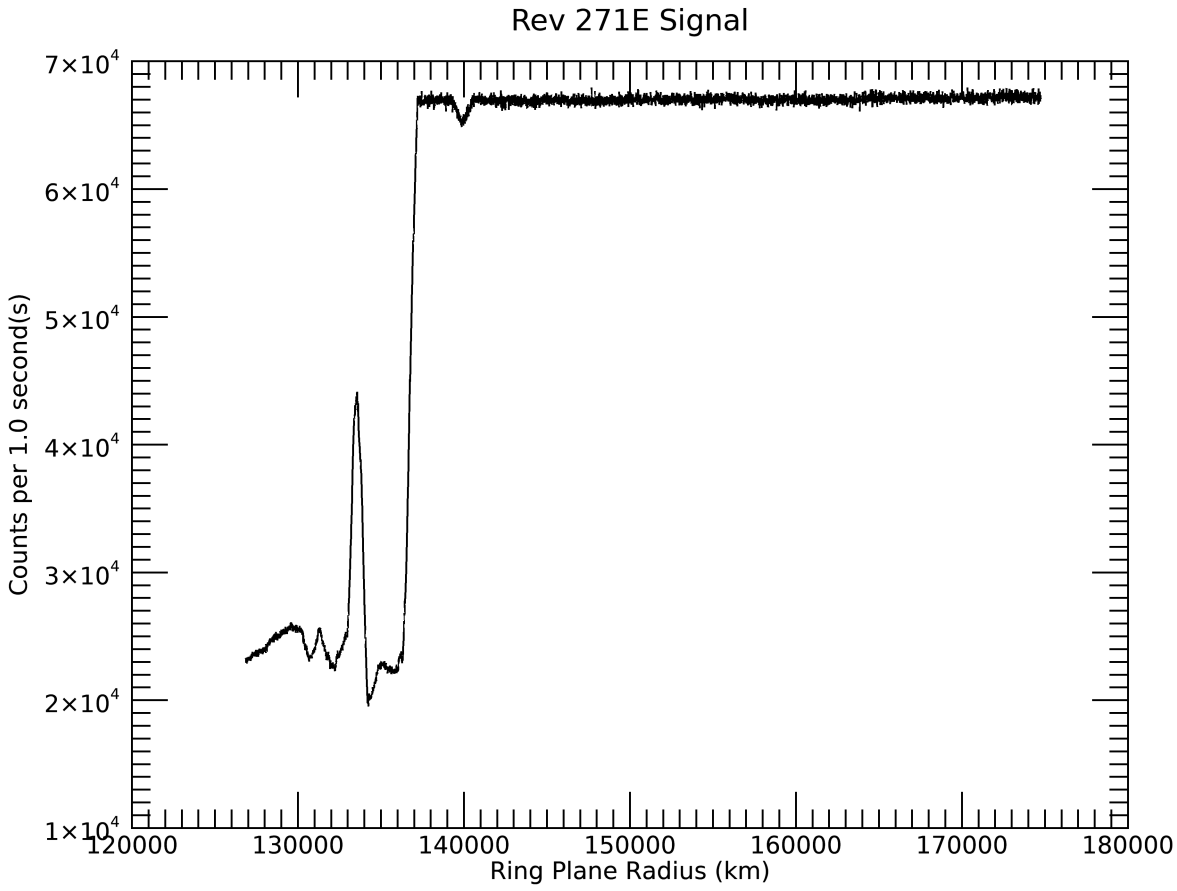
Rev 271E Signal
7×10^4
6×10^4
5×10^4
4×10^4
3×10^4
2×10^4
1×10^4
Counts per 1.0 second(s)
120000
130000
140000
150000
160000
170000
180000
Ring Plane Radius (km)

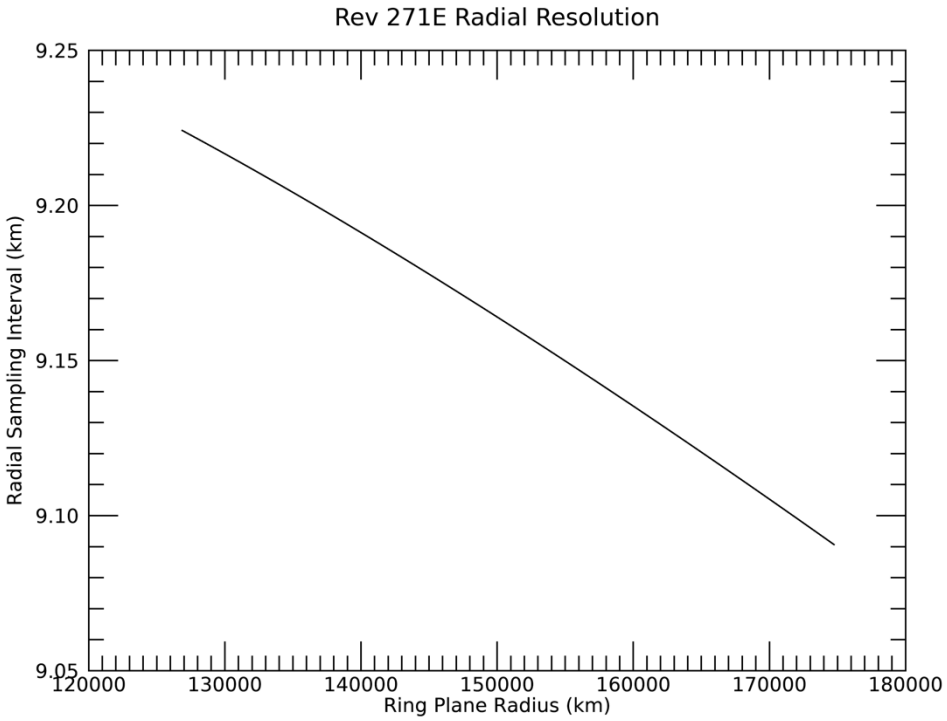
Rev 271E Radial Resolution
Radial Sampling Interval (km)
9.25
9.20
9.15
9.10
9.05
120000
130000
140000
150000
160000
170000
180000
Ring Plane Radius (km)

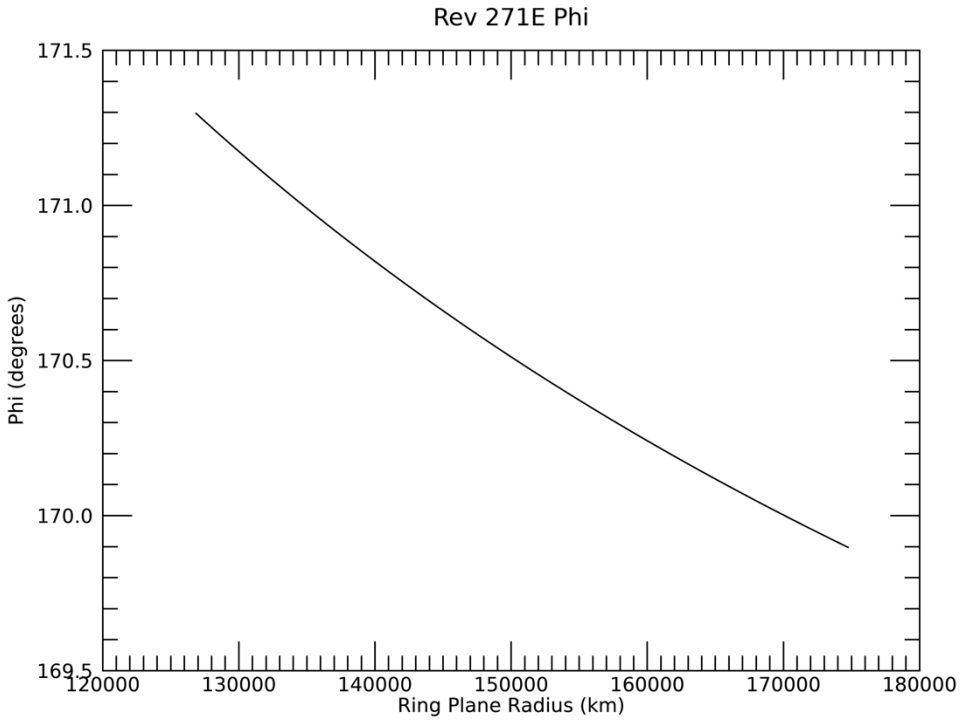
Rev 271E Phi
Phi (degrees)
171.5
171.0
170.5
170.0
169.5
120000
130000
140000
150000
160000
170000
180000
Ring Plane Radius (km)

HYS

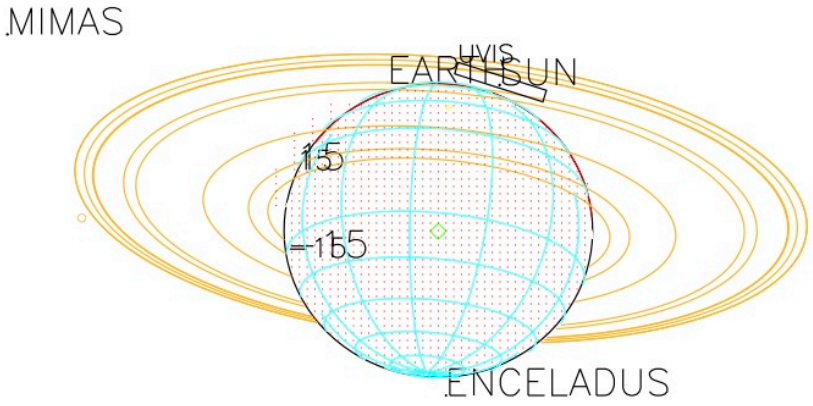

2017-116T22:10:00.000 562341.65 km

Target RA/dec: 84.84, 16.40

Subsolar lat/lon: 22.28, -140.82

Sub-s/c lat/lon: -17.66, 41.38

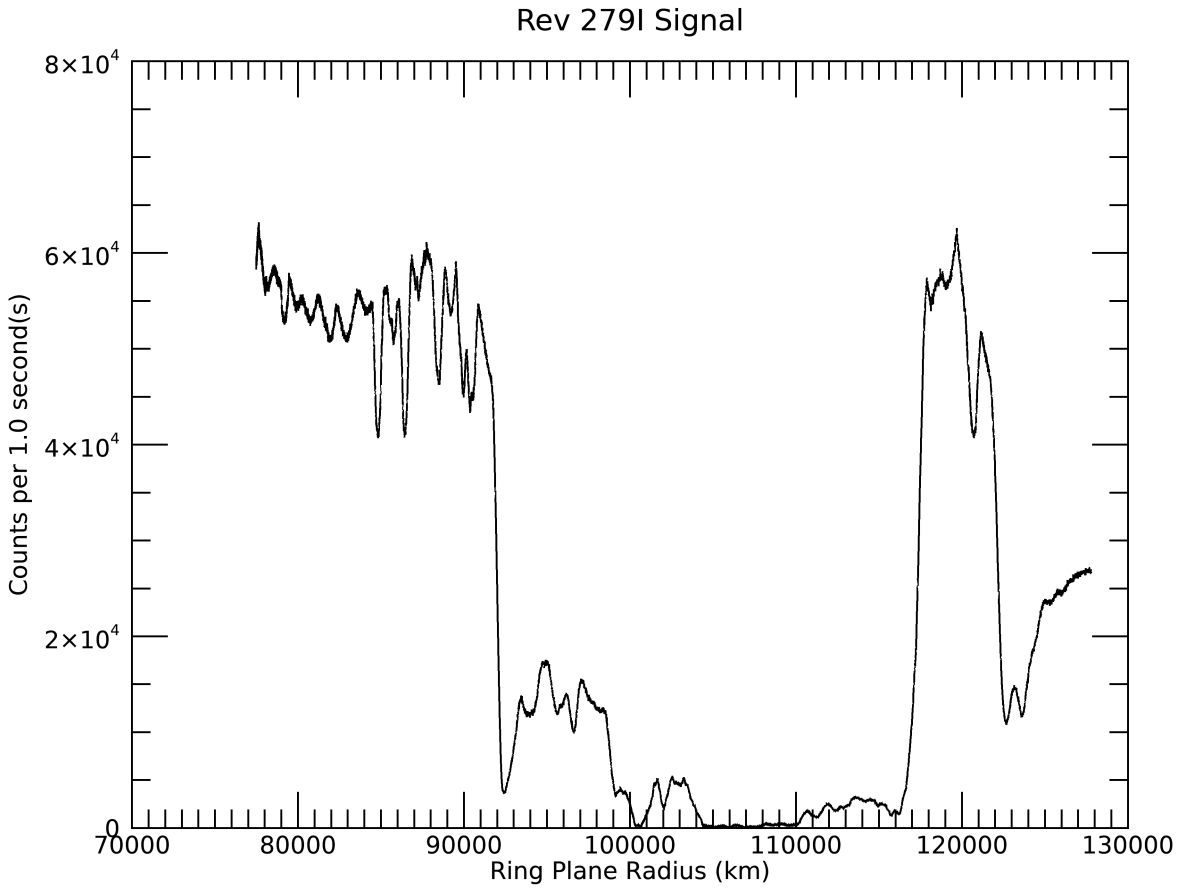
Rev 279I Signal
8×10^4
6×10^4
4×10^4
2×10^4
0
Counts per 1.0 second(s)
70000
80000
90000
100000
110000
120000
130000
Ring Plane Radius (km)

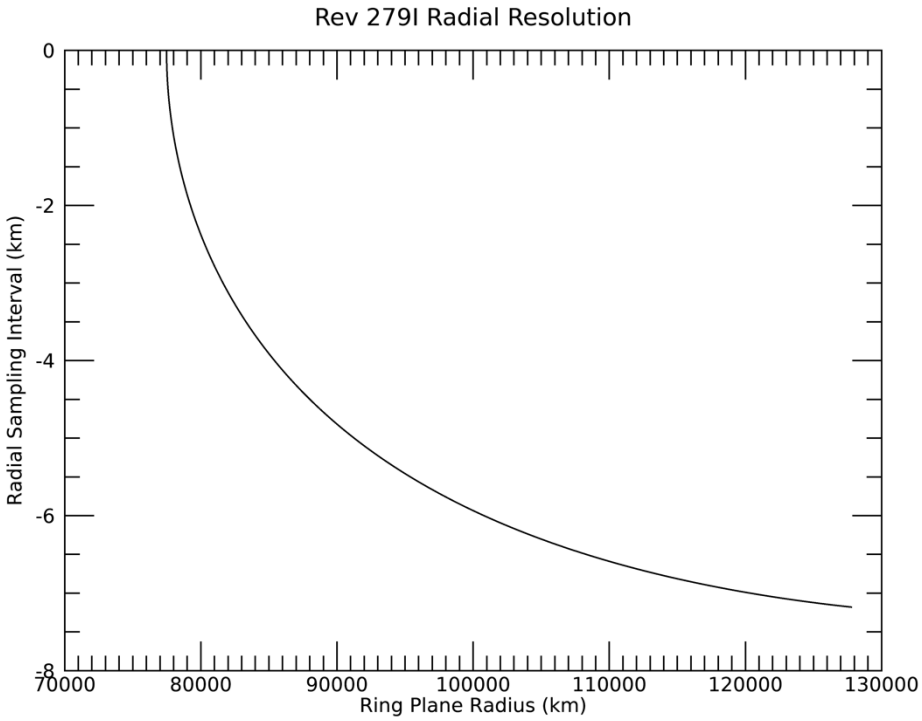
Rev 279I Radial Resolution
Radial Sampling Interval (km)
0
-2
-4
-6
-8
70000
80000
90000
100000
110000
120000
130000
Ring Plane Radius (km)

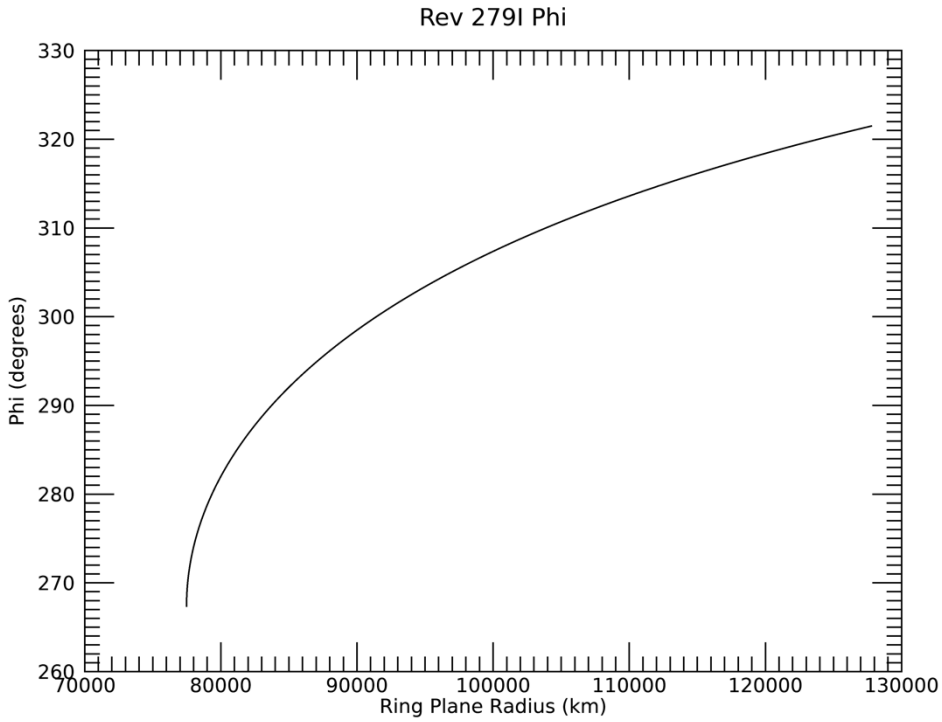
Rev 279I Phi
Phi (degrees)
330
320
310
300
290
280
270
260
70000
80000
90000
100000
110000
120000
130000
Ring Plane Radius (km)

ENCELADU

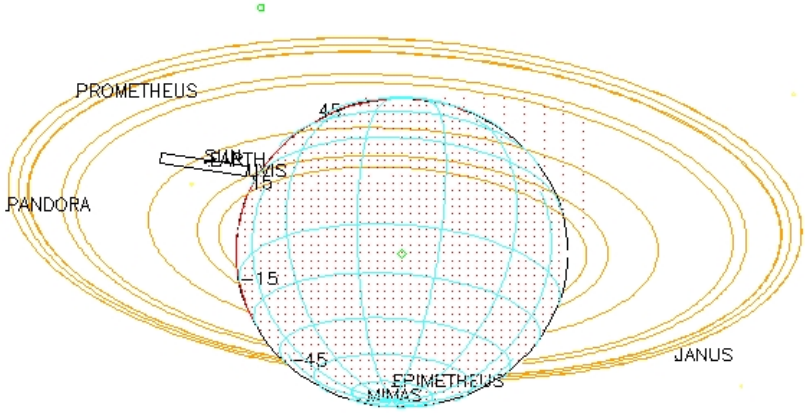

RHEA

TITAN

2017-168T09:50:00.000 486429.69 km
Target RA/dec: 74.79, 18.48
Subsolar lat/lon: 22.28, -123.71
Sub-s/c lat/lon: -20.16, 46.59

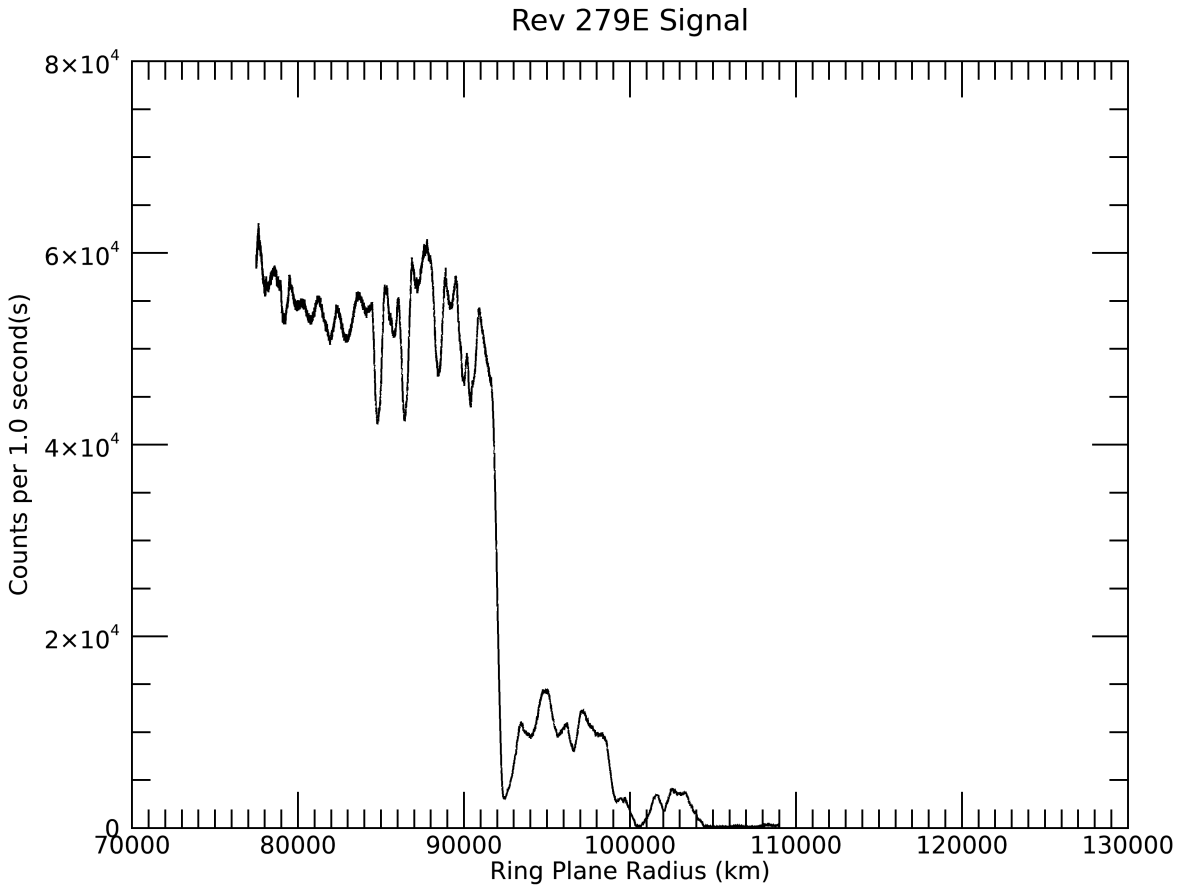
Rev 279E Signal
8×10^4
6×10^4
4×10^4
2×10^4
0
Counts per 1.0 second(s)
70000
80000
90000
100000
110000
120000
130000
Ring Plane Radius (km)

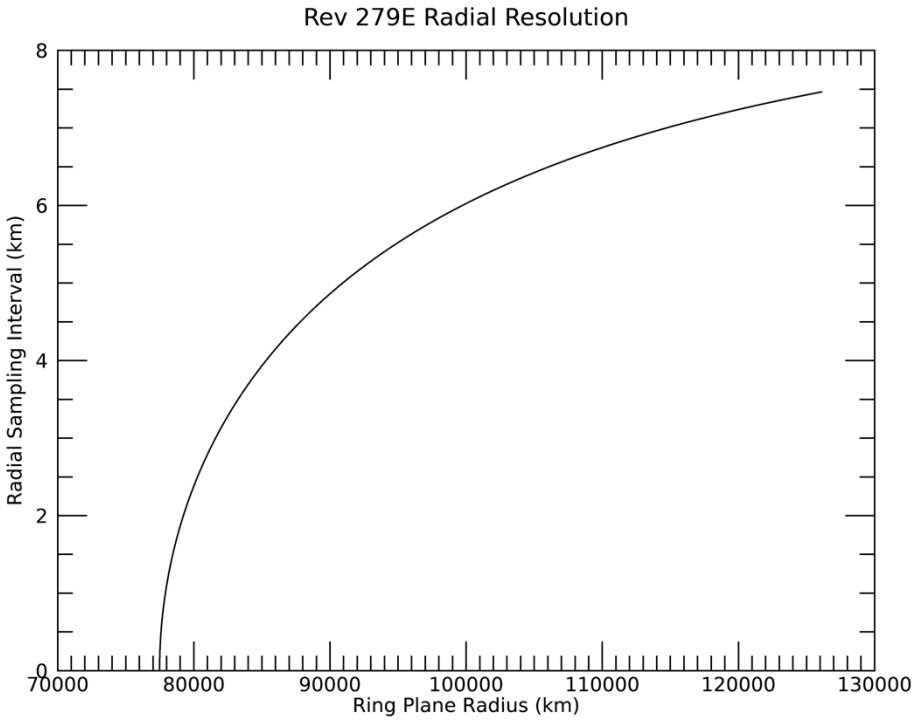
Rev 279E Radial Resolution
Radial Sampling Interval (km)
0
2
4
6
8
70000
80000
90000
100000
110000
120000
130000
Ring Plane Radius (km)

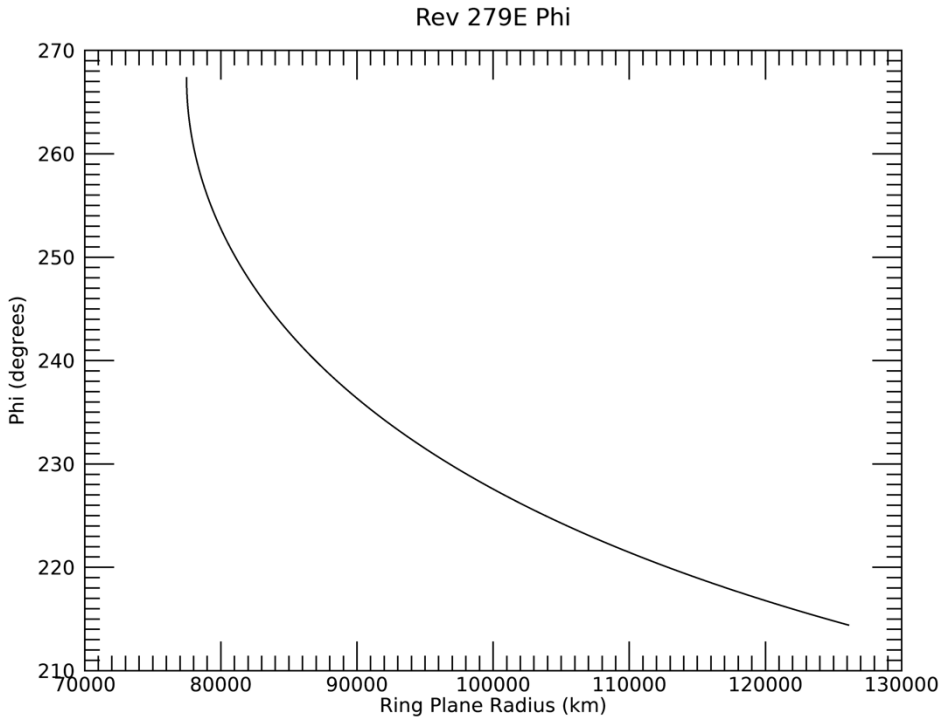
Rev 279E Phi
Phi (degrees)
210
220
230
240
250
260
270
70000
80000
90000
100000
110000
120000
130000
Ring Plane Radius (km)

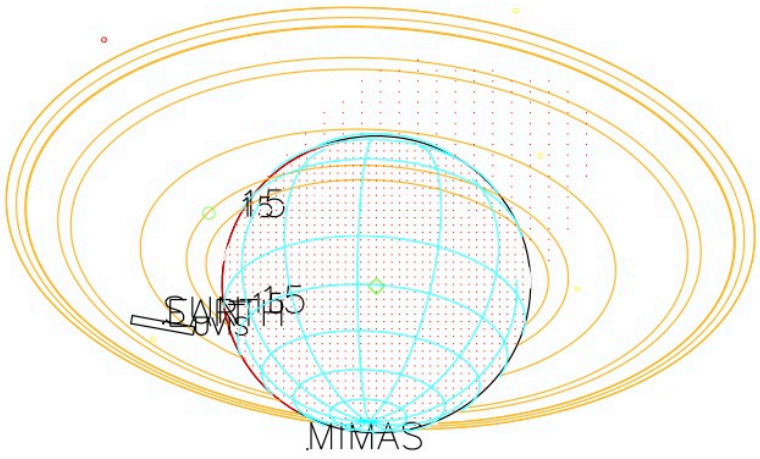

TITAN

RHEA

2017-168T09:58:00.000 372217.16 km

Target RA/dec: 70.09, 24.84

Subsolar lat/lon: 22.28, -128.21

Sub-s/c lat/lon: -26.24, 37.67